Universidade de Aveiro Secção Autónoma de Ciências da Saúde
2013

Luísa Filipe Henriques Martins de Bastos

Caracterização da Interação APP/HB-EGF

Unraveling the APP/HB-EGF Interaction

Universidade de Aveiro Secção Autónoma de Ciências da Saúde
2013

Luísa Filipe Henriques Martins de Bastos

Caracterização da Interação APP/HB-EGF

Unraveling the APP/HB-EGF Interaction

Dissertação apresentada à Universidade de Aveiro para cumprimento dos requisitos necessários à obtenção do grau de Mestre em Biomedicina Molecular, realizada sob a orientação científica da Professora Doutora Sandra Vieira, Professora Auxiliar Convidada da Secção Autónoma de Ciências da Saúde da Universidade de Aveiro.

Este trabalho contou com o apoio do Centro de Biologia Celular (CBC) da Universidade de Aveiro, e é financiado por fundos FEDER através do Programa Operacional Factores de Competitividade – COMPETE e por Fundos nacionais da FCT – Fundação para a Ciência e a Tecnologia no âmbito dos projectos PTDC/QUI-BIQ/101317/2008, PTDC/SAL-NMC/111980/2009 e PEst-OE/SAU/UI0482/2011.

Dedicada aos meus pais pela educação, motivação, dedicação e apoio que me deram ao longo deste percurso.

o júri

presidente

Professora Doutora Ana Gabriela da Silva Cavaleiro Henriques
Prof. Auxiliar Convidada, Secção Autónoma de Ciências da Saúde,
Universidade de Aveiro

Professora Doutora Sandra Isabel Moreira Pinto Vieira
Prof. Auxiliar Convidada, Secção Autónoma de Ciências da Saúde,
Universidade de Aveiro

Professora Doutora Odete Abreu Beirão da Cruz e Silva
Prof. Auxiliar com Agregação, Secção Autónoma de Ciências da Saúde,
Universidade de Aveiro

Professora Doutora Catarina Lídia de Almeida Rodrigues Lemos
Professora auxiliar, Faculdade de Ciências da Saúde,
Universidade Fernando Pessoa

agradecimentos

À minha orientadora, Sandra Vieira, pela inspiração que para mim representa, pelo espírito científico e constante estimulação intelectual. É também de gratificar a sua dedicação, motivação e companheirismo, não só durante elaboração deste projeto científico mas durante todo o meu percurso como estudante universitária.

À professora Odete da Cruz e Silva, pela oportunidade de realizar este trabalho no laboratório de Neurociências do Centro de Biologia Celular.

A cada um dos colegas do Centro de Biologia Celular que sempre se disponibilizaram para ajudar e que, em algum momento do meu percurso, contribuíram com os seus conhecimentos, sempre demonstrando espírito de entreajuda. Um especial agradecimento à professora Margarida Fardilha pelo acolhimento e disponibilidade de ajuda nos procedimentos de YTH.

Aos 3 R's, Regina, Roberto, e Rocha, pela transmissão de conhecimentos, disponibilidade, hospitalidade e pelo agradável ambiente de trabalho proporcionado. Às mais recentes amigas do CBC, em especial à Gi, à Lili e à Pati, pelo reconforto nos momentos de maior angústia, mas principalmente pelos divertidos momentos de lazer.

Aos meus "companheiros de bancada", Patrícia, Ana, Sónia, João, Marta, Juliana, Luís e Emanuel, pela partilha de experiências e solidariedade. Um agradecimento especial à Catarina, a minha grande companheira de viagem, pela sincera amizade e cumplicidade.

Aos amigos de longa data, pela verdadeira amizade, motivação e momentos de descontração.

À minha família, pelo constante suporte, estabilidade e harmonia proporcionada no seio familiar, um importante contributo para o equilíbrio mental e emocional. Ao André pelo constante apoio, compreensão, companheirismo e por me incitar a desafiar-me a mim própria.

palavras-chave

Proteína Precursora de Amilóide de Alzheimer (PPA); Fator de Crescimento de Ligação à Heparina semelhante ao Fator de Crescimento Epidermal (HB-EGF); Fator de Crescimento Epidermal (EGF); sinalização da MAPK; sinalização da STAT3.

resumo

A Doença de Alzheimer (DA) é a doença neurodegenerativa mais prevalente a nível mundial, e a principal causa de demência na população sénior. O processamento anormal da Proteína Precursora de Amilóide de Alzheimer (PPA) e a produção aumentada do seu fragmento beta amilóide (Aβ) constituem eventos centrais na patogénese da DA, o que tem fomentado a investigação da PPA. Esta tem sido descrita como uma proteína envolvida em processos celulares determinantes, como adesão, migração, diferenciação, e sobrevivência celular. Como tal, devido à necessidade imperativa de caracterizar as suas funções biológicas, a investigação de proteínas que interagem com a PPA é de vital importância. Recentemente, diversas proteínas foram identificadas no nosso laboratório como putativos interatores da PPA, através da técnica de Yeast Two Hybrid (YTH). De entre estes, o fator de crescimento de ligação à heparina semelhante ao fator de crescimento epidermal (HB-EGF) revelou-se um interessante alvo de estudo.

O HB-EGF é um membro da família do fator de crescimento epidermal (EGF) com capacidade de ligação à heparina, que se destaca pelas suas capacidades de estimular o crescimento e diferenciação celulares, tendo sido proposto como um relevante fator trófico para o desenvolvimento e manutenção do sistema nervoso central (SNC). Na verdade, o HB-EGF é mais abundante no SNC do que o próprio EGF, o que sugere que o HB-EGF é o principal ligando neuronal para o recetor do EGF (EGFR). O HB-EGF é sintetizado como um precursor de 208 aminoácidos (pre-proHB-EGF), sendo exposto na membrana celular como um precursor transmembranar de 20-30 kDa, o proHB-EGF. Esta forma é subsequentemente proteoliticamente processada, gerando um péptido solúvel que é libertado para o meio extracelular (sHB-EGF). Curiosamente, o HB-EGF apresenta atividades biológicas parácrinas, autócrinas e justácrinas.

O presente trabalho teve como principal objetivo a validação da interação entre a PPA e o HB-EGF, primeiramente alcançado através da técnica de YTH, que revelou também que a interação entre as duas proteínas não é mediada pelo domínio intracelular da PPA. Esta interação foi subsequentemente confirmada por ensaios de GFP-Trap pull-down em cultura de células de mamífero, e a sua relevância fisiológica estudada através de estudos de co-localização e sinalização celulares, usando células HeLa transfectadas com os cDNAs da PPA e do HB-EGF. Apesar do papel funcional do complexo PPA/HB-EGF não ter sido determinado, os resultados obtidos sugerem que as duas proteínas interagem física e funcionalmente, influenciando a sinalização mediada por cada uma delas separadamente, como a ativação da via de sinalização MAPK que verificámos ser também induzida pela PPA. Adicionalmente, descrevemos uma nova interação proteica entre a PPA e uma forma precursora do EGF, e demonstrámos que a PPA atua de forma sinérgica com o EGF. Estes resultados levam a uma maior compreensão da biologia da PPA, uma proteína importante na fisiologia cerebral e na fisiopatologia da DA.

keywords

Alzheimer's Amyloid Precursor Protein (APP); Heparin-Binding EGF-like Growth Factor (HB-EGF); Epidermal Growth Factor (EGF); MAPK signaling; STAT3 signaling.

abstract

Alzheimer's disease (AD) is the most prevalent neurodegenerative disorder worldwide and the leading cause of dementia in the elderly. Abnormal processing of Alzheimer's amyloid precursor protein (APP) and increased generation of its amyloid beta (Aβ) fragment are central events in the AD pathogenesis, propelling major studies on APP biology. APP is thought to be involved in important processes such as cell adhesion, survival, migration and differentiation. Therefore, because of the imperative need to study APP biological functions, the search for APP-binding partners has stand out. Recently in our laboratory, a plethora of putative APP-binding proteins was unraveled through the use of the Yeast Two Hybrid (YTH) system. Among them, the heparin-binding epidermal growth factor-like growth factor (HB-EGF) has emerged as an interesting target of study.

HB-EGF is a heparin-binding member of the EGF family of growth factors that stimulates growth and differentiation. It has been purposed has an important trophic factor in the developing and adult central nervous system (CNS), being expressed at much higher levels than EGF in the CNS, which indicates that HB-EGF may serve as a major ligand for EGFR in neurons. HB-EGF is synthesized as a pre-pro-form of 208 amino acids in length and is expressed at the cell surface as a 20-30kDa type I transmembrane precursor, named proHB-EGF. This larger membrane-anchored precursor is then proteolytically processed, generating the mature soluble HB-EGF (sHB-EGF) that is released to the extracellular medium. Very interestingly, HB-EGF presents autocrine, paracrine and juxtacrine biological activities, with proHB-EGF evidencing unique biological characteristics distinct from sHB-EGF.

In the work here described, we first validated the APP/HB-EGF interaction by yeast co-transformation, and unraveled that the interaction is not mediated by the APP intracellular domain (AICD). We further confirmed it as an *in vivo* interaction by GFP-Trap pull-down assays and accessed the physiological relevance of this novel interaction through co-localization and signaling studies in HeLa cells transfected with the APP-GFP and HB-EGF cDNAs. Although the functional role of the APP/HB-EGF complex was not determined, results suggest that these proteins physically and functionally interact, having potential value in regulating each other signal pathways, with a role for APP in inducing the activation of the MAPK signaling being evidenced. In addition, a putative novel interaction with a proEGF species was also detected and APP was shown to act synergistically with EGF to activate the MAPK signaling. These results deepen our understanding of the APP biology, a crucial protein in cerebral physiology and AD pathophysiology.

Index

1 Abbreviations

AD	Alzheimer's disease
ADAM	A disintegrin and metalloprotease
Ade	Adenine
AICD	APP intracellular domain
APLP	APP-like protein
APP	Amyloid precursor protein
AR	Amphiregulin
Aβ	Amyloid beta-peptide
BCA	Bicinchoninic acid
Bcl-6	B cell lymphoma 6
BSA	Bovine Serum Albumin
BTC	Betacellulin
cDNA	Complementary deoxyribonucleic acid
CNS	Central nervous system
CSF	Cerebrospinal fluid
CTF	C-terminal fragment
DG	Dentate gyrus
DO	Dropout
DT	Difteria Toxin
DTR	Difteria Toxin Receptor
ECL	Enhanced chemiluminescence
EGF	Epidermal growth factor
EGFP	Enhanced Green Fluorescent Protein
EGFR	Epidermal Growth Factor Receptor
ER	Endoplasmic Reticulum
ErbB	Erythroblastic Leukemia Viral Oncogene Homolog
ERK	Extracellular signal regulated kinase
GAL4	Gal4 transcription factor
GAL4-AD	Gal4 activation domain
GAL4-BD	Gal4 DNA binding domain
GFLD	Growth factor-like domain
GFP	Green Fluorescent Protein
GPCRs	G-protein coupled receptors

HBD	Heparin binding domain
HB-EGF	Heparin-binding Epidermal Growth Factor-like Growth Factor
HB-EGF-C	HB-EGF cytoplasmic segment
HeLa	Henrietta Lacks immortalized cell line
His	Histidine
HSPG	Heparan sulfate proteoglycans
JM	Juxtamembrane
JNK	c-Jun N-terminal kinase
KPI	Kunitz protease inhibitor
LB	Loading Buffer
LB medium	Luria Bertani growth medium
Leu	Leucine
LGB	Lower Gel Buffer
LiAc	Lithium acetate
LPA	Lysophophatidic acid
MAPK	Mitogen-activated protein kinase
MDC9	Metalloprotease/disintegrin/cysteine-rich protein 9
MMP	Metalloproteinase
mRNA	Messenger ribonucleic acid
NE	Nuclear envelope
NFKB	Nuclear Factor-Kappa B
NRDc	N-arginine dibasic convertase
O/N	Overnight
OD	Optical Density
ORF	Open Reading Frame
PBS	Phosphate buffered saline
PI3K	Phosphatidylinositol 3-Kinase
PKC	Protein Kinase C
PLCγ	Gamma isoform of phospholipase C
PLZF	Promyelocytic leukaemia zinc finger protein
PM	Plasma Membrane
PMA	Phorbol-12-myristate-13-acetate
P-MAPK	Phosphorylated MAPK
PPIs	Protein-protein interactions

PS1 and PS2	Presenilin-1 and -2
P-STAT3	Phosphorylated STAT3
QDO	Quadruple Dropout
rpm	Rotation per minute
RT	Room Temperature
sAPP	Secreted APP
SD	Supplement dropout medium
SDS	Sodium dodecylsulfate
SDS-PAGE	Sodium dodecylsulfate - Polyacrilamide gel electrophoresis
SEM	Standard error of the mean
sHB-EGF	Secreted HB-EGF
SMC	Smooth muscle cells
STAT	Signal Transducer and Activator of Transcription
SVZ	Subventricular zone
TBS	Tris-buffered saline solution
TBS-T	TBS supplemented with Tween detergent
TDO	Triple Dropout
TEMED	Tetramethylethylenediamine
TGF-α	Transforming growth factor-α
TGN	Trans-Golgi-network
TM	Transmembrane
TPA	Phorbol ester 12-O-tetradecnoylphorbol-13-acetate
Trp	Tryptophan
UGB	Upper gel buffer
WB	Western Blot
YPD	Yeast Peptone Dextrose
YTH	Yeast Two Hybrid

2 Introduction

2.1 Alzheimer's disease (AD)

Alzheimer's disease (AD), first described by the neuropathologist Alois Alzheimer in 1906, is a slowly progressive disorder characterized by an insidious onset and progressive cognitive impairment, loss of memory, and abnormal behavior, leading to a vegetative state and ultimately death. AD has become the most common age related neurodegeneratation, accounting for 50-60% of the cases of dementia. It is generally sporadic, with a late-onset, affecting people over the age of 65. However, around 5% of AD patients develop the disease phenotype at a much younger age (40 to 50 years old) and are classified as early-onset, most of which being familial cases (1). These are mainly caused by missense mutations in the amyloid precursor protein (APP), and in presenilin-1 and -2 (PS1 and PS2) genes (2). Abnormal processing of APP and increased generation of the amyloid beta (Aβ) peptide are central events in the AD pathogenesis (3), but mutations and polymorphisms in multiple genes, along with non-genetic factors, are likely to contribute to sporadic AD pathogenesis (2).

2.1.1 Neuropathological phenotype

The major AD pathological hallmarks are the progressive deposition of protein fragments in senile plaques and the appearance of neurofibrillary tangles (1–4). The combined consequences of the pathological changes lead primarily to massive neuronal and synapse loss at specific brain regions involved in learning, memory and emotional behavioral, such as the hippocampus and cortex (5). These morphological alterations lead to AD characteristic changes, namely cortical atrophy and concomitant enlargement of ventricles and sulci, particularly in the frontal, temporal and parietal lobes (Figure 1).

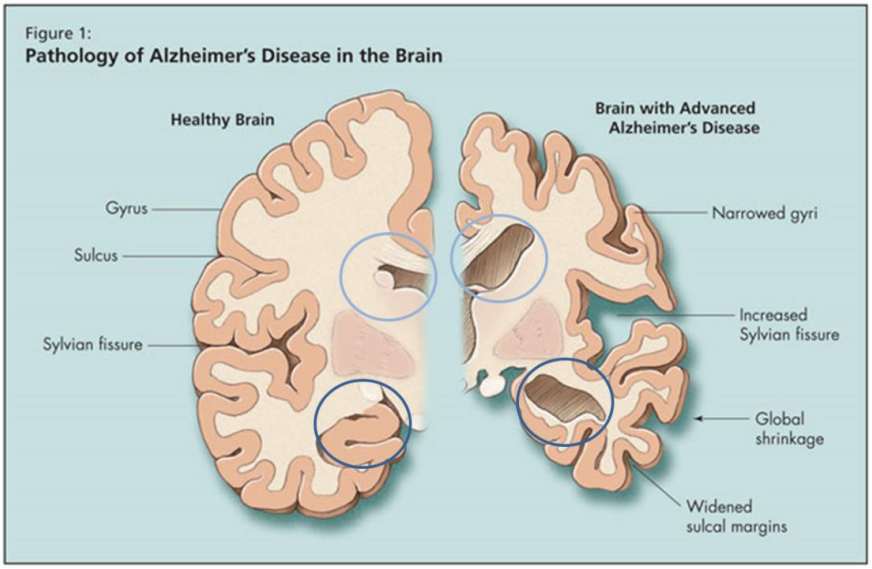

Figure 1 - Representation of a cross-section of brain coronal sections. Left: image of a healthy brain; right: Alzheimer's brain. Note the shrinkage particularly at the hippocampus (dark blue circles) and the widening of the ventricles (light blue circles). Adapted from http://www.healthplexus.net/article/neurobiology-aging (Jun 2013).

The senile/amyloid plaques are extracellular deposits of Aβ peptides, which are a product of the APP proteolytic cleavage (detailed in section 2.2.3). The Aβ peptides are organized in 7-10 nm-thick fibrils intermixed with non-fibrillar forms of the peptide. In addition, mature plaques (Figure 2) contain degenerating axons and dendrites, and are surrounded and invaded by microglia and reactive astrocytes, indicating an inflammatory component in the neurodegenerative process (3,5).

The neurofibrillary tangles are intraneuronal lesions consisting of 10-nm-thick paired helical filaments (Figure 2). The main component of these filaments is the hyperphosphorylated form of the microtubule-associated protein Tau. Tau hyperphosphorylation favours its dissociation from microtubules and stimulates its self-assembly into paired helical filaments that in turn assemble into neurofibrillary tangles (3,5).

2.1.2 The amyloid cascade hypothesis

The amyloid hypothesis states that overproduction of Aβ caused by the imbalance between the production and clearance of Aβ in the brain, and its aggregation into senile plaques is a primary event in AD pathogenesis, triggering an inflammatory response, synapse loss, neuronal dysfunction, cell death, and gradual cognitive decline (Figure 2) (2,5–8). Although the extracellular accumulation of insoluble fibrillar Aβ was previously considered a key causative element in AD, recent evidence suggests that soluble Aβ oligomers, which are

the precursors of the fibrils, are the actual neurotoxic components contributing to neurodegeneration and consequently dementia (2,5,6).

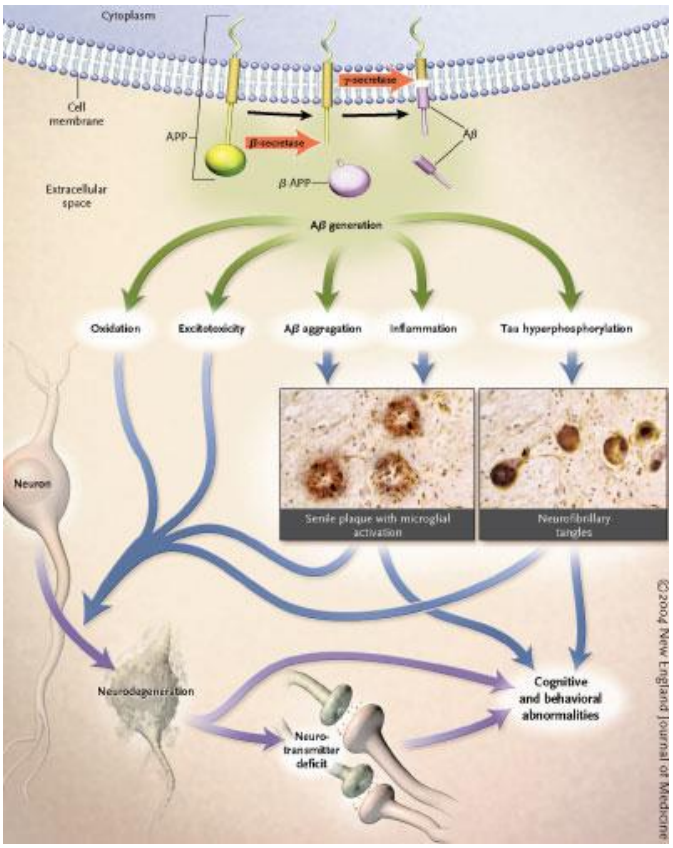

Figure 2 - The putative amyloid cascade, which is still controversial in some of the correlations it defends, states that Aβ generation induces a set of detrimental mechanisms known to be involved in AD pathogenesis, and ultimately leads to the cognitive and behavioral abnormalities observed in AD patients. Reproduced from reference (9).

The amyloid hypothesis generated several predictions that have been the basis for most work on the AD pathogenesis and on researching for a biomarkers-based diagnosis. Nonetheless, several of its predictions are still controversial. Therefore, understanding the normal physiological APP functions remains an issue of major scientific and clinical interest.

2.2 Alzheimer's β-amyloid precursor protein (APP)

As mentioned, the Aβ peptide was found to be a cleavage product derived from the transmembrane domain of a large precursor protein, APP. For that reason, APP has become one of the most studied proteins in the field of AD research (1), and after more than 15 years of intense research, understanding it remains a major scientific and intellectual challenge.

When studying APP (or its homologs) in cell cultures, many researchers have focused on specific fragments and/ or subdomains of APP, to which several functions have been attributed (10). Briefly, APP is thought to be involved in important processes such as cell adhesion, synaptic contact, cell survival, neurite outgrowth, cell migration and differentiation, and in memory regulation (7). APP has also been implied in protease inhibition (11) and in pro- and anti-apoptotic functions (3). The APP protein, as well as the plethora of functions correlated to it, will be further described below.

2.2.1 APP characterization and gene family

In mammalian, APP is part of a larger gene family that includes APP-like proteins 1 and 2 (APLP1 and APLP2) (1,3,12–14). APP is a ubiquitously expressed type I transmembrane glycoprotein (1–3,12,13,15,16), present in many cell and tissue types, including astrocytes, microglia, endothelial cells, smooth muscle cells and all peripheral cells; however, it is detected predominantly in neurons (2,11,17,18). It is encoded by a single gene located on chromosome 21 (21q21) that contains 18 exons, of which exons 7, 8 and 15 can be alternatively spliced (1–3,12,13,15,18). Alternate splicing of the APP transcript generates 8 isoforms, ranging from 365 to 770 amino acids (11,12,15). Among the 8 APP isoforms, the predominant transcripts are APP695 (exons 1–6, 9–18), whose encoding cDNA lacks the gene sequence from exons 7 and 8, APP751 (exons 1–7, 9–18) lacking exon 8, and APP770, encoded with all exons (Figure 3).

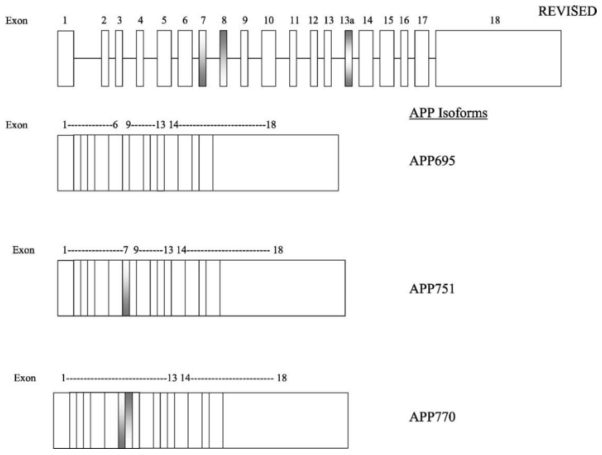

Figure 3 - Schematic representation of the APP gene and its three major isoforms. The human APP gene contains 19 exons. Alternative splicing produces the three major isoforms shown. The relative sizes of exons and introns are not drawn to scale. Reproduced from reference (2).

The three transcripts encode multidomain proteins with a single membrane-spanning region and differ only in the size of their extracellular sequence. APP isoforms are expressed in

a cell-type specific manner, with APP695 being the predominantly transcript in neuronal tissue, whereas APP751 and APP770 are mainly expressed in non-neuronal cells, such as brain glial cells (1,2,4,5,11–14,19). Each isoform exists in immature (N-glycosylated) and mature (sulfated, N- and O-glycosylated) forms (20). Aβ is derived from the region of the protein encoded by parts of exons 16 and 17 (2).

As illustrated in Figure 4, the APP protein is composed of a large glycosylated extracellular portion, a hydrophobic transmembrane domain, and a short C-terminal cytoplasmic domain, referred to as the APP intracellular domain (AICD) (1–3,10,12).

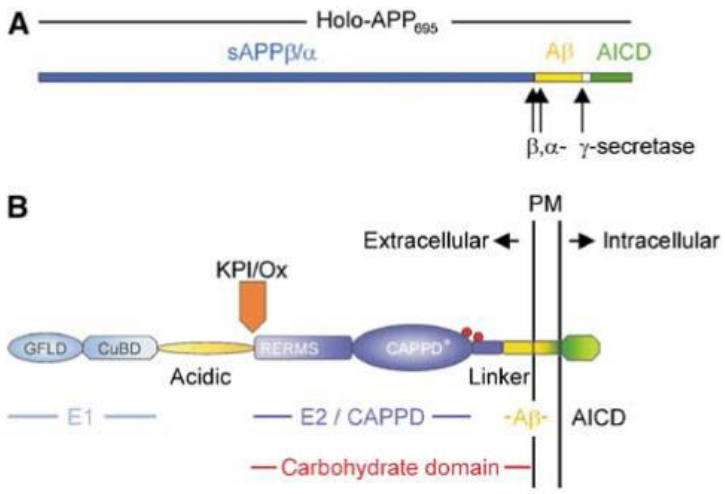

Figure 4 - (A) Schematic representation of the human APP695 holoprotein, including the relative position of the α-, β- and γ-secretase cleavage sites. (B) Schematic representation of the functional domains arrangement in APP: the E1 region consists of the N-terminal growth factor-like domain (GFLD) and the following copper-binding domain (CuBD). The E1 region is linked via the acidic region to the carbohydrate domain, which contains the two N-glycosylation sites of the ectodomain (red spheres). The carbohydrate domain can be subdivided into the E2 domain, also called central APP domain (CAPPD), and a linker or juxtamembrane domain. The carbohydrate domain is followed by the transmembrane and the APP intracellular domain (AICD). Aβ indicates the amyloid β-peptide sequence. The Kunitz-type protease inhibitor domain (KPI), which is present in APP751 and APP770, and the Ox2 sequence, which is present in APP770, are shown above their insertion site. Adapted from reference (10).

The APP extracellular sequence (or ectodomain) can be regarded as a string of several individual functional domains (Figure 4). The APP N-terminal head (a.a. residues 23–128) starts with a 17- residue signal peptide and is followed by the E1 domain, which contains: a growth factor-like domain (GFLD), a copper-binding domain (CuBD) and a zinc-binding motif (10,13). The GFLD is a cysteine-rich domain that constitutes one of the APP heparin-binding sites, and seems to be critical for neurite outgrowth and MAP kinase activation (10,21). Immediately

adjacent to this, is a hydrophobic surface patch; such patches are quite often key players in protein–protein interactions, and may provide a ligand binding site and/or an APP–APP dimerization interface (10,22). CuBD, comprising residues 124–189, may regulate APP proteolysis or act as a metallotransporter; copper binding to this domain affects the APP dimerization state, leading to lower Aβ production (21). Zinc-metal binding to APP modifies its conformation and interferes with APP binding to extracellular matrix components (3).

The N-terminal APP domain (E1 plus acidic) is able to stimulate neurite outgrowth, and is similar to a region identified in a couple of growth factors; thus, some authors suggest that this head domain by itself is responsible for the APP growth factor-like properties (10).

The acidic region precedes the Kunitz protease inhibitor (KPI) domain that is missing in APP695, and an OX2 domain, only present in APP770. The KPI motif has the ability to inhibit serine proteases such as trypsin, chymotrypsin and factors XIa and IXa of the coagulation cascade, functioning in blood coagulation. KPI-containing APP isoforms seem to be more amyloidogenic and their abundance increases in AD brains (1,2). Following the KPI motif, there is a carbohydrate domain, which can be divided into the E2 domain [also called central APP domain (CAPPD)], and the linker (or juxtamembrane) region. The E2 domain is also interesting, since it contains a couple of substructures that might provide interaction sites for binding partners (10). Importantly, the E2 domain possesses a putative growth-promoting motif called "RERMS" (3,10,13,21), and a highly conserved heparan sulfate proteoglycan (HSPG)-binding site. The E2 domain of APP is also able to form an antiparallel dimer in solution. Dimerization and dissociation of APP might regulate various APP functions. It has been hypothesized that cell-bound APP form dimers in trans-regulating cell–cell adhesion, whereas monomeric APP may act either as a growth factor receptor, when still bound to the cell membrane, or as a growth factor itself once it is released by α-secretase cleavage into the external milieu (10). Moreover, the strong homology and conserved domain organization between APP and the APP family members APLP1 and APLP2, imply that not only homo-oligomerization but also hetero-oligomerization might be possible, as demonstrated recently (10,22). Dynamic alterations of the APP ectodomain between monomeric, homodimeric and heterodimeric status could at least partially explain some of the variety in the functions of APP.

The Aβ domain comprises the 28 residues just outside the membrane plus the first 12-14 residues of the single membrane-spanning domain (TM). It contains additionally zinc, cooper and heparin binding sites, and a RHDS motif (amino acids 5-8 of Aβ) that appears to promote cell adhesion.

Near to its C-terminal region, APP has one 23-residue hydrophobic stretch that serves to anchor APP to internal membranes (e.g. ER, Golgi, trans-Golgi network and endosome) and

to the plasmalemma (4). Furthermore, the cytoplasmic region of APP, named APP Intracellular C-terminal domain (AICD) contains several consensus motifs (e.g. the YTSI and the YENPTY protein-sorting domains) that regulate its trafficking, and appears to have a role in signal transduction through interaction with several proteins (3,10,23,24). When liberated by proteolytic cleavage, AICD can be nuclear targeted and form protein complexes with transactivating properties (23,25).

The two mammalian APP homologs, APLP1 and APLP2, are also transmembrane proteins and share conserved structures with APP, including a large extracellular domain containing the E1 and E2 domains and a short intracellular domain (Figure 5). Although these three proteins are functional and structurally related, only APP generates the amyloidogenic fragment Aβ, since the transmembrane domain is not conserved among APP and APLPs (1–3,12–15). In addition, APLP1 does not possess the KPI domain (Figure 5) (1,12,13). Similarly to APP, APLP2 is expressed ubiquitously, while APLP1 is only expressed in the brain and is only found in mammals (1,12,13). However, given the sequence identity between the three genes, it is not unexpected that the mammalian APP homologs play redundant activities *in vivo* (13).

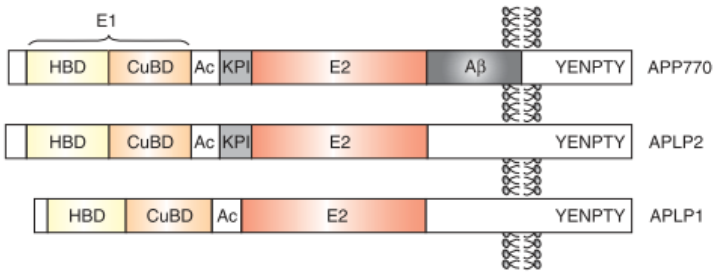

Figure 5 - Schematic overview of domain structure of APP family proteins. All APP family members share conserved E1 and E2 extracellular domains, an acidic domain (Ac) and the YENPTY motif in the carboxyl terminus. Note that Aβ is unique for APP. HBD, Heparin binding domain; CuBD, Copper binding domain; KPI, Kunitz-type protease inhibitor domain. Adapted from reference (26).

2.2.2 APP intracellular trafficking

APP is a transmembrane protein that is dynamically sorted through the membranes of intracellular organelles and the plasma membrane (PM) (23). APP traffic (Figure 6) is tightly regulated and during this process APP can be cleaved by specific proteases. APP is co-translationally translocated into the endoplasmic reticulum (ER) via its signal peptide, and then post-translationally modified ("matured") and trafficked through the Golgi apparatus to the trans-Golgi-network (TGN) and to the cell surface, via the secretory pathway. Classical N- and O-glycosylation occur during transit through the ER and Golgi. Phosphorylation and tyrosine sulfation in the late Golgi and at the cell surface further increases the structural complexity of

APP and APP-like proteins (3,4,7,11,13,14,16,27). APP is indeed a phosphoprotein with several putative phosphorylation sites in both the intracellular and extracellular domains, and APP phosphorylation plays an important role in regulating APP trafficking and processing (19).

In neurons, APP is subjected to the constitutive secretory pathway and after sorting in the Golgi it undergoes fast axonal transport to presynaptic terminals (12,28). However, only a small portion of APP is localized to the PM, most of it remaining in the Golgi, where the highest concentration of APP is found at steady state (7,13). From the TGN, APP can be transported in TGN-derived secretory vesicles to the PM, or be directly to an endosomal compartment (Figure 6, step 1). Clathrin-associated vesicles mediate both these steps. In the PM, where α-secretase is present, APP can either undergo non-amyloidogenic processing or be re-internalized by endocytosis, via its YENPTY motif (Figure 6, step 2). Once endocytosed, APP can be processed in the endosomal-lysosomal pathway. From late endosomes, APP can either be degraded in lysosomes or recycled by vesicles back to the PM or to the TGN (Figure 6, step 3). APP comes in contact with BACE1 in the endosome and the TGN, which promotes its amyloidogenic processing and subsequent Aβ generation (7,11,12,14,16,23,27,28). Aβ is either then dumped into the extracellular space, following vesicle recycling, or is degraded in lysosomes (12). The endocytosis process is determinant for Aβ generation, as 80% of Aβ release is blocked by preventing surface endocytosis (12). Although most APP must pass through the cell surface as part of its processing, this step is very rapid, and few APP is on the surface at a given time point (estimated half-life for surface-expressed APP is less than ten minutes) (3,12). Why some surface APP is internalized into endosomes and some proteolyzed directly by α-secretase is unclear. Finally, to complete the APP cycling loop, retrograde transport occurs between endosomes and the TGN, mediated by a complex of molecules called the Retromer (12,27).

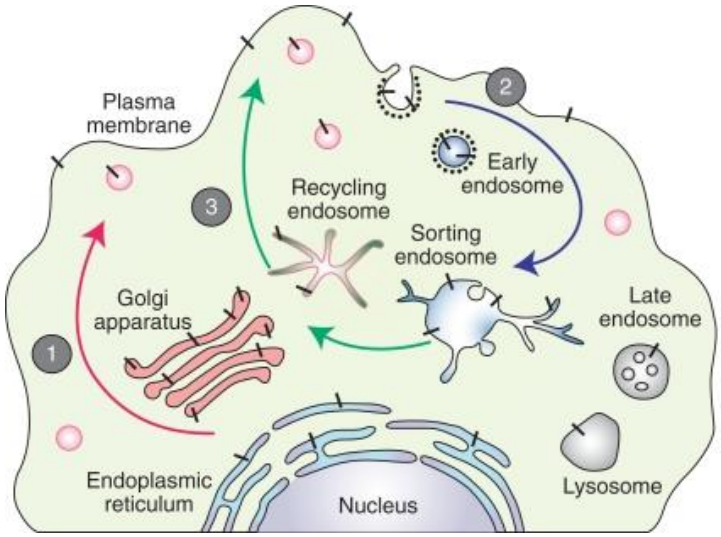

Figure 6- Intracellular APP trafficking. Nascent APP molecules (black bars) mature through the constitutive secretory pathway (step 1). Once APP reaches the cell surface, it is rapidly internalized (step 2) and subsequently trafficked through endocytic and recycling compartments back to the cell surface (step 3) or to the TGN. A small fraction is also degraded in the lysosome. Nonamyloidogenic processing mainly occurs at the cell surface where α-secretases are present. Amyloidogenic processing involves transit through the endocytic organelles where APP encounters β- and γ-secretases. Reproduced from reference (29).

Concerning the complexes involved in APP transport, the NPXY (asparagiNe-Proline-any-tYrosine) amino acid motif (YENPTY domain) governs the targeting of proteins to clathrin-coated vesicles (12,23,24). Several proteins, including members of the Fe65 and of the X11 families have been identified as clathrin adaptor proteins mediating the binding of the APP NPXY motif to clathrin coats, and therefore acting as regulators of APP endocytosis (11,23,30).

2.2.3 APP proteolytic processing

As described above, APP undergoes proteolysis both during and after its trafficking through the constitutive secretory pathway (4,13). APP proteolytic processing is a very important physiological process, since it generates several fragments that are actually biologically active peptides, as it will be further discussed.

The full-length APP is sequentially processed by at least three proteases termed α-, β- and γ-secretases, via two major mutually exclusive pathways (Figure 7). β- and α-cleavage sites are located close to the membrane region, between residues 596 and 597 of APP695. γ-cleavage site is located within the transmembrane domain, between residues 711-712 or 713-714. The α- and β-cleavages are mutually exclusive events, defining the processing pathway that APP undergoes.

In the **Nonamyloidogenic Pathway**, APP is sequentially cleaved by α-secretase and γ-secretase. α-cleavage occurs at the Lys_{16}–Leu_{17} bond within the Aβ peptide sequence (Fig. 1), releasing a large soluble N-terminal fragment (sAPP-α) and a membrane-bound C-terminal fragment (CTF) consisting of 83 amino acids (C83). The 10kDa C83 is further cleaved by γ-secretase (a complex whose catalytic component are presenilins) to release a non-pathogenic p3 peptide (3 kDa product) and the AICD, both of which are degraded rapidly (1–4,6,12,13). In the **Amyloidogenic Pathway**, APP is primarily processed by β-secretase at the first residue (β-cleavage site) or at the 11th residue (so called β' site) of the Aβ peptide sequence, yielding soluble sAPP-β and generating a membrane-tethered CTF consisting of 99 amino acids (C99). γ-secretase further cleaves the 12kDa C99 to release AICD and the 4kDa Aβ peptide (1–4,6,12,13,24). Figure 7 is a schematic representation of the APP cleavage sites and its proteolytic products. Aβ is indeed a normal soluble cellular metabolite comprising two predominant forms with different COOH-termini length, Aβ40 and Aβ42. Of note, comparable levels of Aβ are detected in both cerebrospinal fluid and plasma in sporadic AD and healthy subjects throughout life, and intracellular Aβ40 is innocuous (2).

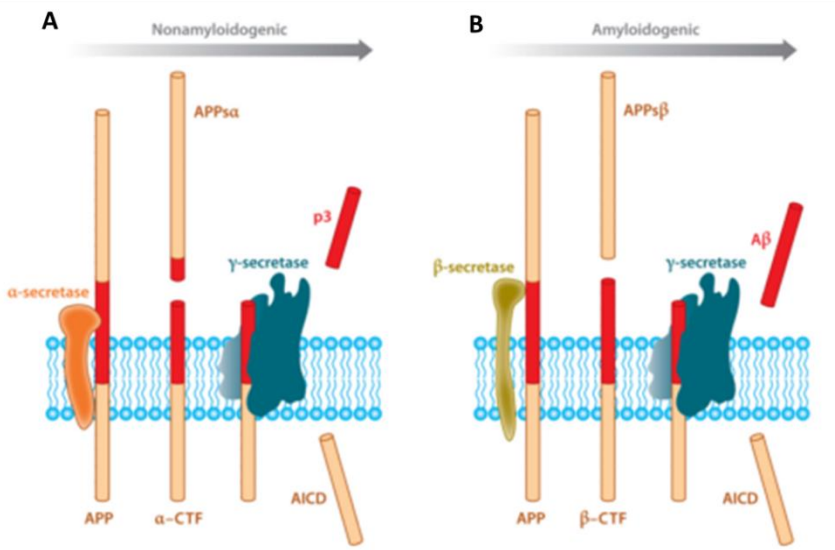

Figure 7- Schematic Diagram of APP proteolytic processing and its metabolic derivatives. (b) Nonamyloidogenic processing of APP involving α-secretase followed by γ-secretase cleavage. (c) Amyloidogenic processing of APP involving BACE1 followed by γ-secretase is shown. Both processes generate soluble ectodomains (sAPPα and sAPPβ) and identical intracellular C-terminal fragments (AICD). Adapted from reference (12).

2.2.4 Functions of APP and its fragments

2.2.4.1 Full-length APP

The *in vivo* gain- and loss-of-function phenotypes associated with the APP family of proteins in model systems are consistent with a role for APP in the development of the peripheral and central nervous systems, relating to synapse structure and function, as well as in neuronal migration or adhesion. These may be mediated either by the full-length protein or by its proteolytic products (13). Indeed, the search for a physiological role of full length APP is inseparably linked to the functions of APP cleavage products (6).

Cell Surface Receptor. Mainly due to its highly similar structure to Notch, APP has been proposed to function as a cell surface receptor (13). Studies have reported that certain ligands, including Aβ, F-spondin, Nogo-66, netrin-1 and BRI2, bind to the extracellular domain of APP, resulting in modulated APP processing and sequential downstream signals (1,3,13). However, it is unclear whether any of the candidates are *bona fide* ligands and definitive evidence supporting a physiological role of APP as a cell surface receptor is still lacking (13).

Cell and Synaptic Adhesion. APP is widely accepted as a protein contributor to cell adhesion via its extracellular domain. The E1 and E2 regions of APP were reported to interact with extracellular matrix proteins and heparin sulfate proteoglycans, supporting its role in cell-substratum adhesion. For example, APP co-localizes with integrins on the surface of axons and at sites of adhesion, and it was recently shown that APP and integrin-β1 do interact (13). Furthermore, the E1 and E2 regions were found also to interact with themselves, in parallel or anti-parallel, forming homo- (with APP) or hetero-dimers (with APLPs), with the trans-dimerization promoting cell-cell adhesion (1,13,22). Further, heparin binding to the E1 or E2 regions was reported to induce APP dimerization (13). Of note, recent studies suggest that homodimerization can be also promoted by the GxxxG motif near the luminal face of the membrane (13). The “RHDS” tetra-peptide motif between the sAPP C-terminus and the Aβ sequence also appears to promote cell adhesion (13). Recent studies in which trans-cellular APP/APLP interaction induced presynaptic specializations in co-cultured neurons, also suggest APP/APLPs as synaptic adhesion molecules (SAM) (1,13,31). Both the extracellular and intracellular domains of APP are required to mediate the synaptogenic activity (13,31).

2.2.4.2 APP Ectodomain - sAPPα

Synaptotrophic and Neuroprotective Functions. In most studies, APP overexpression shows a positive effect on cell health and growth, functions that can be reproduced by the soluble ectodomain, which is released by APP cleavage. sAPP has been shown to modulate cell

growth, motility, neurite outgrowth, and cell survival (12). Interestingly, sAPP-α alone is able to rescue most of the abnormalities of APP deficient mice, implying that most of the physiological functions of APP are conducted by its extracellular domain (1,6).

The constitutively secreted sAPP-α is neuroprotective, protecting neurons against oxygen-glucose deprivation and excitotoxicity (1,6,12,24). Several lines of evidence point also to a neurotrophic role, a function that may be related to APP adhesive properties described above, either in its full-length form or as a secreted molecule (sAPP). Thus, APP may exert these activities in both autocrine and paracrine fashions, the later via sAPP-α (13).

sAPP-α acts as a growth factor in dividing cells of epithelial origin, and regulates the proliferation of embryonic and adult neural stem cells (1,3,6,12,13). The RERMS sequence of APP is the region that appears to have growth-promoting properties (3). sAPP-α was also shown to promote neurite outgrowth, synaptogenesis as well as cell adhesion (1,6,12,13,24). sAPP promotes neurite outgrowth in neural stem cells, in a function where APLP2 (but not APLP1) was redundant (13). The biologically relevant sites for these actions appears to be the APP two heparin-binding domains (6,12). *In vivo* studies also shown that sAPP-α can improve cognitive function and synaptic density in animal models, promoting learning and memory (1,6,13). Because sAPP levels have been reported to be reduced in individuals with AD, the loss of its trophic activity and pro-survival mechanisms may contribute, at least in part, to the AD neurodegeneration (13).

2.2.4.3 APP Ectodomain - sAPPβ

Axonal Pruning and Degeneration. Although there are only 17 amino acids difference between sAPPβ and sAPPα, sAPPβ lacks most of the synaptotrophic and neuroprotective effects that have been associated with sAPPα. A recent study suggested that sAPP-β can be cleaved to generate an N-terminal fragment that is a ligand for the Death Receptor 6 (DR6), activating caspase 6, which further stimulates axonal pruning and neuronal cell death (Figure 8) (1,6,13).

2.2.4.4 APP Ectodomain - Aβ

Aβ is secreted constitutively by normal cells in culture and detected as a circulating peptide in the plasma and cerebrospinal fluid (CSF) of healthy humans and other mammals (4). The physiological and pathological functions of Aβ have been extensively investigated because of its central role in AD. Studies have demonstrated that Aβ overproduction results in a neurodegenerative cascade leading to synaptic dysfunction, neuronal tangle formation and eventually neuron loss in the pathologically affected brain regions. Among the various Aβ

peptides generated by the multiple-site cleavages of secretases, Aβ42 is the most toxic specie, being more hydrophobic and amyloidogenic. Most mutations related to hereditary familiar AD either increase Aβ generation or the ratio of Aβ 42/ Aβ 40 (1,6,14), suggesting that elevated levels of Aβ42 relative to Aβ40 is critical for AD pathogenesis (1,14). In AD patients Aβ42 levels in the CSF are reduced, which reflects the reduced clearance of Aβ through the CSF and increased accumulation in amyloid plaques (6).

Although excessive Aβ causes neurotoxicity, some studies have shown that Aβ40 protects neurons against Aβ 42-induced neuronal damage and is required for the viability of central neurons (1). Moreover, it has been showed that the Aβ peptide itself plays an important role in synaptic physiology, regulating synaptic scaling and synaptic vesicle release (12). In addition, two groups recently reported that low doses of Aβ can positively modulate synaptic plasticity and memory by increasing long-term potentiation, revealing a novel physiological function of Aβ under normal conditions (1,14).

2.2.4.5 APP Intracellular Domain

The high degree of sequence conservation between the intracellular domains of APP proteins predicts that it is a critical domain mediating APP function. Indeed, this relatively short cytoplasmic domain contains phosphorylation sites as well as multiple functional motifs and multiple binding partners that contribute to trafficking, metabolism, and possibly cell signaling functions of APP (13).

Phosphorylation and Protein-Protein Interaction. Depending on the exact cleavage site of γ-secretase, AICD may have 59, 57, 53 or 50 residues. However, because AICD is quickly degraded after γ-cleavage, the biochemical features and physiological functions of AICD *in vivo* are difficult to study. There are several conserved regions located on AICD: a YTSI (653–656 residues) sorting motif near the cell membrane, a VTPEER (667–762 residues) helix capping box and a YENPTY (682–687 residues) motif that regulates APP trafficking and mediates the interaction between APP/AICD and phosphotyrosine-binding domain containing proteins (1). The YENPTY domain regulates clathrin-coated pit internalization through a series of binding partners. Mutation at this site alters endocytosis of APP and diminishes Aβ production (12). Some of the AICD-binding proteins identified, including kinesin light chain (KLC), Fe65, Shc, JNK-interacting protein (JIP), Numb, X11, Clathrin and mDab1, were found to share one or several common phosphotyrosine-binding domains that specifically interact with this YENPTY motif (1,13). Other proteins, such as protein interacting with APP tail 1 (PAT1), suppressor of variegation, enhancer of zeste, Trithorax (SET) and 14-3-3c, are believed to bind to the YTSI or

VTPEER motif of AICD (3). AICD, therefore, may have different functions when interacting with its' various binding partners (1).

AICD also contains three phosphorylation sites, including two threonine residues at 654 and 668 and a serine residue at 665. AICD has been found to be phosphorylated by PKC, calcium-calmodulin dependent-kinase II, GSK3-b, Cdk5 and c-Jun N-terminal kinase (JNK) at the Ser/Thr sites mentioned above, which may affect APP localization, conformation, processing or the binding of AICD-interacting proteins, thus affecting the function of AICD (1,12,13).

Cell Signaling. The generation of AICD is very similar to that of many other signaling molecules, such as NICD, which is also generated by γ-cleavage, is translocated to the nucleus and mediates gene transcription important for development. AICD seems to function in a similar fashion, with a role for AICD in gene transactivation being supported by several studies. The most widely accepted mechanism is that AICD, together with Fe65 and Tip60, forms a transcriptionally-active complex. Fe65, a cytoplasmic adaptor protein, binds to the YENPTY motif of AICD and mediates an indirect interaction between AICD and the histone acetyltransferase Tip60, stabilizing AICD. This complex regulates the expression of genes such as KAI1, Neprilysin, LRP1, p53, GSK-3β, EGFR, and APP itself (1–3,6,7,12,13). In addition, cellular Ca2+ homeostasis is modulated by AICD-induced mediated transcription (1,13).

Apoptosis. Many studies have documented that AICD is cytotoxic and that over-expressing different AICDs (C31, C57, C59) in Hela, H4, N2a or PC12 cell lines, as well as neuronal cell lines, induces cell death (1,13,32). Results indicate that this AICD-induced cytotoxicity may be mediated by its interacting proteins or by its target genes such as GSK-3β. However, C31, a short form of AICD generated by caspase cleavage, has been reported to directly activate caspase 3 in the tumor cell death process (1,13,32). C31 also appears to induce a caspase-independent toxicity by selectively increasing Aβ42.

Figure 8 summarizes some of the functions attributed to APP proteolytic fragments.

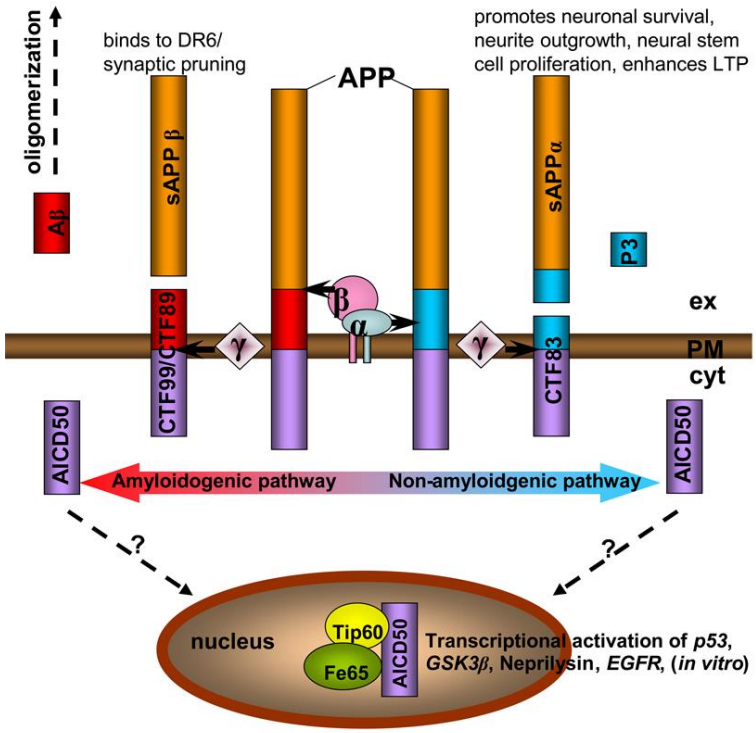

Figure 8 - Schematic representation of the correlation between APP processing metabolic derivatives and some of their functions. ex, extracellular; PM, plasma membrane; cyt, cytosol. Reproduced from reference (6).

2.2.5 APP-binding proteins

A very useful way to approach APP function, besides addressing its functional domains and motifs, is the identification of its protein binding partners (10). Protein-protein interactions (PPIs) are fundamental to all cellular processes and they are often very useful to infer the function of a target protein.

APP can actually bind to a large number of proteins (Table 1). Proteins that were reported to bind APP, but are also known to be quite generally involved in protein processes such as maturation or endocytosis, were not included in the overview.

Table 1 - Various protein interactions and functions of APP.

Function		APP Domain	Binding Partners
Surface Receptor		CAPPD	F-spondin
		Aβ, undefined	ApoE
		Undefined	Aβ
Adhesion molecule	**Cell/substratum**	Undefined, Aβ	ECM (laminin, collagen, etc)
		E1 (GFLD)	Fibulin-1
		E1, E2	HSPG
		AICD	Fe65
	Cell/cell	CAPPD	CAPPD
		E1	E1
Regulator of neuronal processes	**Neurite outgrowth**	sAPP	APP/Integrin? MAPK?
		Aβ	Undefined
	Dendritic arborization	CAPPD	Undefined
		AICD (C99)	Abl, profiling, JIP
	Synaptogenesis	sAPP	Undefined
		Undefined, AICD	Fasciclin II, X11/Mint
	Synaptic plasticity	sAPP	Undefined
	Neuronal excitability	sAPP	Undefined
	Axonal transport cargo receptor	AICD	JIP
	Regulator of neuronal stem cell division	sAPP	Undefined
Signaling molecule	**GPCR signaling pathway**	AICD	G(o)
	Kinase-mediated signaling cascades	AICD	Abl, Shc/Grb2, JIP, Dab
		sAPP	MAPK, STAT3, NFkB
	Gene transcription	AICD	Fe65, Fe65L, JIP, Mint/X11, Numb
Regulator of calcium homeostasis		Aβ, undefined	Undefined
		AICD	Undefined
Regulator of metal homeostasis		CuBD	Cu^{2+}
Regulator of cell survival/death	**Neurotrophic**	sAPP	Undefined
	Neurotoxic	Aβ	Undefined, APP
		AICD casp (C31)	Caspases, APP-BP1
		AICD (C59, C57)	Undefined
		AICD (a.a. 649-664)	Undefined

ECM, extracellular matrix; HBD, heparin-binding domain; HSPG, heparin sulfate proteoglycans; SVZ, subventricular zone

It is interesting to note that many of the proposed functions of APP (Table 1) and its derived fragments can be grouped into a series of common biological processes. For example, neurite outgrowth, dendritic arborization and synaptogenesis all require highly organized cell–cell and cell–substratum interactions, to which APP indeed appears to contribute. From the table, it also becomes clear that both the extra- and intracellular APP regions are involved in

similar biological functions, like neurite outgrowth or arborization. It is tempting to speculate that holoAPP could function in these processes at both sides of the plasma membrane linking extracellular cues (e.g. ligand or substratum binding) to intracellular signaling pathways (via scaffolding proteins, Ca^{2+} regulation, interactions with the cytoskeleton and/or protein kinases). In this context, APP could function as a receptor-like modulatory protein in neuronal processes (10).

Because of the imperative need to study in detail the APP proteome and better characterize APP functions, the search for APP-binding proteins has stand out in the laboratory. In a previous doctoral thesis developed at our laboratory, Dr. Sara Domingues has unraveled a plethora of putative APP-binding proteins, through the use of the Yeast Two Hybrid system in a brain cDNA library. The heparin-binding epidermal growth factor-like growth factor (HB-EGF) has emerged as a very interesting target of study. Among the known factors that regulate proliferation and neuronal generation, growth factors have been widely accepted as the most important mediators, which supported HB-EGF as our object of study. Additionally, several structural and functional features are shared between APP and HB-EGF proteins, which really made HB-EGF stand out. Of note, the identification of growth factor receptors binding to APP would also greatly support the growth factor hypothesis for APP.

2.3 Heparin-Binding Epidermal Growth Factor-Like Growth Factor (HB-EGF)

2.3.1 Membrane-anchored growth factors

Growth factors, a diverse group of polypeptides that regulate diverse processes from cell survival and proliferation to migration and programmed cell death, constitute a distinct subgroup in endocrinology (33–35). The biology of these factors differs somewhat from classical hormones as neither their site(s) of synthesis nor site(s) of action is restricted to defined tissues. Many growth factors probably operate in a paracrine fashion, binding to receptors in distant cells of the same tissue and, in certain instances, their action may be autocrine in nature, binding to receptors on the same cell (33).

Recent studies revealed that several growth factors and cytokines are synthesized as membrane-anchored proteins, and that such membrane-anchored forms are not only the precursor forms of soluble factors but also biological active molecules. The epidermal growth factor (EGF) family of growth factors, tumor-necrosis factor-α (TNF-α) and the colony-stimulating factor-1 are examples of ligands that are synthesized as membrane-anchored forms (36). Interestingly, the membrane-anchored forms have different biological activity from their soluble counterparts. In fact, membrane-anchored growth factors present distinct and unique features respecting their modes of action comparing to those of the soluble growth factors in the following respects: (1) The membrane-anchored forms do not diffuse in fluids and thus, they act in a juxtacrine manner (i.e. through cell-cell contact) to signal neighboring cells. (2) Membrane-anchored growth factors can form a complex with other membrane proteins, and their activity can be regulated by associating molecules, as shown by proHB-EGF-associating CD9 (mentioned later). (3) In addition, bidirectional signaling between membrane-anchored growth factors and their receptors is also plausible (36).

2.3.2 The Epidermal Growth Factor (EGF) family and their receptors

Epidermal Growth Factor (EGF) is the founding member of the EGF superfamily of peptide growth and differentiation factors. Members of this group include EGF, HB-EGF, transforming growth factor-α (TGF-α), vaccinia growth factor (VGF), amphiregulin (AR), betacellulin (BTC), epiregulin, neuregulin-1 (NRG-1) - including the Neu differentiation factor (NDF), heregulin (HRG), acetylcholine receptor-inducing activity (ARIA), and glial growth factor (GGF) - and neuregulin-2 (NRG-2) (37).

Members of this protein family have highly similar structural and functional characteristics. These ligands have in common a motif of about 40–45 amino acids containing six cysteine residues, known as the EGF-like domain. The highly conserved six cysteine-residues of the EGF-domain form the consensus sequence $CX_7CX_4CX_{10}CXCX_8C$, with the six cysteine residues forming three intra-molecular disulfide bonds (C_1–C_3, C_2–C_4, C_5–C_6) (37). Another common feature of the EGF-family members is that they are synthesized as transmembrane precursor molecules which are then proteolytically processed to release the soluble mature growth factor from the cell surface (37). Besides these similarities, high binding affinity to their receptors and production of mitogenic responses in EGF-sensitive cells are also characteristic of the EGF-family members (33,35).

The EGF-like growth factors achieve their effects by binding to and activating ErbB (Erythroblastic Leukemia Viral Oncogene Homolog) receptor tyrosine kinases. The ErbB receptors are class I transmembrane proteins and represent a subfamily of four closely related receptor tyrosine kinases: the EGF receptor (EGFR) also known as HER1/erbB1, HER2/erbB2 also known as p185/neu, and more recently HER3/erbB3 and HER4/erbB4 (37–39). The four EGF receptor sub-types share a high degree of homology, most notably in the 290 amino acid cytoplasmic tyrosine kinase domain. Also conserved are two cysteine-rich regions in the extracellular ligand-binding domain. On the other hand, very little homology exists in the C-terminal 100 amino acids which are essential for the activation of intracellular signal transduction pathways after ligand binding.

EGF family ligands show specificity when it comes to binding and activating receptors. EGF, TGF-α and AR bind exclusively to HER1; NRG-1 and NRG-2 bind to HER3 and HER4 but activate only HER4; HB-EGF, BTC and epiregulin bind and activate both HER1 and HER4. HER2 is an orphan receptor, with no known ligand, whereas ErbB3 lacks functional intrinsic tyrosine kinase activity (35,37,38). Peptides that bind to EGFR compete with EGF for receptor binding and therefore they are referred to as EGF agonists or antagonist (34).

2.3.2.1 EGF and EGFR structure

Epidermal growth factor acts as a potent mitogen with a very important role in the growth, proliferation and differentiation of numerous cell types, with the deregulation of this gene, as well as of its receptor (EGFR), being associated with oncogenesis (39).

Regarding cellular proliferation and neuronal generation, EGF was shown to promote cell proliferation in the subventricular zone (SVZ) and the dentate gyrus (DG) neurogenic brain niches, and the generation and migration of striatal-specific neurons following ischemic injury, being the EGFR signaling required. Other evidence showed that EGF exerts a neuroprotective

effect rather than a neurogenic effect in promoting recovery following traumatic brain injury (40).

EGF is synthesized as a large precursor molecule that is proteolytically cleaved to generate the 53-amino acid mature epidermal growth factor peptide (39). This growth factor can be found in many human tissues including submandibular gland, parotid gland, and some other biological sources of EGF are platelets, macrophages, urine, saliva, milk, and plasma. The mature EGF receptor (EGFR/erbB1) is composed of a single polypeptide chain of 1186 amino acid residues and a substantial amount of N-linked oligosaccharides. A single hydrophobic membrane anchor sequence separates an extracellular ligand binding domain from a cytoplasmic domain that encodes an EGF-regulated tyrosine kinase (33). The extracellular domain of the EGFR is characterized by its capacity to bind EGF and EGF-like ligands with high affinity. Chemically, this portion of the receptor contains 10-11 N-linked oligosaccharide chains, an unusually high content of cystine residues (10%) that could give rise to as many as 25 disulfides, and, in several cell lines, mannose phosphate. It is proposed that the region between the two half-cystine-rich clusters is involved in ligand binding (33). The hallmark of the cytoplasmic portion of this receptor is the sequence defining the tyrosine kinase domain, whose activity has a central role in the regulation of cell proliferation. Near the carboxyl terminus of the receptor are present four sites of EGF-dependent tyrosine autophosphorylation. Present data suggest that these COOH-terminal tyrosines define an autoinhibitory region that can be relieved by autophosphorylation. Cells exposure to EGF markedly induces the phosphorylation of Ser, Thr, and Tyr residues on the EGF receptor (33).

2.3.2.2 EGFR Signal Transduction

EGFR ligands act by binding the extracellular domain of this high affinity cell surface receptor. Upon ligand-binding, EGFR undergoes a transition from an inactive monomeric form to an active homodimer, or heterodimer if EGFR pair with another member of the EGFR family, a process known as transmodulation (33,38,39,41). Since in this process there is a cross-talk occurring between ErbB receptors, it allows a diversification of the nature of the intracellular signal elicited by a specific growth factor (34). EGFR dimerization then stimulates its intrinsic intracellular protein tyrosine kinase activity, resulting in auto-phosphorylation of several tyrosine residues within its cytoplasmic domain (e.g. Tyr 1092, 1172, 1197, 1110 and 1016). These phosphorylated tyrosine residues then act as docking sites for effector molecules (Figure 9) eliciting downstream activation and signaling by several other transducers.

In Figure 9, it is represented the EGF/EGFR signaling pathway. Upon EGF binding to EGFR, one of the activated adapter proteins, GRB2, is responsible for Ras activation, which in turn

activates the protein kinase activity of Raf. Raf initiates a cascade of phosphorylation events including the phosphorylation and activation of the MAPK kinase (MEK), which in turn phosphorylates MAPK (Mitogen-activated protein kinase, also called ERK - extracellular signal regulated kinase). MAPK activates a number of transcriptional regulators to induce cell growth and proliferation. PI3K (phosphatidylinositol 3-Kinase) is another major mediator of EGFR signaling that, once activated, phosphorylates membrane bound PIP2 (Phosphatidylinositol-4,5-bisphosphate) to generate PIP3 (Phosphatidylinositol-3,4,5-trisphosphate). PIP3 binds to Akt, which in turn regulates the activity of various proteins that mediate cell survival.

EGFR also activates PLCγ (Gamma isoform of phospholipase C), which hydrolyses PIP2 to generate IP3 (inositol trisphosphate) and DAG (1,2-Diacylglycerol). IP3 induces the release of Ca2+ from the ER to activate calcium-regulated pathways. DAG is the physiological activator of protein kinase C (PKC), which regulates NFKB (Nuclear Factor-Kappa B).

Stimulation of EGFR induces also tyrosine phosphorylation of STAT1 and 3 (Signal Transducer and Activator of Transcription 1 and 3) leading to its nuclear translocation, where they are active in gene transcription. PAK activates JNK (c-Jun Kinase) that once activated enter the nucleus and causes phosphorylation of transcription factors such as c-Fos and c-Jun.

EGFR also activates several other proteins including FAK (Focal Adhesion Kinase), Paxillin, Caveolin, E-Cadherin and Ctnn-Beta (Catenin-Beta). FAK1 take part in cell motility, whereas Caveolin, Cadherin and Ctnn-Beta are involved in cytoskeletal regulation. EGFR also translocates from the plasma membrane to other cellular compartments, including the nucleus where it directly regulates the expression of several genes in cooperation with other transcriptional regulators.

This signal transduction will result in a variety of biochemical changes within the cell and in an increase in the expression of certain genes including the EGFR gene itself, ultimately leading to DNA synthesis and cell proliferation (36,38,41,42,44).

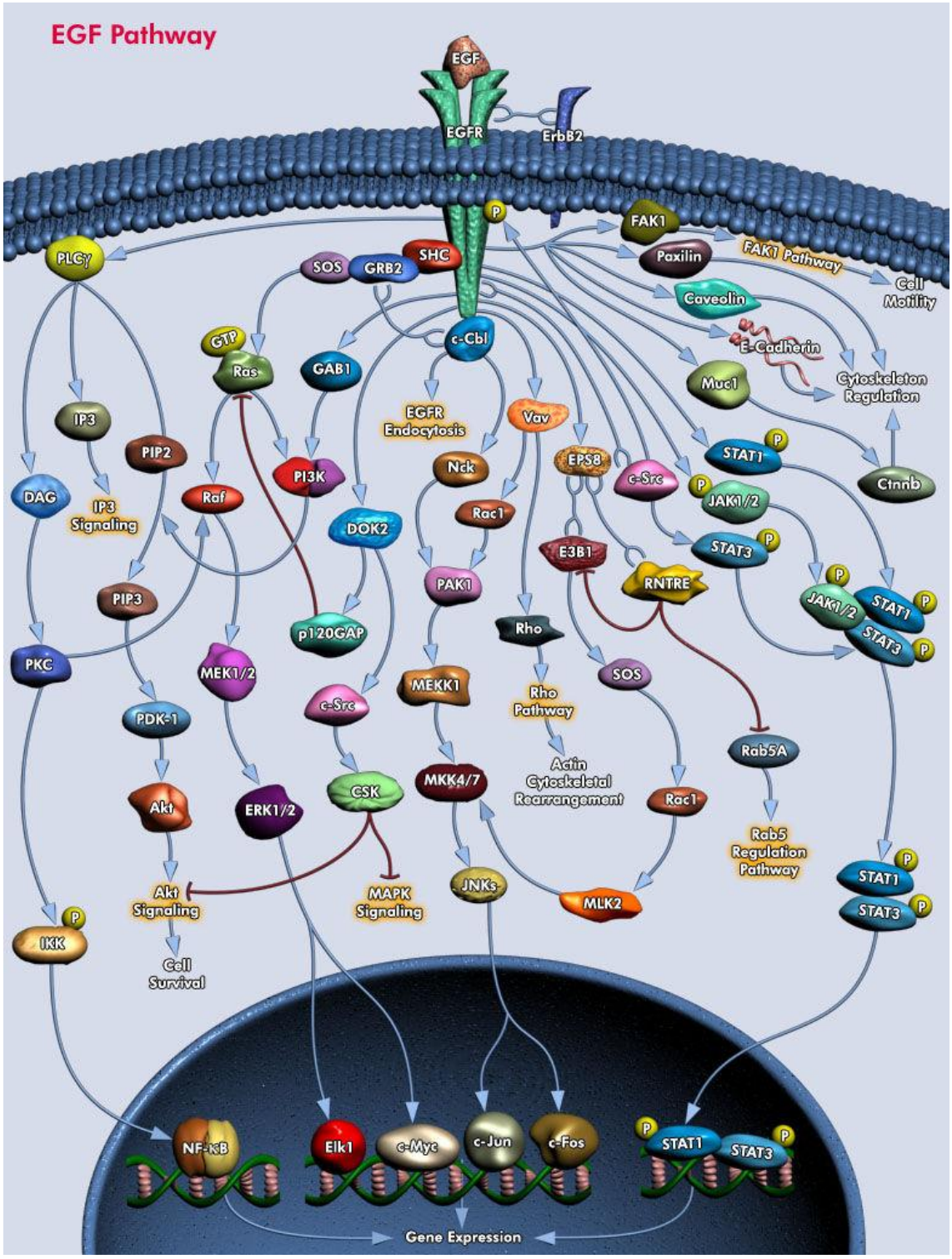

Figure 9 – Diagram showing key components of the EGFR signal transduction pathway. Upon ligand binding, activated EGFR recruits various cytoplasmic proteins, which transduce and regulate the EGFR function. Transduction by activated EGFR leads to downstream effect on proteins that are associated with cell proliferation, motility and survival, such as Ras, Raf and MAPK, PLC, PI3K, Akt, and STATs. The arrows point to signaling proteins that are subsequently recruited by upstream transducers, leading to several changes within the cell. Reproduced from reference (39).

2.3.3 HB-EGF as an EGF-family growth factor

HB-EGF is a heparin-binding member of the EGF family of growth factors that stimulates growth and differentiation. It was first identified as a 20±22 kDa glycoprotein in the conditioned medium of human macrophages (36,37). Like other members of the EGF family, HB-EGF is synthesized as a transmembrane protein (proHB-EGF) and can be cleaved at the plasma membrane to yield the 14-20kDa soluble HB-EGF (sHB-EGF) (36,37,41–43). Among the EGFR ligands, HB-EGF is notable for the number of proteins and other molecules with which it interacts, including transmembrane receptors, adhesion molecules, and transcriptional regulators (35).

HB-EGF is expressed in a variety of tissues, predominantly lung, heart, skeletal muscle and brain, and in a large number of cultured cells including vascular endothelial cells and smooth muscle cells (SMC), monocytes/macrophages, skeletal muscle cells, renal mesangial cells, keratinocytes and tumor cells (36,37,41). HB-EGF is widely expressed in the central nervous system (CNS), including the hippocampus, cerebral cortex, thalamus, hypothalamus, basal ganglia, midbrain, olfactory bulb, and so on. HB-EGF is highly expressed in neurons, as well as astrocytes and oligodendrocytes (44–47).

2.3.4 HB-EGF Physiological and Pathological role

HB-EGF biological activities influence cell cycle progression, molecular chaperone regulation, cell survival, cell adhesion, and mediation of cell migration (37).

Expression of proHB-EGF is detected in most tissues. This protein is involved in several developmental processes such as skeletal muscle cell development, heart muscle cell differentiation (37,41,44), and renal tubular formation (36,37,44), and in wound-healing and response to injury in the adult body (36,37,41,44). More recently, a role for HB-EGF in trophoblast survival (48), in neurogenesis stimulation (49,50) and as a neurotrophic factor (50) was supported by several studies. Among the pathological process in which HB-EGF plays a role, tumor growth, Smooth Muscle Cells Hyperplasia, Cardiac Hypertrophy and Atherosclerosis are the most prominent (36–38,41,44).

2.3.5 Roles of HB-EGF in the CNS and higher brain function

HB-EGF expression is much higher in brains of young animals than in adults, which is in accordance with its marked function during early developmental stages (44). However, HB-EGF is also considered to play pivotal roles in the adult nervous system (44–47). HB-EGF has been implicated in neuronal survival, glial/stem cell proliferation, and differentiation. Recently, a

research group has found that HB-EGF also enhances neurite outgrowth by activation of the ERK signaling pathway (50). This has never been reported for EGF, which suggests that HB-EGF may have more potent effects on the promotion of neurite outgrowth when compared to EGF. In fact, recent evidence has shown that HB-EGF is expressed at much higher levels than EGF in the central nervous system, indicating that HB-EGF may serve as a major ligand for EGFR in neuronal cells (44,50). Another study also reports that HB-EGF contributes to adult neurogenesis in the DG of the hippocampus (49). These reports suggest that HB-EGF may be one of the important contributors to neuronal development and synaptic plasticity in the hippocampus. Additionally, HB-EGF KO mice were impaired in spatial memory in the Morris water maze and in fear learning conditioning (51), which suggests that HB-EGF plays a significant, but yet to be fully identified, role in synaptic plasticity and memory formation. Several studies have also shown that HB-EGF appear to exert a neuroprotective effect and to modify neurogenesis after ischemic brain injury (44,52).

Besides these several actions, HB-EGF affects the development and function of nigrostriatal dopaminergic neurons, as it was found to enhance the survival of midbrain dopaminergic neurons by activation of the MAPK and the Akt signal pathway (53).

Finally, it was purposed that HB-EGF signaling may play a pivotal role in psychomotor behavior and neuronal transmission, and alterations affecting HB-EGF signaling could represent a contributing factor for the development of psychiatric disorders such as schizophrenia (44).

In conclusion, evidences indicate that the HB-EGF signal may be an important trophic factor in the developing central nervous system and a contributor to higher brain functions (Figure 10).

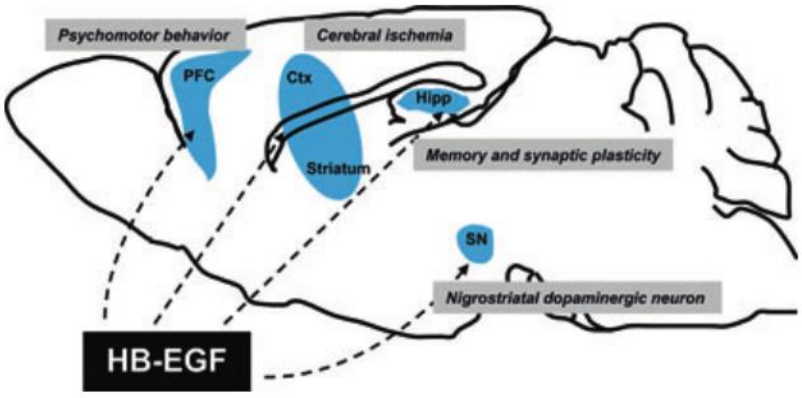

Figure 10 - HB-EGF roles in CNS and higher brain function. HB-EGF is widely expressed throughout the brain, being implicated in psychomotor behavior, cerebral ischemia, nigrostriatal dopaminergic neuron, memory, and synaptic plasticity. PFC, prefrontal cortex; Hipp, hippocampus; SN, substancia nigra; Ctx, cortex. Reproduced from (44).

2.3.6 HB-EGF gene

2.3.6.1 Gene structure

The HB–EGF gene locus has been mapped to the long arm of chromosome 5, at 5q23, in humans, and to chromosome 18 in mice (35,37). The longest form of a HB-EGF cDNA cloned so far is approximately 2.4 kb in length and corresponds in size to the predominant mRNA typically revealed by Northern blot analysis. The human and mouse *HB-EGF* genes encompass approximately 14 kb, and consist of 6 exons and 5 introns consistent with the overall gene structure of other ligands of the EGF family. The sequences contributing to the 208 amino acid ORF are found on exons 1–5 (Figure 11) (37).

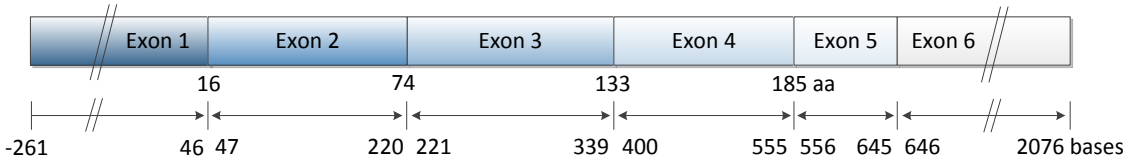

Figure 11 – The 6 exons structure of HB-EGF. Adapted from reference (37).

The expression of the *HB-EGF* gene is highly regulated by several transcriptional regulatory factors in a tissue-specific manner (37,41). A number of putative transcription factor binding sites were identified in the mouse and human *HB-EGF* promoters including binding sites for Sp1, AP1, Ets-2, NFkB and the muscle specific transcription factor MyoD. The HB–EGF promoter contains two E-box sequences, at -1606 bp and -510 bp upstream the transcription start site, respectively. The HB-EGF proximal E-box (at -510 bp) has been shown directly to be responsible for binding MyoD and activating the promoter. Further, the HB–EGF promoter contains two putative NFkB binding sites, a proved positive regulator of *HB–EGF* expression. In addition, platelet-activating factor, which has been considered to contribute to atherogenesis, activates *HB-EGF* gene expression in human peripheral blood monocytes (37). Several lines of evidence have suggested that HB-EGF is a direct transcriptional target downstream the Ras/Raf/MEK pathway, being upregulated by these MAPK pathway components, and playing an important role in the autocrine activation of signaling pathways in transformed cells. More recently, *HB-EGF* induction was proved to depend on the activation of two of the three major MAPKs, ERK and p38, and inhibiting either of them results in decreased *HB-EGF* expression. *HB-EGF* can be induced by a variety of stimuli, and in all cases its induction depends on the activation of MAPKs, a pathway that also contributes to *EGFR* gene transactivation (54).

2.3.7 HB-EGF Structure

Although HB-EGF shares approximately 40% sequence identity in its C-terminal domain with EGF and TGF-α, determination of the primary peptide sequence of HB-EGF revealed the presence of an extended N-terminal domain that was absent in EGF and TGF-α (35,37). Notably, the N-terminal sequence of HB-EGF is enriched in basic amino acids that are positively charged at physiological pH and enable interaction with negatively charged heparin sulphate proteoglycans both on the cell surface and in the extracellular matrix (35).

HB-EGF is synthesized by ER-bound ribosomes as a pre-pro-form of 208 amino acids in length and is expressed at the cell surface as a 20-30kDa type I transmembrane precursor, named proHB-EGF, consisting of an ectodomain, a single membrane-spanning domain and a cytoplasmic domain (37,38,55,56). Pre-proHB-EGF is composed by signal peptide (ORF_{1-23}), propeptide (ORF_{24-62}), mature HB–EGF (ORF_{63-149}), juxtamembrane ($ORF_{150-160}$), transmembrane ($ORF_{161-184}$) and cytoplasmic ($ORF_{185-208}$) domains (Figure 12). Within the mature HB-EGF domain, HB-EGF has an EGF-like domain ($ORF_{103-150}$) (Figure 12) typical of all members of the EGF family, namely 6 conserved cysteine residues, which form three intra-molecular disulfide bonds (C1-C3 , C2.C4 , C5-C6) essential for HB-EGF mitogenic activity (37). The EGF-like growth factor domain alone is sufficient to elicit EGFR phosphorylation via autocrine, juxtacrine, and paracrine signaling pathways (55,56). Also within the mature HB-EGF domain, there is a Difteria Toxin (DT)-binding domain ($ORF_{106-149}$) and a Heparin-binding domain (ORF_{93-113}) (Figure 12 B). The HB-EGF heparin-binding domain lies mostly N-terminal to the EGF-like domain but partially overlaps the first Cys residue in this domain. It contains two consensus sequences for heparin recognition, X-B-B-X-B-X and X-B-B-B-X-X-B-X (with B being basic amino acid). Within the 21-amino acid stretch, the highly basic sequences $KRKKK_{93-97}$, $KKR_{103-105}$ and $RKYK_{110-113}$ contribute the most to heparin-binding (37). It appears that the transmembrane HB-EGF associated with cells consists of ORF_{63-208}, suggesting that the HB-EGF propeptide domain is cleaved rapidly intracellularly after synthesis of the precursor or very rapidly once it has reached the cell surface (37,57), and the endopeptidase furin was implicated in this rapid constitutive cleavage at Arg_{62}–Asp_{63} (37,58,59).

This larger membrane-anchored precursor named proHB-EGF is then proteolytically processed, generating the mature or soluble HB-EGF (sHB-EGF) (Figure 12 A), which is released to the extracellular medium (36,37). Several N-terminal truncated isoforms of mature HB-EGF have been purified. The longest form contains 87 amino acids encompassing the sequence Asp_{63} –Pro_{149} of the ORF. The other three forms have as N-terminal amino acids Arg_{73}, Val_{74} and Ser_{77}, thereby yielding proteins of 76, 75 and 72 amino acids respectively, all of which

mitogenically active (37). The apparent molecular mass of cell-derived HB-EGF is about 14-20 kDa, much larger than would be predicted for a protein of 73–87 amino acids. This discrepancy is in part due to HB-EGF being heavily *O*-glycosylated at glycosylation sites, such as Thr_{75} and Thr_{85}. Discrepancies might also be due to highly positively charged domains in HB-EGF that retard the protein mobility in the SDS-PAGE (37).

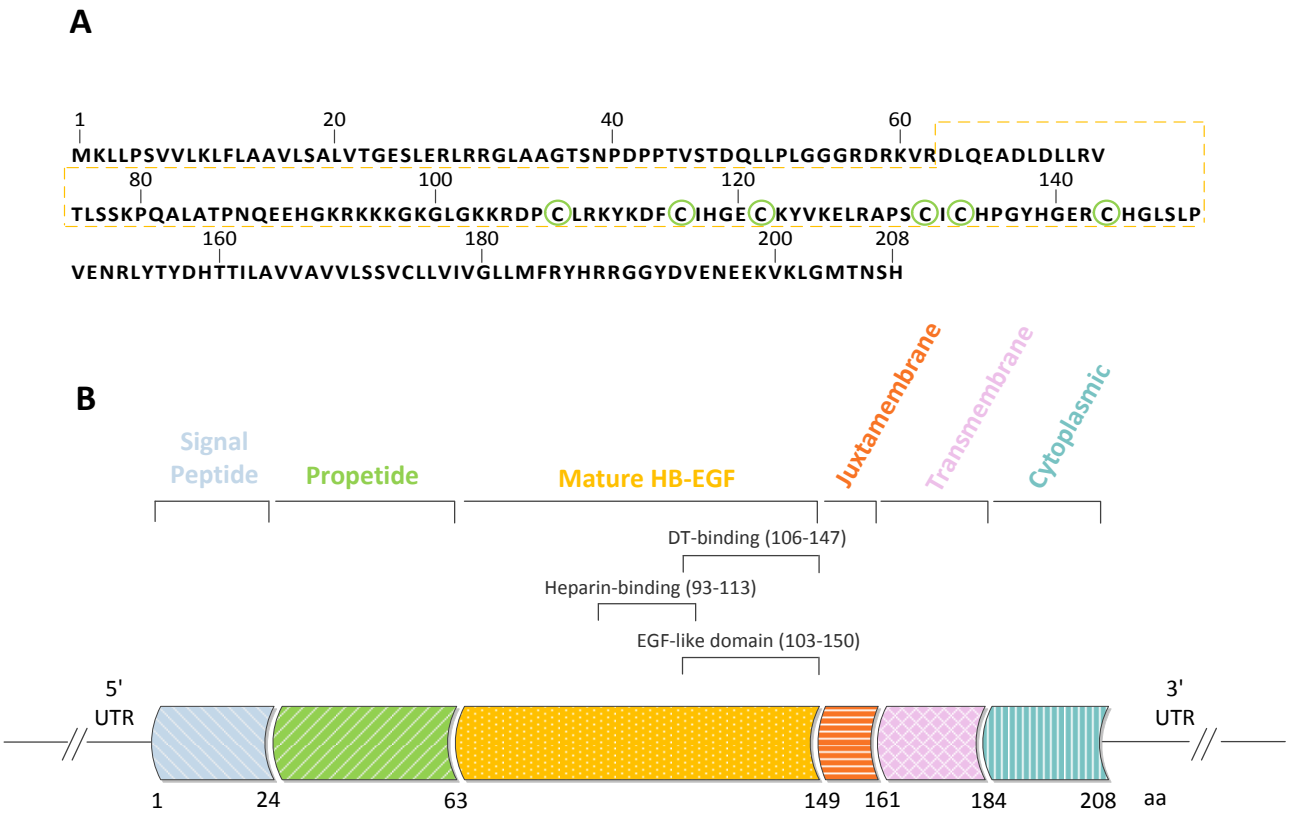

Figure 12 - HB–EGF protein structure. A) Predicted amino acid sequence of the human HB-EGF open reading frame. The 87 amino acid form of mature HB–EGF is shown within the yellow box and the six cysteine residues of the EGF-like domain are highlighted in green circles. B) Domain structure of pre-proHB-EGF is depicted including signal peptide, propeptide, mature HB-EGF, juxtamembrane, transmembrane and cytoplasmic domains. Also depicted are the EGF-like domain, Heparin-binding domain and the Diphtheria Toxin (DT)-binding domain within the mature HB-EGF domain. Adapted from reference (37).

2.3.8 Proteolytic processing of proHB-EGF (Ectodomain shedding)

Post-translational modifications of transmembrane proteins are critical mediators of cellular processes such as proliferation, differentiation, migration, adhesion, and death. Membrane-anchored proHB-EGF undergoes a number of post-translational modifications ranging from O-linked glycosylation of the N-terminal ectodomain, N-terminal truncations, phosphorylation of the cytoplasmic domain and regulated cleavage of the entire ectodomain (35). Ectodomain shedding is the term used to describe the proteolytic cleavage that releases

the ectodomains of transmembrane proteins from cell surface into extracellular spaces (60), a process widely observed in growth factors, growth factor receptors, cell-adhesion molecules, extracellular matrix proteins and other membrane proteins (36,58). The processing of membrane-anchored EGFR ligands is essential for the complete repertoire of functions those ligands play in development, emphasizing the significance of ectodomain shedding for EGFR-mediated signaling (60,61). Regulated processing of the juxtamembrane (JM) domain of proHB-EGF represents a critical control point in HB-EGF function since it converts the membrane-anchored non-diffusible form into the soluble protein that has a greatly expanded sphere of influence on surrounding cells and tissues, altering its actions from juxtacrine to paracrine (35,36).

Ectodomain shedding of membrane-anchored growth factors and cytokines is primarily mediated by metalloproteinases that cleave within the ectodomain of the ligand, particularly by members of “a disintegrin and metalloprotease” (ADAM) family that also cleave APP to sAPP. Metalloproteinases inhibition prevents HB-EGF release induced by different stimuli, with the former being postulated to regulate HB-EGF ectodomain shedding (60,61). In order to the cleavage to take place, both proHB-EGF and the metalloproteinase need to be membrane-anchored (61). Proteolytic cleavage at the proHB-EGF JM site yields at least two fragments, soluble HB-EGF (sHB-EGF) and the carboxyl-terminal fragment containing the transmembrane and cytoplasmic segments (HB-EGF-C) (Figure 13) (55,56,60). Release of soluble HB-EGF has been found to occur both constitutively and in a regulated manner. Monocytes/ macrophages and T lymphocytes are among the cell types that release HB-EGF constitutively. In the case of adherent cells such as MDA-MB-231 and Vero, the membrane-anchored precursor is the predominant form and processing is inducible, for example, by addition of phorbol esters (58).

In mammalian cells, two membrane-anchored enzymes, ADAMs 10 and 17, have emerged as key molecules in the shedding of the seven ErbB1-ligands. ADAM17 is considered the principal ‘sheddase’ for HB-EGF, whereas ADAM10 was identified as the major ‘sheddase’ for EGF (35,41,62). A matrix metalloproteinase-3 (MMP-3) has also been implicated in the cleavage of HB–EGF in the juxtamembrane region, since it releases sHB-EGF from an insoluble substrate *in vitro* (37,58). So far, it has been reported that proHB-EGF can be processed by MMP-3, MMP-7, ADAM9, 10, 12, and 17 (60).

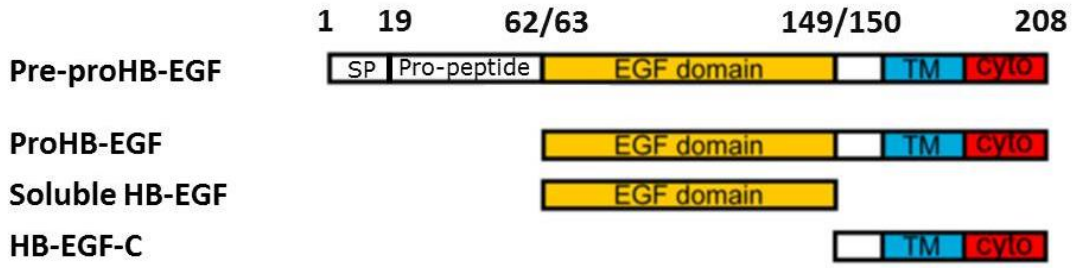

Figure 13 - Schematic representation of HB-EGF processing. HB-EGF is synthesized as pre-proHB-EGF by ER-bound ribosomes, and expressed at the plasma membrane as proHB-EGF. ProHB-EGF is cleaved at the juxtamembrane domain, yielding soluble HB-EGF and HB-EGF-C. Adapted from reference (55).

2.3.8.1 Regulation of proHB-EGF processing

Regulation of ectodomain shedding by different stimuli. Ectodomain shedding must be strictly regulated. Several stimuli, which include calcium ionophores, activation of G-protein coupled receptors (GPCRs) by lysophophatidic acid (LPA), and phorbol ester-mediated PKC activation are known to induce ectodomain shedding of HB-EGF by metalloprotease activation (Figure 14) (36,55,56,61–64). Activators of protein kinase C (PKC), such as phorbol ester 12-O-tetradecnoylphorbol-13-acetate (TPA), were among the first identified activators of protein ectodomain shedding (36,59,61–64). Therefore, PKC is involved in the intracellular signaling pathway for proHB-EGF processing, with PMA inducing the loss of cell-surface associated transmembrane HB-EGF, the acquisition of cell resistance to DT, and release of the mature sHB-EGF into conditioned medium (61). Stimulation of G-protein-coupled receptors (GPCRs) also leads to proHB-EGF ectodomain shedding, and shed sHB-EGF, in turn, activates and further induces EGFR signaling, mediating the reported *EGFR* transactivation by GPCR signaling. Transactivation of EGFR-dependent pathways has been known to be critical for the mitogenic activity of GPCRs ligands such as lysophosphatidic acid, endothelin and thrombin. It was shown that the sHB-EGF generated by GPCR-induced ectodomain shedding of proHB-EGF is the only growth factor mediating *EGFR* transactivation (36). Several growth factors, including sHB-EGF itself, may be involved in activation of receptor tyrosine kinases, activating the Ras-MAPK pathway that also leads to proHB-EGF ectodomain shedding.

Cellular stresses caused by inflammatory cytokines, reactive oxygen and osmotic shock can also induce ectodomain shedding (41). In addition, protein phosphorylation may also be involved in the regulation of this process, since it was observed that tyrosine phosphorylation and phosphatase inhibitors promote shedding (61). The cochaperone BAG-1 (an antiapoptotic protein) that binds to HB-EGF C-terminus, also increases the secretion of soluble HB-EGF.

Furthermore, Nardilysin, a metalloendopeptidase and linker protein, potentially regulates HB-EGF ectodomain cleavage by binding to ADAM17 (64).

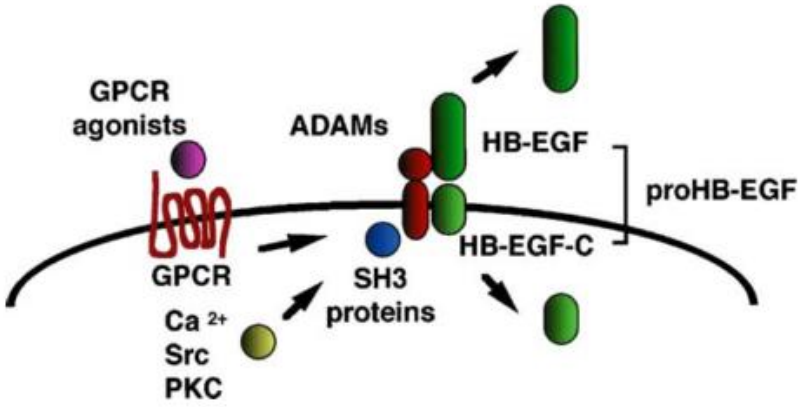

Figure 14 - Model of proHB-EGF ectodomain shedding induction. ADAM proteins are activated by various stimuli including GPCR signaling, PKC activation, and binding of cytoplasmic docking proteins, which lead to proHB-EGF processing yielding sHB-EGF and HB-EGF-C. Adapted from reference (60).

Regulation of proHB-EGF shedding by signaling pathways. ProHB-EGF ectodomain shedding is regulated by at least two distinct intracellular signaling pathways, including the PKC pathway and the Ras-MAPK pathway.

It has been shown that the regulated processing of proHB-EGF requires PKCδ and MDC9 (metalloprotease/disintegrin/cysteine-rich protein 9), a member of the ADAM family of metalloproteases which is a PKCδ-specific binding protein. Importantly, MDC9 overexpression results in the shedding of the proHB-EGF ectodomain (63). PKCδ may trigger proHB-EGF shedding by binding and subsequent phosphorylation of the cytoplasmic domain of MDC9, recruiting MDC9 to the proximity of proHB-EGF (63). The direct interaction with PKCδ supports the hypothesis that MDC9 is the initial protease in the TPA-induced mechanism of ectodomain proHB-EGF shedding (63).

In many types of mammalian cells, the Ras-MAPK cascade is the main mitogenic signaling pathway, and MAPK activation is essential for cell growth (65). PMA is known to induce MAPK activation and this activation was shown to precede HB-EGF shedding, comprising an intermediate step in the shedding mechanism (61). As an inducer of proHB-EGF shedding, MAP kinase may be a mediator of sustained and amplified growth factor activity. One of the hypothesis is that HB-EGF binds to its receptor, which in turn activates MAPK, leading to cell proliferation but also to the release of more growth factor from the proHB-EGF membrane-anchored precursor, resulting in an autocrine amplification loop (61). Since it has been demonstrated that Raf-1 induces proHB-EGF shedding via the MAPK cascade, it was

postulated that the activation of the MAPK cascade by PMA is in part due to the activation of certain PMA-responsive PKC isoforms that activate Raf-1. Therefore, results suggest that HB-EGF-induced binding to ErbB receptors regulates proHB-EGF shedding via Raf-1/MEK/ERK signaling pathway (61), and MAPK (p42 and p44) activation was shown to mediate the serum starvation-induced HB-EGF cleavage (61).

Another suggested novel regulator of proHB-EGF shedding is the degree of cell adhesion and spreading. Surprisingly, it was observed that when cells are placed into suspension, PMA failed to induce shedding, with the ability of PMA to induce proHB-EGF shedding being fully restored after plating suspended cells on fibronectin. However, this inability of PMA to induce the cleavage of proHB-EGF in suspended cells was not due to an impaired activation of the MAPK, suggesting that MAPK activity is necessary but not sufficient to promote proHB-EGF shedding, since cell adhesion is also required. The degree of cell spreading also appears to regulate proHB-EGF shedding. It was observed that when cells are plated on increasing fibronectin densities, the extent of PMA-induced shedding of proHB-EGF increases in proportion to the degree of cell spreading (61).

In summary, activation of the Ras-MAPK pathway promotes G1 phase progression in the cell cycle, and MAPK activation can induce proHB-EGF shedding in a process that is dependent on cell adhesion and spreading, suggesting that the cellular architecture and cytoskeleton may play a role in this signaling pathway (61,65).

2.3.9 Mature HB-EGF: Autocrine and Paracrine biological activities

Mature HB-EGF is a potent stimulator of cell proliferation and migration. It has a broad spectrum of activities, but in particular it targets fibroblasts, SMC and epithelial cells. HB-EGF is a potent mitogen for a number of cell types including mouse 3T3 fibroblasts, SMC, epithelial cells, keratinocytes, hepatocytes, renal tubule cells, and breast and ovarian carcinoma cells. HB-EGF is also a potent stimulator of cell motility, being also chemotactic for SMC, fibroblasts and keratinocytes (36,37,41), and stimulating intensive random migration (chemokinesis) of astrocytes (37). On the other hand, HB–EGF is not mitogenic for endothelial cells, unlike other heparin-binding growth factors such as Fibroblast Growth Factor-1 and -2 (FGF-1 and -2) and Vascular Endothelial Growth Factor (VEGF) (36,37,41). Noticeably, the HB-EGF mitogenic activity on SMC is much stronger than that of EGF, and it appears to involve interactions with heparan sulfate proteoglycans in the extracellular matrix (37).

HB–EGF might also stimulate cells indirectly by inducing the transcription of other growth factors and growth factor receptor genes. For example, in SMC, HB-EGF stimulates an increase in the mRNA levels of the SMC mitogens Platelet-derived Growth Factor (PDGF) and

FGF-2. HB-EGF also induces an increase in the mRNA levels of other EGF-like ligands such as TGF-α, AR and BTC in keratinocytes, epithelial cells and colon adenocarcinoma cells. Induction of macrophage colony-stimulating factor (M-CSF) receptor gene expression in SMC by HB-EGF suggests it has a role in the phenotypic change of SMC to macrophage-like foam cells in atherosclerosis (37).

2.3.10 Transmembrane HB-EGF (proHB-EGF): Juxtacrine activities

Although HB-EGF was first identified as a soluble growth factor, the existence and relative abundance of HB-EGF in its membrane-anchored form, the existence of protein complexes of proHB-EGF with other membrane proteins, and its localization at cell-cell contact sites suggest that proHB-EGF is not only a precursor for sHB-EGF but also plays some role in intercellular interactions. In fact, proHB-EGF has unique biological characteristics distinct from sHB-EGF (36,37,41). Several properties of transmembrane HB-EGF, including juxtacrine growth factor activity and adhesion, DT-binding, and proteolytic processing to produce mature HB-EGF are depicted in Figure 15. Juxtacrine activity is a term coined to describe the interactions of an immobilized growth factor with neighboring cells in a non-diffusible manner.

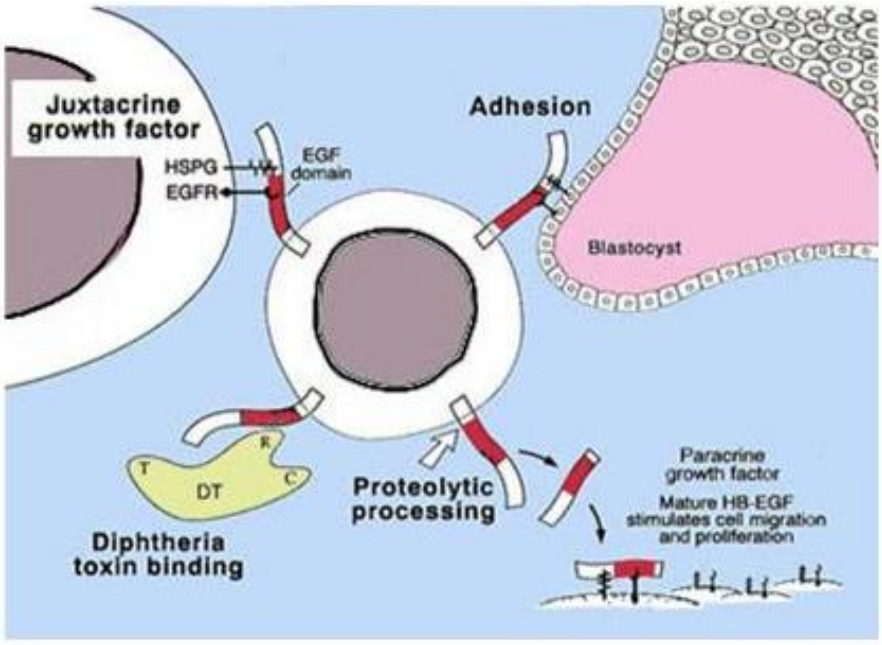

Figure 15 - Scheme of activities associated with the transmembrane form of HB–EGF. Transmembrane HB–EGF is depicted clockwise as a juxtacrine growth factor, as an adhesion molecule for the cells of the mouse blastocyst, as a target for proteolytic processing and as the receptor for DT. Interactions with EGFR and heparan sulfate proteoglycans (HSPG) are depicted. Reproduced from reference (37).

An important and apparently unique property of transmembrane HB-EGF is that it is the specific receptor for Diphtheria Toxin (DT), which explains its denomination as DTR (Difteria Toxin Receptor) (66). DT binds specifically to the EGF-like domain of transmembrane human HB–EGF (Asp_{106} –Pro_{149}), with Glu_{141} being a critical residue for DT-binding and toxin-sensitivity (37,67). Most mammalian cells expressing proHB-EGF are sensitive to DT, however, mice and rat are DT-resistant, since DT does not bind to their proHB-EGF due to amino acid substitutions in the EGF-like domain (36,67). After DT binding, the DTR/transmembrane HB-EGF complex is internalized by receptor-mediated endocytosis and enters the cytoplasm, where the A-fragment of the toxin exerts its cytotoxicity (36,37). HB-EGF must be in the transmembrane form to convey DT toxicity. When cells possessing the transmembrane form are treated with phorbol ester, the precursor is processed to release mature HB-EGF and cells become DT-resistant (37,66).

Transmembrane HB-EGF was also reported to stimulate juxtacrine tyrosine phosphorylation of EGFR/HER1 and proliferation (68), and acts as an adhesion factor, e.g. for blastocysts (69).

There are also evidences suggesting that proHB-EGF has the ability to suppress the growth of cancer cells through up-regulation of EGFR, an effect completely opposite to that of sHB-EGF that always presents growth-promoting activity. In fact, proHB-EGF is expressed in various tissues that are not thought to be involved in cell proliferation, suggesting that its original function *in vivo* is not always promotion of cell growth. While both forms of HB-EGF induce EGFR phosphorylation, in the case of proHB-EGF the phosphorylation state is prolonged, which may explain the distinct actions (70). It was also observed that the prolonged EGFR stimulation possibly up-regulates the expression of the cyclin-dependent kinase inhibitor, p21, which leads to an increased resistance to apoptosis. Of note, the cell growth arrest and induction of p21 in tumor cells expressing high amounts of EGFR have been reported to be mediated by STAT1 (37,70).

The juxtacrine activities of transmembrane HB-EGF are modulated by CD9, which acts as a co-factor for proHB-EGF juxtacrine activity (see in section 2.3.11.3) (36,37,68).

2.3.11 HB-EGF receptors and proHB-EGF protein complexes formation

2.3.11.1 Tyrosine kinase receptors

HB-EGF, EGF, TGF-α and AR all stimulate qualitatively similar patterns of EGFR/HER1 tyrosine phosphorylation suggesting that these ligands are functionally identical in activating

HER1. HB-EGF is also capable of activating HER4/ErbB4, a receptor first shown to be activated by NRG (37,42). High-affinity interactions with receptors are mediated via the 3-looped EGF-like motif and result in receptor autophosphorylation and initiation of downstream signaling cascades. Interestingly, the biological outcomes evoked by HB-EGF binding to ErbB1 and ErbB4 are distinct, with the former typically promoting proliferation (mitogenic function) and chemotaxis and the latter stimulating strong chemotaxis and migration but no proliferative response (37,42,43,50).

Interactions between the membrane-anchored form of HB-EGF and the respective ErbB receptors expressed on adjacent cells also mediate both cell survival and intercellular adhesion functions (35).

In complex systems, where several EGF receptor subtypes are expressed and heterodimerization occurs, HB-EGF can activate HER1 and HER4, as well as HER3 and HER2, by EGF receptor transmodulation (37). An interesting recent discovery is that HB-EGF plays a critical role in *EGFR* transactivation induced by G-protein-coupled receptor ligands, such as lysophosphatidic acid, endothelin-1, and angiotensin-II, being the ectodomain shedding of proHB-EGF required for this process (38,71).

2.3.11.2 Heparan sulfate proteoglycans (HSPG)

One functional difference and unique feature of HB-EGF is that, unlike EGF and TGF-α, it is a heparin-binding protein, showing a high affinity for heparin and heparan sulfate. The interaction of HB-EGF with heparin, in the form of HSPGs present on cell surfaces (Figure 16), is known to modulate HB-EGF binding to EGFR and activity at least for certain cell types, such as SMC and CHO cells (35–37). For this, HB-EGF is a much more potent chemoattractant for SMC than EGF or TGF-α, and reduction of SMC surface HSPG levels reduces the chemotactic activity of HB-EGF to about the level of EGF and TGF-α, suggesting that interaction with HSPG enhances HB–EGF activity relative to EGF and TGF-α.

Cell surface HSPG also modulates other transmembrane HB-EGF activity, particularly DT-binding activity. Cells expressing transmembrane HB-EGF/DT receptor, but deficient in cell surface HSPG were less sensitive to DT toxicity than were wild type cells and the DT-sensitivity was restored by addition of either Heparan Sulfate (HS) or heparin. Apparently, heparin increases DT-binding to the cells by increasing the affinity of HB-EGF/DTR for DT.

In conclusion, binding of this growth factor to HSPG, which has lower affinity to HB-EGF but exists in higher receptor/cell number when compared to the high affinity tyrosine kinase erbB receptors, results in an additional level of growth factor activity regulation (37).

2.3.11.3 DRAP27/CD9

HB-EGF forms a complex with a cell-associated protein, DRAP27 (Figure 16), the monkey homologue of CD9, a tetraspan membrane protein that belongs to the transmembrane 4 superfamily (TM4SF) and that is suggested to be involved in cell growth, adhesion and migration (37,67). CD9 serves as a co-factor of proHB-EGF for DT binding and, therefore, greatly upregulates the binding of DT to proHB-EGF. Juxtacrine mitogenic activity of proHB-EGF is also upregulated by the association of CD9. This up-regulation of proHB-EGF activities occurs due to protein-protein interaction between proHB-EGF and CD9, which increases the number of effective binding sites for DT (35,36,67). This binding appears to stabilize transmembrane HB-EGF on the cell surface by preventing its processing and/or internalization (37). The second extracellular domain of CD9 and the EGF-like domain of proHB-EGF are essential for the proHB-EGF up-regulation. It was also showed that CD9 and also CD63, CD81, and CD82, can be found associated with proHB-EGF and integrin $\alpha_3\beta_1$. However, among these TM4SF proteins, only CD9 up-regulated the DT binding activity of proHB-EGF (67).

2.3.11.4 Integrin $\alpha_3\beta_1$

In addition to CD9, proHB-EGF forms a complex with integrin $\alpha_3\beta_1$, a protein localized at cell-cell contact sites in epithelial cells (36,37). Together with integrin $\alpha_3\beta_1$, transmembrane HB-EGF and CD9 were found to co-localize at cell–cell contact sites near adherence junctions (Figure 16). It seems that transmembrane HB-EGF binds to CD9, which in turn binds to integrin $\alpha_3\beta_1$. Since EGF receptors are also localized to adherence junctions, the notion that proHB-EGF plays a role in intercellular communication in a juxtacrine manner at cell-cell contact sites is supported. In conclusion, it may be that direct interactions of juxtacrine growth factors, receptors and cell adhesion molecules control cell proliferation during the cell–cell adhesion process (37).

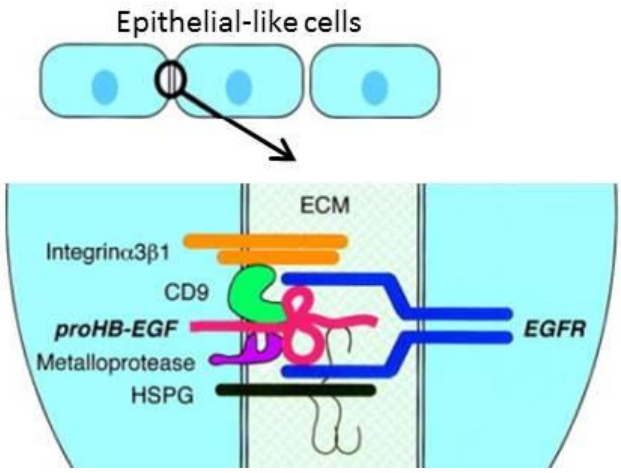

Figure 16 - Hypothetical model of the proHB-EGF complex. ProHB-EGF forms a complex with associated molecules including CD9, Integrin α3β1 and HSPGs at cell-cell contact sites. EGFR localized at cell-cell contact sites transmits growth stimulatory or inhibitory signals into the cells. Metalloproteases may also be localized at the site for the processing of proHB-EGF. Adapted from reference (36).

2.3.11.5 N-arginine dibasic convertase (NRDc)

Recently, NRDc, a metalloendopeptidase associated with the cytoplasm and the cell surface, was identified as a specific receptor for sHB-EGF, although not being one of the known members of the ErbB family (38,42,60). Its name derives from its *in vitro* substrate specificity, since it generally cleaves precursor polypeptides at the N-terminus of arginine (R) residues in dibasic sites. NRDc is mainly expressed in developing neural tissue and adult testis, heart and skeletal muscle, tissues that also express HB-EGF (42).

Within the EGF family of ligands, NRDc was found to be a highly selective receptor for HB-EGF. This specificity suggests that there is a specific NRDc-binding domain within HB-EGF. In fact, evidence suggests that the interaction is mediated by the HB-EGF heparin-binding domain. Interestingly, NRDc was shown to enhance sHB-EGF-induced, but not EGF-induced, cell migration. Furthermore, this occurs in an EGFR/ErbB1-dependent manner, since EGFR inhibition totally abolishes HB-EGF-induced cell migration. Therefore, although the mechanism by which NRDc induces cell migration is not known, it is certain that NRDc is a modulator of HB-EGF migration activity via ErbB1 (42).

2.3.11.6 Cytoplasmic tail interactors

Several binding partners for the cytoplasmic domain of proHB-EGF were identified, including the cochaperone BAG-1 and the transcriptional repressors promyelocytic leukaemia zinc finger protein (PLZF) and B cell lymphoma 6 (Bcl-6). As mentioned above, interaction between BAG-1 and proHB-EGF was found to lead to rapid secretion of sHB-EGF, decreased

cell adhesion, and increased resistance to apoptosis. Basically, this interaction augments the pro-survival function of proHB-EGF. Conversely, association between the C-terminal fragment of HB-EGF, that is liberated following ectodomain shedding, with PLZF or Bcl6, leads to nuclear export and degradation of these transcriptional repressors, respectively, and a resulting inhibition of their repressive activity (35,41,50).

2.3.12 ProHB-EGF dual intracellular signaling

2.3.12.1 Mature HB-EGF-induced signaling

Soluble HB-EGF generated by proHB-EGF processing binds to EGFR and ErbB4 directly, and binds/activates ErbB2 and ErbB3 indirectly by receptor heterodimerization. This induces ErbBs signaling into cells and promotes G1-phase progression in the cell cycle by regulating the expression of cyclin D via the Ras-MAPK signaling cascade (Figure 17) (38,41,60).

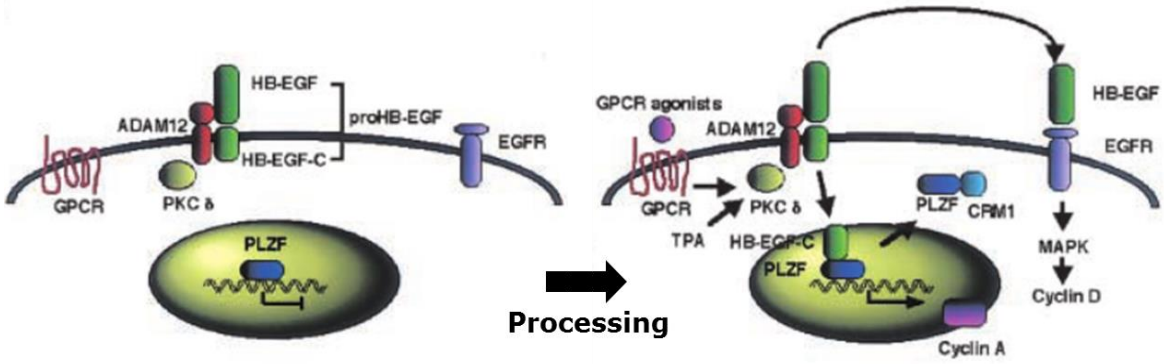

Figure 17 - Gene transcription control by HB-EGF-C and sHB-EGF. HB-EGF-C and sHB-EGF generated by proHB-EGF processing mediate signaling into the nucleus directly, and indirectly via ErbB receptors, respectively, and this dual intracellular signaling regulates gene transcription. Adapted from references (60,72).

Upon HB-EGF binding to the receptor, auto-phosphorylation occurs due to the intracellular tyrosine kinase activity of EGFR, HER2 and HER4. Phosphorylated tyrosine residues then serve as docking sites for intracellular proteins that direct downstream signaling pathways, including PI3K and MAPK cascades. Very recently, the downstream signaling circuitry that regulates the ability of HB-EGF to autoregulate, to induce migration, and to inhibit apoptosis of human trophoblasts has been examined (73). In human cytotrophoblast cell lines, HB-EGF induces a rapid, transient activation of the MAPK14, ERK and PI3K pathways (marked phosphorylation of MEK, MAPK14, ERK, and AKT is observed 15 min after treatment with HB-EGF), but a slower or delayed activation of the JNK pathway (occurring after 1h of

treatment). The authors verified that the presence of an inhibitor of PI3K or of any of the three MAPK pathways (MAPK14, MEK, or JNK), blocked the HB-EGF-induced increase in trophoblast migration (73). Interestingly, it was also reported that HB-EGF prevents apoptosis induced by oxygen fluctuations (Hypoxia/Reperfusion) by signaling through MAPK14 but not through the other kinases. Another very interesting finding was that HB-EGF signaling increases HB-EGF protein levels via the three MAPK pathways (but not PI3K) in hypoxia conditions (73).

2.3.12.2 HB-EGF-C-induced signaling

In addition to the well-known signaling pathways mediated by the extracellular EGF-like growth factor domain, subsequent to shedding, the carboxyl-terminal cell-associated remnant, HB-EGF-C, is phosphorylated and migrates from the PM to the ER and nuclear envelope (NE), where it directly regulates gene expression (55,56) and functions as an intracellular signal coordinating cell cycle progression (Figure 17) (41,60,72).

The interactions between HB-EGF-C and PLZF and Bcl-6 (55,56,60,72) evoke a novel intracellular signaling that is independent of EGFR activation. PLZF is localized in the nucleus, being a transcriptional repressor of several proteins and a negative regulator of the cell cycle by the suppression of cyclin A expression (60,72). HB-EGF-C translocates from the PM to the nucleus, where it binds to PLZF and triggers its nuclear export, which results in the prevention of cyclin A transcription suppression and allowing progression of the cell cycle into the S-phase (Figure 17, Figure 18) (60,65,72). This process also lead to Bcl6 degradation and attenuation of its negative regulatory activity on gene repression (Figure 18) (35,37,65).

Therefore, proHB-EGF has two functional domains (HB-EGF and HB-EGF-C) affecting mitogenic signaling, and the coordination of the dual mitogenic signals generated by the processing may be important for cell cycle progression (60,72). BAG-1L, an isoform of BAG-1 is another potential binding protein of nuclear HB-EGF-C. While BAG-1 was first identified as a proHB-EGF cytoplasmic-binding protein in the cytoplasm and PM, its isoform BAG-1L possesses a nuclear localization signal and is localized in the nuclei of some cell types, being therefore a potential binder of nuclear HB-EGF-C (60).

Recent experiments have indicated that the cytoplasmic region of proHB-EGF also acts to regulate the distribution of proHB-EGF at the plasma membrane. These findings indicate that the proHB-EGF cytoplasmic region is, unexpectedly, a multifunctional protein domain (60).

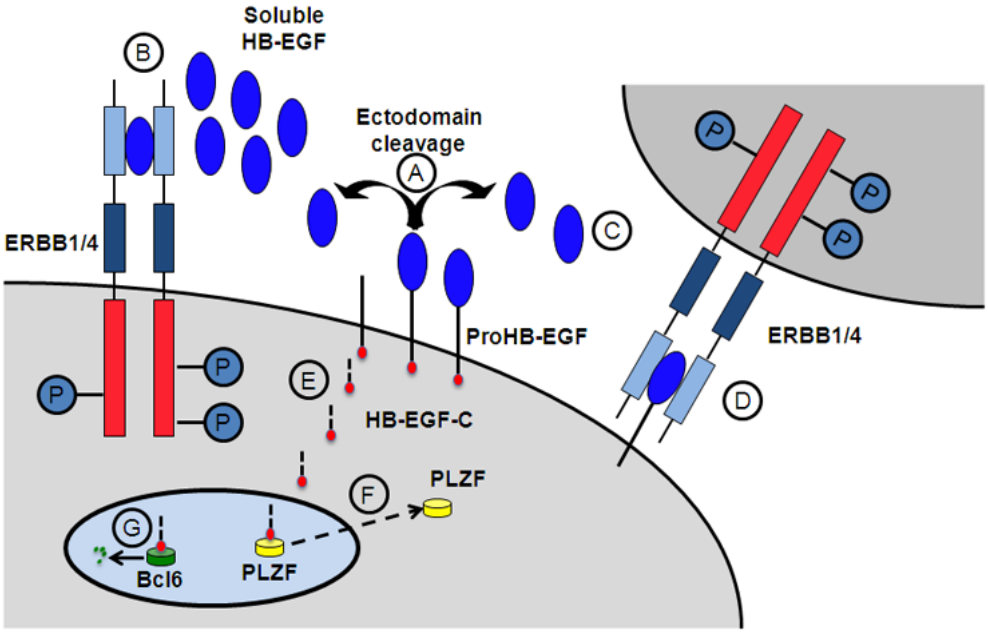

Figure 18 - Regulated processing and activity of HB-EGF. ProHB-EGF expressed on the PM undergoes ectodomain cleavage (A). Release of the mature, soluble protein facilitates both autocrine (B) and paracrine (C) activation of ERBB receptors expressed on the same or adjacent cells, respectively. ProHB-EGF can also activate ERBB receptors via juxtacrine signaling (D). The HB-EGF-C translocates to the nucleus (E) to effect either nuclear export (F) or degradation (G), respectively, of the transcriptional repressors PLZF or Bcl6. Reproduced from reference (35).

It is then well accepted that HB-EGF-C is able to function in the nucleus, thus raising two intriguing questions: How is the newly synthesized proHB-EGF, which possesses ER retrieval activity, delivered to the PM? And how is HB-EGF-C targeted to the nucleus in response to shedding stimuli? In fact, HB-EGF shows bidirectional intracellular trafficking, anterograde and retrograde transport between the plasma membrane and ER (Figure 19), and is able to localize to five different subcellular compartments: the plasma membrane, Golgi apparatus, ER, nuclear envelope, and perinuclear vesicles.

In a recent study, the shedding of proHB-EGF and the subsequent trafficking of the cleaved HB-EGF-C fragment were analyzed in relation to the cell cycle and accordingly, with cellular proliferation (65). It was observed that in the early G1 phase, proHB-EGF is localized to the PM, with its shedding occurring during late G1 phase, where proHB-EGF is localized to the cytoplasm, and the HB-EGF-C migration into the nucleus was observed at the beginning of early S phase. During the S and G2 phases, HB-EGF-C is localized to the nucleus. Following internalization of endogenous HB-EGF into the nucleus, endogenous PLZF translocation to the cytoplasm occurs late in S phase, with complete migration of PLZF into the cytoplasm occurring in the G2 phase (65). ProHB-EGF shedding, nuclear translocation of HB-EGF-C, and nuclear export of PLZF might thus be a main mechanism for cell cycle progression of normal cells (65).

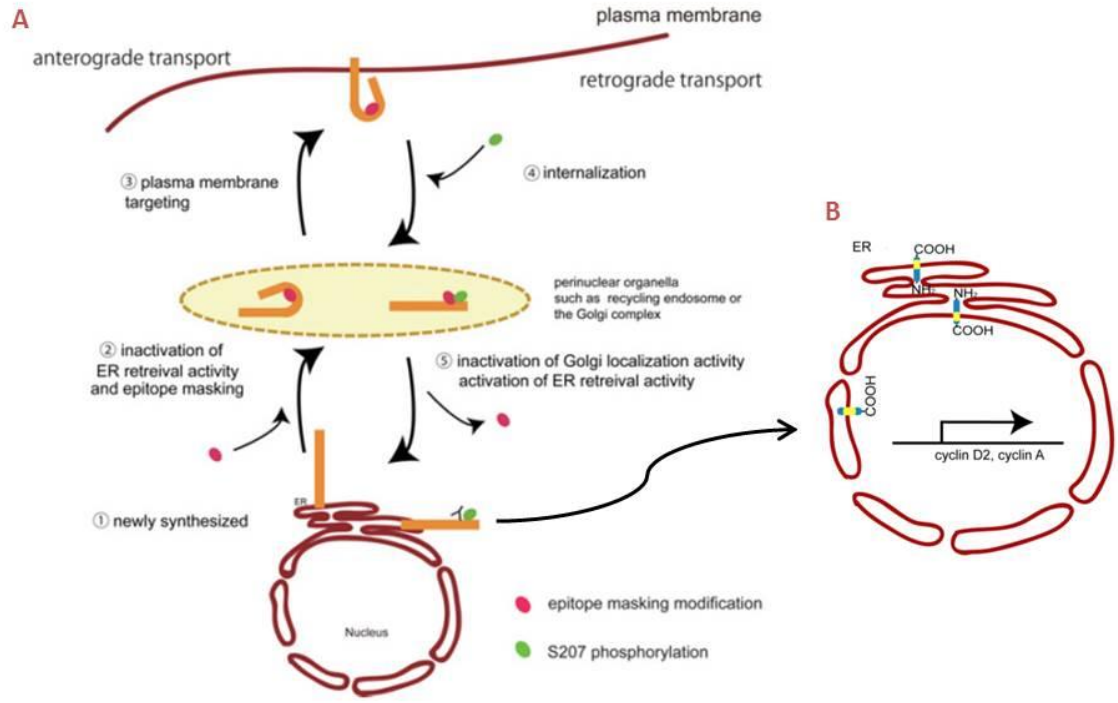

Figure 19 - A working model for the intracellular trafficking of proHB-EGF and HB-EGF-C regulated by post-translational modification. A, anterograde and retrograde transports. B, nuclear envelope targeting of HB-EGF-C. Since the newly synthesized proHB-EGF is sorted to the plasma membrane, it indicates that the ER/NE retrieval activity of HB-EGF-C is inactivated when proHB-EGF is synthesized. Evidences have shown that during or just after proHB-EGF is synthesized by ER-bound ribosomes, an epitope-masking posttranslational modification occurs in the cytoplasmic tail region - amino acids 199–208 - which suppresses ER retention/retrieval activity (185-198) via a conformational change. With ER targeting blocked, proHB-EGF is instead targeted to the plasma membrane. After exposure to shedding stimuli, a phosphorylation at S207 occurs in the carboxyl-terminal, which induces a conformational change and exposes the previously masked-epitope, which appear to regulate the activation of the retrograde transport to the Golgi apparatus and ER. Adapted from references (55,56).

In synthesis, APP and HB-EGF have functions, a complex cellular processing, and signaling pathways that partially overlap, with a putative interaction between these two proteins being innovative and of major importance in APP and HB-EGF physiologies, besides its potential contribution to our understanding of the AD pathogenesis.

3 Aims of the thesis

Given the several distinct roles that have been purposed for APP and its physiological relevance in developing and adult CNS, it is important to identify novel APP-binding proteins in order to better characterize APP function. From a large scale yeast two-hybrid screening of a human brain cDNA library using APP as bait, a novel promising APP interactor was identified, the EGF-like growth factor HB-EGF. Therefore, this master thesis focused on validating and characterizing the interaction between APP and HB-EGF, with the specific aims being:

- To confirm the interaction between APP and HB-EGF by yeast co-transformation;
- To validate the physiological APP/HB-EGF interaction *ex vivo* by GFP-Trap® pull-down assays;
- To monitor the subcellular localization of the APP/HB-EGF complex in mammalian cells;
- To evaluate the influence of APP and HB-EGF co-expression in MAPK and STAT3 signaling;
- To study the effect of APP:HB-EGF co-expression in the induction of cellular morphological changes.

4 Materials and Methods

4.1 Yeast two Hybrid Screening

4.1.1 YTH Screening workflow - Background

The original two-hybrid system was based on the yeast GAL4 transcription factor, involved in galactose metabolism, and is known as the GAL4 system (74). The two functional domains of a transcriptional activator, the DNA-binding domain (BD) and the transcription activation domain (AD), can be split apart and each fused to one of a pair of putative partner proteins in order to reconstitute the activator's ability to turn on a reporter gene. These two elements can be co-introduced into yeast strains modified with one or more reporter genes (the use of multiple reporter genes decreases the number of false positives obtained). These reporter genes have a binding site specific to the BD on their promoter region, causing the transcription of those genes to be dependent on the interaction between prey and bait proteins. Interaction of the BD-bait fusion with the AD-prey fusion, positions the AD in the proximity of the reporter gene, thus activating its transcription (75).

The MATCHMAKER GAL4 Two-Hybrid System 2 (Clontech) was used to perform yeast two-hybrid screens according to the manufacturer's instructions. The key components and features of the MATCHMAKER Two-hybrid System 2 (Clontech) are the reporter genes used, the yeast host strains, the optimized plasmids and the cDNA libraries, as detailed below.

Reporter genes. The reporter genes used in this system are the MEL1 gene (coding for α-galactosidase that is secreted into the culture medium) and the auxotrophic reporter genes HIS3 and ADE2, which allow yeast cells carrying interacting proteins to grow in medium lacking histidine and adenine. Additionally, the YTH bait plasmid pAS2-1 and the library plasmid pACT2, which contain the TRP1 and LEU2 genes, respectively, allow for selection in medium lacking tryptophan and leucine. Hence, the high-stringency selection consists of medium lacking tryptophan, leucine, histidine and adenine, and also in the presence of X-α-Gal (5-bromo-4-chloro-3-indolyl alpha-D-galactopyranoside). If the two proteins (bait and prey) interact, the reporter genes will be activated and the yeast will grow with a blue appearance of the colonies. The selection of positive clones with the "five" reporter genes was designed to reduce the number of false positives, thus allowing faster identification of true interactions with the bait protein.

Yeast host strains. The AH109 Saccharomyces cerevisiae strain was used, since it virtually eliminates false positives by using three reporters – ADE2, HIS3 and MEL1 – under the control of distinct GAL4-responsive upstream activating sequences (UAS) and promoter elements (TATA boxes).

Plasmids. The Gal4 DNA-BD fusion vector pAS2-1 and the Gal4-AD fusion vector pACT2 have multiple cloning sites that allow for the insertion of bait or library cDNA, respectively. They also carry a bacterial replication origin and an ampicilin resistance gene, for selection in bacteria. pAS2-1 contains the TRP1 gene for selection in Trp^- auxotrophic yeast strains (AH109, Y187 or diploids) and pACT2 contains the LEU2 gene for selection in Leu^- auxotrophic yeast strains (AH109, Y187 or diploids). Additionally, the YTH system includes yeast plasmids carrying Gal4-BD and Gal4-AD fusion cDNAs (pVA3-1 and pTD1-1) that provide controls for positive interactions, which were used to validate the method.

Baits and prey for the YTH screening. Bait-1 cDNA, coding for full-length human APP (isoform 695) and Bait-2 cDNA, coding for the intracellular domain of human APP_{695} with 50 amino acids, the AICD, had been previously PCR amplified and inserted in Clontech's GAL4 DNA-binding domain (GAL4-BD) expression vector pAS2-1, using *Nco*I/*Sma*I restriction enzyme sites, in frame with the GAL4 DNA-BD. The bait proteins were expressed as a fusion with the Gal4-BD in the yeast strain AH109.

The Human Brain MATCHMAKER cDNA Library (Clontech) used to perform the YTH screen (previous work from Dr. Sara Domingues in our laboratory) is a high-complexity cDNA library, expressing fusions of the prey proteins with the yeast Gal4-AD vector pACT-2 and pretransformed into the *S. cerevisiae* Y187 host strain.

YTH screening by Yeast Mating. A large scale yeast mating screening of several independent clones from human brain Matchmaker cDNA library (Clontech) was previously carried out in our laboratory (76). In this method, a yeast strain expressing the bait protein is mated with another yeast strain of opposite mating type pretransformed with the cDNA library. The diploid cells were plated in selective media with X-α-Gal and three reporter genes: HIS3, ADE2, and MEL1, allowing for the identification of the positive clones.

HB-EGF was identified as a positive clone when using the full-length human APP (isoform 695) cDNA as bait, which has propelled its selection for validation and further functional investigation during the current project. Yeast plasmid DNA was then extracted from the positive clones using the breaking buffer method (Yeast Protocols Handbook, Clontech) and the pACT2-library plasmids were rescued by transformation in *E. coli* XL-1 Blue.

The library cDNAs were identified by partial sequencing of the library insert with a primer that targets the GAL4-AD (Clontech), using an ABI PRISM 310 Genetic Analyzer (Applied Biosystems).

4.1.2 YTH cDNAs amplification and purification

The pACT2, pAS2-1 (vectors alone), pVA3-1, pTD1-1 (positive controls), pAS2-1-APP, pAS2-1-AICD (baits 1 and 2) and pACT2-HB-EGF (prey) cDNAs were all subjected to bacterial transformation, DNA isolation by "Midiprep" and were ultimately purified by ethanol precipitation as follows.

4.1.3 Bacteria transformation with plasmid DNA

Preparation of *E. coli* XL1-blue competent cells. A single colony of *E. coli* XL1-Blue was incubated in 10 ml of SOB medium at 37°C overnight. Then, 1 ml of this culture was used to inoculate 50 ml of SOB and the culture was incubated at 37°C with shaking at 220 rpm for 1-2 h, until OD_{550nm}=0.3. The culture was cooled on ice for 15 min and centrifuged at 4,000 g at 4°C for 5 min. The supernatant was discarded and then resuspended in 15 ml of Solution I (solutions in Appendix). After standing on ice for 15 min, cells were centrifuged at 4,000 g for 5 min at 4°C and 3 ml of Solution II were added to resuspend the cell pellet. The cells were immediately divided in 100 µl aliquots and stored at -80°C.

Bacteria transformation with plasmid DNA. *E. Coli* XL1-Blue competent cells were thawed on ice and the appropriate amount of DNA (plasmid DNA: 0.1-50 ng) was added to a 100 µl aliquot of competent cells and gently swirled. Cells were incubated on ice for 30 min and then subjected to an heat shock at 42°C for 90 sec, followed by a quick cooling on ice for 2 min. 900 µl of SOC medium was added to cells and a 45 min incubation at 37°C followed. The culture was then centrifuged at 14000 rpm for 30 sec, the supernatant was removed and the pellet was resuspended in the remaining volume (100 µl), and spread on the appropriate agar medium (LB/ampicillin or kanamycin agar plates). Plates were incubated at 37°C for 16-18 h.

4.1.3.1 Isolation of plasmid DNA from bacteria - Promega "Midiprep"

One colony of transformed bacteria with each cDNA was isolated, transferred to 3 ml of LB medium containing the appropriate antibiotic, and incubated for 16-18 h at 37°C with shaking (180 rpm). After bacterial growth, 250 µl of the culture was transferred to 250 mL of LB medium, also with the appropriate antibiotic, and again incubated overnight (O/N) at 37°C with agitation. Cells were then centrifuged at 5000 *g*, for 10 min (Beckman Avanti J-25 I -

Beckman Coulter), the supernatant was discarded and 6 ml of Cell Resuspension Solution was added. After resuspension, 6 ml of Cell Lysis Solution was added, gently mixed and incubated at RT for 3 min. Once the solution became clear and viscous, 10 ml of Neutralization Solution was added to the lysed cells and mixed. After precipitate formation, a PureYield™ Clearing Column was placed into a 50 ml disposable plastic tube and the lysate was poured into the column. After 2 min incubation, the PureYield™ Clearing Column was centrifuged at 1500 *g* for 5 minutes (Eppendorf Centrifuge 5810R). Then, a PureYield™ Binding Column was placed into a new 50 ml disposable plastic tube and the filtered lysate poured into it. Following an additional centrifugation step at 1500 *g* for 3 min, 5.0 ml of Endotoxin Removal Wash solution (with isopropanol added) was added to the PureYield™ Binding Column. Another centrifugation at 1500 *g* for 3 min followed, and the flow-through was discarded. The column was then washed with 20 ml of Column Wash Solution (with ethanol added) and centrifuged once again at 1500 *g* for 5 min. The flow-through was discarded and the centrifugation step was repeated for an additional 10 min, to ensure the removal of ethanol. To elute the DNA, the column was transferred to a new 50 ml disposable plastic tube and 600 µl Nuclease-Free Water was added to the DNA binding membrane in the PureYield™ Binding Column. The column was centrifuged at 1500-2000 *g* for 5 min one last time and the filtrate was collected and transferred to a microtube.

4.1.3.2 Purification of plasmid DNA by ethanol precipitation

Ethanol precipitation was also performed in order to concentrate nucleic acids as well as to increase DNA purification, which is essential for optimal transfections. Approximately 1/10 volume of 3M sodium acetate (pH 5.2) was added to the DNA solution, to adjust the salt concentration. Then, 2.5 volume of ice-cold 100% ethanol was added, mixed and incubated O/N at -20°C to allow the DNA precipitate to form. The DNA was recovered by centrifugation (14000 *g*, 15 min, 4 °C), the supernatant was carefully discarded and the pellets rinsed with 750 µl of ice-cold 70% ethanol (half of the tube capacity). The solutions were incubated for 15 min, at -20 °C, and then centrifuged (14000 *g*, 5 min, 4 °C). The supernatant was once again removed and the pellet allowed to dry. After all traces of ethanol have disappeared, the DNA was resuspended in Milli Q water and stored at -20°C. The DNA concentration and the 260/280 nm purity ratio was calculated by absorbance measurements.

4.1.4 Yeast transformation with plasmid DNA

4.1.4.1 Preparation of competent yeast cells

One yeast colony was inoculated into 1 ml of YPD medium in a microtube and vortexed vigorously to disperse cell clumps. The culture was transferred into a 250 ml flask containing 50 ml of YPD and incubated at 30°C with shaking at 230 rpm overnight, until it reached the stationary phase with OD_{600nm}>1. An amount of this culture (20-40 ml), sufficient to produce an OD_{600nm}=0.2-0.3, was transferred into 300 ml YPD in a 2 L flask. The culture was incubated at 30°C with shaking at 230 rpm, until OD_{600nm}=0.4-0.6, and then centrifuged at 4000 *g* for 5 min at room temperature. The supernatant was discarded and the cells resuspended in 25 ml of sterile H_2O. The cells were recentrifuged and the pellet resuspended in 1.5 ml of freshly prepared, sterile 1x TE/LiAc (lithium acetate solution).

4.1.4.2 Yeast transformation by the LiAc-mediated method

In a microtube, 200 ng of plasmid DNA were added to 100 µg of salmon testes carrier DNA. Then, 100 µl of freshly prepared competent cells were added to the microtube, followed by 600 µl of sterile PEG/LiAc (40% PEG 4000/ 1x TE/1X LiAc). The mixture was incubated at 30°C for 30 min with shaking (200 rpm). After adding 70 µl of DMSO, the solution was mixed gently and then heat-shocked for 15 min in a 42°C water bath. The cells were chilled on ice for 1-2 min and pelleted by centrifugation for 5 sec at 12,000 *g* and resuspended in 0.5 ml of sterile 1x TE buffer. Cells were then plated in the appropriate SD selection medium, and incubated at 30°C for 2-4 days, until colonies appeared.

4.1.5 Bait and Prey auto-activation test

In order to analyze the ability of the recombinant constructs to autonomously activate the reporter genes HIS3, ADE2 and MEL1, the bait plasmids pAS2-1-APP and pAS2-1-AICD, the prey plasmid pACT2-HB-EGF, and the pAS2-1 and pACT2 empty vectors were independently transformed into the AH109 yeast strain (Clontech), using the lithium acetate transformation method, as described above. The transformants were selected on medium without tryptophan (for APP, AICD and pAS2-1) and without leucine (for HB-EGF and pACT2), since the respective vectors contain the nutritional selection reporter genes TRP1 and LEU2. To verify that the Gal4-BD and the Gal4-AD fusion constructs do not intrinsically activate reporter genes, the transformants from the previous step were assayed for growth in medium lacking histidine and adenine and for blue appearance of the colonies in the presence of X-α-Gal. Briefly, the AH109 yeast cells independently transformed were plated on SD/-Trp/X-α-Gal, SD/-Trp/-His/X-α-Gal

and SD/-Trp/-Ade/X-α-Gal (for baits), and on SD/-Leu/X-α-Gal, SD/-Leu/-His/X-α-Gal and SD/-Leu/-Ade/X-α-Gal (for prey). The plates were incubated at 30°C for 2-4 days.

4.1.6 Verifying protein interactions in yeast by co-transformation

After testing APP, AICD and HB-EGF for HIS3, ADE2 and MEL1 reporter genes' intrinsic activation, protein interactions were verified by co-transformation of the AH109 yeast strain with each BD-bait (full-length APP and AICD) and the AD-prey (HB-EGF), using the lithium acetate method described above. In parallel, the pAS2-1 and pACT2 empty plasmids were co-transformed as an interaction negative control. A positive control is given by co-transformation of pVA3-1 and pTD1-1 vectors, which express the Gal4-BD-p53 and the Gal4-AD-SV40 large T antigen fusions, respectively. AH109 was thus co-transformed using the following plasmid pairs: pAS2-1/pACT2; pVA3-1/pTD1-1; pAS2- 1/HB-EGF-pACT2; APP-pAS2-1/pACT2; AICD-pAS2-1/pACT2; APP-pAS2-1/HB-EGF-pACT2; AICD-pAS2-1/HB-EGF-pACT2. The co-transformants were selected in SD/-Trp/-Leu medium. To confirm protein-protein interactions (reporter genes activation), fresh colonies of the co-transformants were assayed for growth on SD/TDO (SD/-Trp/-Leu/-His) and SD/QDO (SD/-Leu/-Trp/-His/-Ade) plates, and later on SD/QDO/X-α-Gal plate (SD/-Leu/-Trp/-His/-Ade/ X-α-Gal).

4.2 APP-GFP and Myc-HB-EGF mammalian expression cDNAs

The green fluorescent protein (GFP), obtained from *Aequorea victoria*, is widely used in transfection experiments to study the dynamics and characteristics of gene expression in a non-invasive manner. For this reason, the generation of GFP-fusion proteins is one of the favorite methodologies for immunofluorescence analysis. Wt APP cDNA (isoform 695) fused to GFP was already available at the laboratory, having been one of the constructs selected for performing the several studies in the scope of this master thesis. Briefly, parental APP cDNA was subcloned into the pEGFP-N1 vector (Clontech), a plasmid that encodes GFP. The result was a fusion gene of APP with GFP in its C-terminal (77,78).

The HB-EGF clone cDNA was obtained from Human Brain Matchmaker cDNA library (Clontech), which contains fusions of the prey proteins with the yeast Gal4-AD vector pACT-2. The pACT2-HB-EGF DNA had been previously extracted from the positive clones obtained in the screening by large scale yeast mating and was rescued by transformation in *E. coli* XL-1 Blue.

4.2.1 APP-GFP and pACT2-HB-EGF cDNAs amplification and purification

Both constructs were amplified and recovered from *E.coli* XL-1 Blue. Isolation and purification of plasmid DNA was performed using the Promega Pure Yield Plasmid Midiprep System. Both DNAs were further purified by ethanol precipitation. These procedures were previously described in section 4.1.3.

4.2.2 Generation of the Myc-HB-EGF construct

The HB-EGF cDNA was digested and inserted into pCMV-Myc (Clontech), a mammalian expression vector containing the human cytomegalovirus (CMV) promoter and a Myc tag N-terminal to the multiple cloning site (MCS). The Myc epitope tag was chosen due to its small size, unlikely to affect the tagged protein's biochemical properties. The pCMV-Myc-HB-EGF construct was thus created from pACT2-HB-EGF, using standard cloning procedures (Table 2), having the insert been cloned in frame with the Myc coding sequence.

Table 2 - Cloning strategy followed to obtain the pCMV-Myc-HB-EGF fusion construct.

Vector and Insert
DNA amplification in *E.coli* XL1-Blue
DNA isolation by "Midiprep"
Ethanol precipitation
Simultaneous digestion with *EcoR*I and *Xho*I
Incubation with alkaline phosphatase
Restriction fragment analysis of DNA
DNA extraction from the Agarose Gel
Vector and Insert DNA purification
Ligation of Vector and Insert
Transformation of ligation mixtures into *E.Coli* XL1-Blue
Isolation of plasmids from transformants by "Miniprep"
Identification of insert-containing plasmids by restriction analysis
DNA "Midiprep"

4.2.2.1 Plasmid DNA digestion with restriction enzymes

Firstly, to express a recombinant Myc-tagged HB-EGF protein, the plasmid DNA pCMV-Myc (Clontech) was simultaneously digested with *Eco*RI and *Xho*I (both from New England

Biolabs, NEB) restriction endonucleases. The pACT2-HB-EGF DNA was simultaneously digested with the same restriction enzymes. For a typical DNA digestion the manufacturer's instructions were followed. In a 1.5 ml microtube the following components were added:

- 100 µg/ml DNA
- 1x reaction buffer (specific for each restriction enzyme)
- 1 U/µg DNA of restriction enzyme
- 0.1 µg/µl BSA
- Milli Q water to make the volume up to 20 µl

The mixture was incubated at the appropriate temperature (37°C for both enzymes) for 4 hours before further analysis.

4.2.2.2 Alkaline phosphatase treatment

In order to prevent self-ligation of pCMV-Myc vector molecules, the digested plasmid DNA was first incubated with shrimp alkaline phosphatase (SAP) (ROCHE) before ligation. According to the manufacturer's instructions, the reaction mixture was adjusted with 1/10 volume 10X concentrated dephosphorylation buffer, and incubated with 1 µl of SAP at 37°C for 1 h. Finally, SAP was inactivated by heating the reaction mixture at 65°C for 15 min.

4.2.2.3 Restriction fragment analysis - DNA Gel Electrophoresis

The electrophoresis apparatus was prepared and the electrophoresis tank was filled with 1x TAE buffer to cover the agarose gel. The appropriate amount of agarose was transferred to an Erlenmeyer with 50 ml 1x TAE. The slurry was heated until the agarose was completely dissolved and allowed to cool to 60°C before adding 1,25 µl GreenSafe (Nzytech). The agarose solution was poured into the gel cast and the comb was positioned. After the gel became solid the comb was carefully removed and the gel immersed in the tank. The DNA samples were mixed with 6x loading buffer and the mixture was loaded into the slots of the submerged gel using a micropipette. Marker DNA was also loaded into the gel (1 Kb plus DNA ladder, Invitrogen). The lid of the gel tank was closed and the electrical leads were attached so that the DNA migrated towards the anode. The gel run at 90-100V until the bromophenol blue had migrated the appropriate distance through the gel. At the end, the gel was examined by UV light and analyzed on a Molecular Imager (Biorad).

4.2.2.4 DNA extraction from Agarose Gels

The QIAquick Gel Extraction Kit Protocol (Qiagen) was used to extract and purify the cleaved pCMV-Myc and pACT2-HB-EGF plasmids from the agarose gel. Firstly, the DNA fragments were excised from the agarose gel with a clean, sharp scalpel, minimizing the size of the gel slices. Each gel slice was then weighted and 3 volumes of Buffer QG to 1 volume of gel (100 mg ~ 100 µl) were added. The sample was incubated at 50°C until the gel slice had completely dissolved. After checking the yellow color of the mixture, which corresponds to a pH<7.5, a QIAquick spin column was placed in a provided 2 ml collection tube. To bind DNA, the sample was applied to the QIAquick column, and centrifuged for 1 min. The flow-through was discarded and the QIAquick column was placed back in the same collection tube. Then, 0.5 ml of Buffer QG were added to QIAquick column and centrifuged for 1 min, to remove all traces of agarose. To wash, 0.75 ml of Buffer PE were added to QIAquick column and centrifuged for 1 min. The flow-through was discarded and the QIAquick column was centrifuged for an additional 1 min. The QIAquick column was then placed into a clean 1.5 ml microcentrifuge tube and the DNA was eluted by adding 30 µl of Buffer EB to the center of the QIAquick membrane and centrifuging the column for 1 more min. All centrifugation steps were carried out at ~13,000 rpm in a conventional table-top microcentrifuge.

4.2.2.5 Vector and Insert DNA purification

The QIAGEN DNA Purification kit was used to purify the DNA fragments from the enzymatic reactions. It allowed DNA purification by using QIAquick spin columns (silica-membrane-based columns). Briefly, 5 volumes of buffer PB (QIAGEN) were added to 1 volume of the solution to be purified and mixed. The spin column was placed in a collection microtube and the sample was applied to the column and centrifuged for 1 min at 12,000 *g* to bind the DNA. The flow-through was discarded and the column was washed with 0.75 ml of buffer PE (QIAGEN), centrifuged for 1 min at 12,000 *g* and the flow-through discarded. The column was placed back in the same microtube and centrifuged again to remove traces of washing buffer. Then, the column was placed in a clean microtube, 30 µl of Buffer EB (QIAGEN) were added and allowed to stand for 1 min. To elute the DNA, the column was centrifuged for 1 min at 12,000 *g*.

4.2.2.6 Ligation of Vector and Insert

The T4 DNA ligase (NEB) was used to join the *EcoR*I/*Xho*I-digested pCMV-Myc and the HB-EGF fragment, in order to obtain the pCMV-Myc-HB-EGF construct. To carry out the ligation reaction, 50 ng of vector DNA from the previous step was transferred to a microtube with

three times the equimolar amount of insert DNA. 2 µl of 10x T4 DNA ligase buffer and 1 µl of T4 DNA ligase (New England Biolabs) were added to the reaction mix and H_2O was added to a final volume of 20 µl. The reaction was carried out for 16 h at 16°C. An aliquot (5 µl) of the DNA ligation mixture was then subjected to bacterial transformation and plated onto ampiciline-containing selective media as described previously (section 1.1.3).

4.2.2.7 Isolation of plasmids from transformants - "Miniprep"

In order to screen for the recombinant plasmid in the transformants, the plasmid DNA was extracted from several isolated bacterial colonies by alkaline lysis "miniprep", for subsequent restriction fragment analysis, as follows. A single bacterial colony was transferred into 3 ml of LB medium containing ampicillin (50 µg/ml) and incubated overnight at 37°C with vigorous shaking (220-250 rpm). 1.5 ml of this culture was transferred into a microtube and centrifuged at 12,000 *g* for 1 min at 4°C and the supernatant was discarded. The cell pellet was resuspended in 100 µl of ice-cold Solution I by vigorous vortexing. Then, 200 µl of freshly prepared Solution II were added to the microtube that was mixed by inverting several times. Keeping the microtube on ice, 150 µl of ice-cold Solution III were added and again the microtube inverted several times. After the microtube was allowed to stand on ice for 5 min, it was centrifuged at 12,000 *g* for 10 min at 4°C and the supernatant transferred to a clean microtube. The DNA was purified by ethanol purification as previously described (section 4.1.3.2) and stored at -20°C.

4.2.2.8 Identification and purification of insert-containing plasmids

After plasmid DNA extraction from bacteria, the DNA was further analyzed by restriction digestion with the endonucleases *Eco*RI and *Xho*I and the restriction fragments submitted to electrophoretic analysis as described above. Once confirmed that the ligation procedure had been successful for the selected transformants, the pCMV-Myc-HB-EGF construct was once again amplified by bacteria transformation and isolated by Promega "Midiprep", which yielded transfection-quality plasmid DNA. The manufacturer's instructions were followed, as described previously in section 4.1.3.

4.3 Mammalian cell asssays

4.3.1 Culture and maintenance of the HeLa cell line

Immortal cell lines are a very important tool for research into the biochemistry and cell biology of multicellular organisms. HeLa cells are an immortalized cell line derived from human

cervical epithelia cancer cells, originally taken from a cancer patient, Henrietta Lacks. Since this is an immortalized cell line, HeLa cells have evaded normal cellular senescence and instead can keep undergoing division, allowing their growth for prolonged periods *in vitro*. Indeed, this cell line was found to be remarkably durable and prolific, which made this cell line our choice for all the research experiments performed.

HeLa cells were cultured in Dulbeco's Minimal Essential Media supplemented with 1% Non-Essential amino acids (Gibco), 10% heat inactivated Fetal Bovine Serum (FBS; Gibco) and 1% antibiotic/antimycotic (AA) mix (Gibco). Cultures were maintained at 37°C under 5% CO_2 in a humidified incubator. Cells were subcultured whenever 80-90% confluence was reached.

4.3.2 Transient transfection of the HeLa cell line with APP-GFP and Myc-HB-EGF cDNAs

In order to be able to study the effects of APP and HB-EGF activity and interaction through transient transfection experiments, HeLa cells were grown on plastic culture dishes (12-well, 6-well and 60 mm), having been seeded 24 h before transfection, so that cells could be around 70 to 80% confluence at the time of the transfection. The growth medium was changed immediately prior to the transfection procedure and HB-EGF, along with Wt APP-GFP cDNA, was transfected into HeLa cells. Single-transfection of HB-EGF and Wt APP-GFP cDNA was also performed for some experiments. As experimental controls, single-transfection of pEGFP-N1 and pCMV-Myc vectors, or co-transfection of both empty vectors (EGFP:Myc) was also accomplished.

4.3.3 Transfection using the Turbofect™ Reagent

All the transfection procedures were performed using the TurboFectTM reagent (Fermentas Life Sciences). The TurboFect™ transfection reagent is a cationic polymer that forms a positively charged complex with DNA that is easily endocytosed by eukaryotic cells. Briefly, for each well of a 12-well plate, 1 µg of cDNA was diluted in 50 µl of serum-free growth medium and for each well of a 6-well plate, 2 µg of cDNA were diluted in 100 µl of serum-free growth medium. When using a 60 mm plate, 4 µg were diluted in 400 µl of serum-free growth medium. After gently vortexing the plate, a ratio of 1.5-2:1 µl of TurboFect™ reagent was added to the DNA, mixed and incubated during 15-20 min at RT. It was then added to each well and mixed by gently agitating the plate. The cells were incubated at 37°C in a 5% CO2 incubator. After 6 h the cell medium was changed, and at 24 h of total transfection time, cells were collected.

4.3.4 Cells stimulation with EGF

Confluent cell monolayers were stimulated with 100 ng/ml of Human Epidermal Growth Factor (EGF; Cell Signaling). For signaling studies purposes, EGF was added 1 hour before cell collection 23h post-transfection. When the aim was to visualize the EGF effect on cells morphology through immunocytochemistry procedures, EGF was added to the cell medium 1 hour after transfection with plasmid DNA, and left until a total of 24h of transfection, after which cells were fixed.

4.3.5 Protein synthesis inhibition with CHX

HeLa cells independently transfected for 23h with the pCMV-Myc vector or the pCMV-Myc-HB-EGF constructs were treated for 1h with 50 µg/ml cycloheximide (CHX; Sigma) in FBS-DMEM, and harvested with 1% SDS. The total protein content of the cellular lysates was determined and samples subjected to western blotting, as described below, to evaluate the APP levels.

4.4 Proteomic assays

4.4.1 Cell collection and quantification of protein content (BCA)

Transfected cells were harvested in 150 µl (12-well), 250 µl (6-well) or 550 µl (60 mm plate) 1% SDS for WB and boiled at 90°C for 10 min, followed by a 10 sec sonication period, and storage at -20°C. The cell collection procedure for GFP-Trap® Pull-Down Assay is slightly different and is described further ahead.

The protein content of cell lysates was carried out using the Pierce's bicinchoninic acid (BCA) protein assay kit (Thermo Scientific), following the manufacturer's instructions. The whole procedure was performed using a 96-well plate for spectrophomotmetric analysis. Standard samples were prepared using increasing known amounts of bovine serum albumin (BSA), as depicted in Table 3. The remaining samples were prepared by mixing 5 µl of the cell lysate with 20 µl 1% SDS. Duplicates of all samples were assayed by this method.

Table 3 - Standards used in the BCA protein assay method. BSA, Bovine serum albumin solution (2 mg/ml).

Standard	BSA (µl)	1% SDS (µl)	Protein Mass (µg)
Blank	0	25	0
P1	1	24	2
P2	2	23	4
P3	5	20	10
P4	10	15	20
P5	20	5	40

The working reagent was prepared by mixing the BCA reagent A with the BCA reagent B in a 50:1 proportion, and 200 µl of this mixture were added to each well. The plate was incubated for 30 min at 37°C, after which the absorbance at 562 nm was measured using a microplate reader (Infinite M200, Tecan). A standard curve was obtained by plotting BSA standard absorbance vs BSA concentration, and used to determine the total protein concentration of each sample.

4.4.2 GFP-Trap Pull-Down assays

For biochemical interaction studies, GFP-fusion proteins and their binding partners can be fast and efficiently isolated via pull-down of the GFP moiety with GFP-Trap® (Chromotek). Therefore, GFP-Trap Pull-Down assays were performed in order to confirm and further analyze APP binding to HB-EGF. After HeLa cells co-transfection with the APP-GFP and the Myc-HB-EGF cDNAs for 24h, cells were incubated with the DSP crosslinker (Pierce) for 45 min at room temperature. Then, cells were washed in 1x PBS and subsequentely collected with a scrapper in 1 ml of cold PBS with 1x PMSF solution. Samples were then centrifuged for 5 min at 3000 *g* (4°C), the supernatant was removed and 500 µl of freshly prepared lysis buffer was added to the pellet. The cell membranes were further disrupted by sonication for 10 s. Samples were maintained on ice for 30 min and vortexed twice, with 10 min intervals. Meanwhile, the GFP-Trap beads (Chromotek) were washed 4 times in freshly prepared wash buffer, isolated by a magnet and kept at 4°C. After 30 min, the sample was centrifuged for 5 min at 10,000 *g* (4°C), and the supernatant transferred to a new microtube, being the pellet discarded. 25 µl of supernatant were transferred to a microtube with 12 µl of Loading Buffer/10% SDS, always keeping the sample on ice (“Cell Lysates”). 10 µl of supernatant were collected to perform BCA protein quantification in order to aliquot mass-normalized lysates. The volume of the mass-normalized lysates was adjusted to 300 µL with freshly prepared dilution buffer and 5-10 µl of GFP-Trap beads were transferred to each sample, followed by an incubation step of 4h with orbital shaking at 4°C. The mixture was then subjected to magnetic separation with a magnet, the supernantant was fully discarded and the magnetic complexes magnetically washed with 300 µl of wash buffer for 3 times. The magnetic complexes were then ressuspended in 100 µl of Loading Buffer/1% SDS (“Pull-Down”) and boiled for 10 min to dissociate the GFP-Trap beads from the protein complexes. Afterwards, the GFP-Trap was magnetically separated and the supernatant transferred to a new microtube. Lysates, supernatants and precipitates were then resolved in a 5-20% SDS–PAGE followed by immunoblotting. For the pull-down assays in 60 mm culture dishes, an initial step was added in the beginning of the procedure to minimize

protein degradation, with cells being washed 2x in cold PBS and kept on ice in the first 10 min of incubation with the DSP cross-linker.

4.4.3 Western Blot (WB) assays

Mass-normalized samples were resolved by electrophoresis on a 5-20% gradient sodium dodecylsulfate polyacrylamide gel (SDS-PAGE). The samples were prepared by the addition of ¼ volume of loading gel (4x LB) buffer and subjected to electrophoresis, after what protein samples were electrotransferred to a nitrocellulose membrane.

4.4.3.1 Ponceau Red staining of protein bands

Ponceau Red staining is normally applied to assess successful electrotransfer of proteins to the nitrocellulose membrane. It can also be used as a loading control in an alternative to actin or β-tubulin, when these proteins levels vary with the experimental conditions. This type of staining is fast, inexpensive, nontoxic, and it is fully reversible in a few minutes (79). The nitrocellulose membranes were incubated in Ponceau S solution (Sigma Aldrich) for 7 min, followed by a wash with deionized water for making the protein bands clearly visible. Membranes were then scanned in a GS-800 calibrated imaging densitometer (Bio-rad), after which membranes were washed with 1X TBS-T and water for complete removal of the staining.

4.4.3.2 Immunodetection

Concerning the immunological detection, briefly, after transferring the proteins, membranes were first hydrated in 1X TBS for 10 min, and then blocked for unspecific antibody binding sites. This was ensured by incubating the membrane for 1-2 h with 5% non-fat dry milk (or BSA, according to the manufacturers' instructions) in 1X TBS-T. Incubation with the primary antibody was performed according to the manufacturer indications, or according to previously optimized experiments with the incubation time ranging from 2 h to O/N incubation. After 3 washes with 1x TBS-T, membranes were incubated for 2 h with the secondary antibody, diluted either in 3% non-fat dry milk or BSA in 1X TBS-T solution. Antibodies dilutions are further presented in Table 4. Membranes were subsequently washed 3 times with TBS-T before submission to signal development.

Immunodetection was carried out using horseradish peroxidase-conjugated secondary antibodies, and membranes were submitted to signal development using either homemade enhanced chemiluminescence (ECL) or Luminata^{TM} Crescendo (Millipore) reagents. Both of the reagents work as a substrate to horseradish peroxidase, producing a chemiluminescent signal.

In a dark room, membranes were incubated for 1 min at RT with ECL or for 5 min with Luminata™ Crescendo, and then an autoradiography film (GE Healthcare) was placed on the top of the membrane and placed inside an x-ray film cassette. The excess of detection reagent was drained off the membrane. After the exposure (with time varying depending on the protein being detected), the film was developed in developing solution (Sigma Aldrich), washed in water and fixed in fixing solution (Sigma Aldrich). The membrane was further washed with 1x TBS-T and deionized water before drying. The autoradiograms were scanned in a GS-800 calibrated imaging densitometer (Bio-Rad) and immunoreactive bands were quantified by densitometric analysis with QuantityOne software (Bio-Rad Laboratories), using Ponceau Red Staining as an internal control.

4.4.3.3 Antibodies used in WB assays

In the WB assays, several antibodies were used. The monoclonal anti-APP 22C11 (Chemicon), directed against APP N-terminus, and the polyclonal anti-APP CT695 (Invitrogen) directed against APP C-terminus, both recognizing full-length APP, enabled the evaluation of APP and APP-GFP cDNA levels. The monoclonal anti-Myc-Tag (Cell Signaling Technology) and the polyclonal anti-HB-EGF antibodies (Antibodies online) were used to detect Myc-HB-EGF and HB-EGF.

To evaluate the effect of HB-EGF and APP in MAPK/Erk signaling, two antibodies were used: the monoclonal anti-phospho-MAP Kinase (Millipore), directed against the phosphorylated Tyr185/Tyr187 residues, and the polyclonal anti-MAP Kinase (Millipore) antibody; both of these recognize the p44 and the p42 MAP kinases (ERK 1 and 2).

To evaluate the effect of HB-EGF and APP in STAT3 signaling, two antibodies were used: the monoclonal anti-phospho-STAT3 (Millipore), directed against the phosphorylated Tyr705 residue, and the monoclonal anti-STAT3 (Cell Signalling Technology) antibody; both of these recognize the alpha and beta STAT3 isoforms. All the secondary antibodies, either recognizing mouse or rabbit IgGs, were goat antibodies labeled with horseradish peroxidase (GE Healthcare).

The polyclonal anti-EGF and anti-EGFR antibodies were used to evaluate EGF and EGFR protein levels, respectively, and to test for interaction with APP. In Table 4 are represented the primary and secondary antibodies used, as well as their respective dilutions.

Table 4 - Antibodies used in the Western Blotting, respective target proteins and their sizes, and specific dilutions used.

Target Protein	Size (kDa)	Primary Antibody	Secondary Antibody
APP (N-terminal)	100-150	Monoclonal 22C11 (Chemicon); Dilution: 1:250	Horseradish Peroxidase conjugated α-Mouse IgG; Dilution: 1:5000
APP (C-terminal)	100-150	Polyclonal CT695 (Invitrogen); Dilution: 1:500	Horseradish Peroxidase conjugated α-Rabbit IgG; Dilution: 1:5000
Myc-Tag	NA	Monoclonal Anti-Myc-Tag (9B11) (Cell Signaling Technologies) Dilution: 1:5000	Horseradish peroxidase conjugated α-Mouse IgG; Dilution: 1:5000
Phospho-Thr185/Tyr187 MAP kinase	42 and 44	Monoclonal Anti-phospho-MAP Kinase 1/2 (Erk 1/2) (Thr185/Tyr187), clone AW39 (Millipore) Dilution: 1:1000	Horseradish peroxidase conjugated α-Rabbit IgG; Dilution: 1:5000
MAP Kinase	42 and 44	Polyclonal Anti-MAP Kinase 1/2 (Erk1/2), CT (Millipore); Dilution: 1:1000	Horseradish peroxidase conjugated α-Rabbit IgG; Dilution: 1:5000
Phospho-Tyr705 STAT3	76 and 84	Monoclonal Anti-phospho-STAT3 (Tyr705) (Millipore); Dilution: 1:3000	Horseradish Peroxidase conjugated α-Rabbit IgG; Dilution: 1:1000
STAT3	76 and 84	Monoclonal Anti-STAT3 (124H6) (Cell Signaling Technology); Dilution: 1:2000	Horseradish Peroxidase conjugated α-Mouse IgG; Dilution: 1:2000
HB-EGF (mature domain)	14-30	Polyclonal Anti-HB-EGF (Antibodies-online); Dilution: 1:500	Horseradish Peroxidase conjugated α-Rabbit IgG; Dilution: 1:1000
EGF	5.8/133	Polyclonal Anti-EGF (C-Term) (Antibodies-online); Dilution: 1:500	Horseradish Peroxidase conjugated α-Rabbit IgG; Dilution: 1:1000
EGFR	180	Polyclonal Anti-EGFR (Millipore); Dilution: 1:500	Horseradish Peroxidase conjugated α-Rabbit IgG; Dilution: 1:5000

4.5 Immunocytochemistry (ICC) assays

In order to evaluate if and were APP and HB-EGF co-localize in mammalian cells, subcellular localization studies were carried out using HeLa cells. Immunocytochemistry of HeLa cells co-transfected with EGFP:Myc, APP-GFP:Myc, EGFP:HB-EGF, and APP-GFP:HB-EGF were performed. Besides these conditions, a set of immunocytochemistry analysis with transfected cells under sEGF influence was also performed.

4.5.1 Sample preparation and immunodetection

After 24h of transfection with the Turbofect Reagent, HeLa cells grown on coverslips were fixed with 4% paraformaldehyde in PBS for 30 min. Fixed cells were washed 3 times with 1x PBS and permeabilized with a 0.2% TRITON PBS solution during 10 min. After another 3 washes, cells were covered with 1x PBS/3% BSA blockage solution for 30 min. Cells were then incubated with the primary antibodies diluted in 1x PBS/3% BSA for 2 h at RT (respective dilutions are presented in Table 5). The antibodies were removed by washing 3 times with 1x PBS and the specific secondary antibodies were incubated for 1 h at RT (see Table 5). After another 3 washes with 1x PBS and one additional wash with deionized water, coverslips were mounted on microscope glass slides and embedded in VECTASHIELD® antifading-reagent, with or without DAPI for nucleic acid staining (Vector Laboratories).

Fluorescence microscopy was carried out in a LSM 510 Meta confocal microscope (Zeiss) using an Argon laser line of 488 nm (green channel), a 561 nm DPSS laser (red channel), and a Diode 405-430 laser (blue channel). Images were acquired with a 63x water immersion objective.

4.5.2 Antibodies used in ICC assays

For the immunocytochemistry procedures, the monoclonal anti-Myc-Tag antibody (Cell Signaling Technology) and the polyclonal anti-HB-EGF antibody (antibodies-online) were used. These antibodies were used to visualize the co-localization of APP and HB-EGF and to analyze the effects of HB-EGF and APP-GFP overexpression in the cell. The secondary antibodies used were the anti-mouse and the anti-rabbit Texas Red-conjugated antibodies, the anti-rabbit Alexa Fluor 350, and the anti-mouse Alexa Fluor 488-conjugated antibodies (Molecular Probes). The list of the primary and secondary antibodies used for the immunocytochemistry procedures as well as their respective dilutions are present in Table 5.

Table 5 - Antibodies used in immunocytochemistry, respective target proteins and specific dilutions used.

Target Protein /Epitope	Primary Antibody	Secondary Antibody
Myc-Tag	Monoclonal Anti-Myc-Tag (9B11) (Cell Signaling Technologies) Dilution: 1:5000	Texas Red® Goat Anti-Mouse IgG (Life Technologies) or Alexa Fluor® 488 Goat Anti-mouse (Molecular Probes) Dilution: 1:300
HB-EGF	Polyclonal Anti-HB-EGF (antibodies-online); Dilution: 1:100	Texas Red® Goat Anti-Rabbit IgG (Life Technologies); Dilution: 1:300

4.6 Data analysis

The protein bands resultant from the immunobloting procedures were quantified using the Quantity One densitometry software (Bio-Rad). Data from HB-EGF and APP-GFP cDNAs transfected cells were compared to cells transfected only with the pCMV-Myc and EGFP-N1 empty vectors. All applicable data are shown as mean values ± SEM (standard error of the mean). The Student's *t*-test was used to determine the significance of differences between population means. Statistical significance analysis was conducted by one way analysis of variance (ANOVA) followed by the Tukey test.

5 Results

5.1 Confirmation of APP - HB-EGF binding by Y2H

As previously mentioned, HB-EGF was identified as a positive clone in a large scale yeast mating, when using the full-length human APP (isoform 695) cDNA as bait, which propelled its selection for further investigation.

Although the Y2H system offers numerous advantages comparing to biochemical methods, the novel PPIs identified by large-scale YTH screening should be validated, at first in the YTH system, and then confirmed by other methods, in order to exclude all classes of false positives. Therefore, from this point forward, our primary goal was to validate APP/HB-EGF interaction. Additionally, we also tested whether the interaction was mediated by the AICD using the yeast two hybrid system.

5.1.1 Bait and prey autoactivation test

Firstly, before studying any possible interactions between baits and prey, it was necessary to demonstrate that the bait and the prey proteins do not autonomously activate the reporter genes HIS3, ADE2 and MEL1, for example, due to intrinsic DNA-binding and/or transcriptional activation sequences.

In order to address this topic, both bait plasmids (pAS2-1-APP and pAS2-1-AICD) and the prey plasmid (pACT2-HB-EGF) were independently transformed into the AH109 yeast strain and tested for growth in selective media lacking His and Ade.

None of the bait plasmids neither the prey plasmid were able to drive the expression of the nutritional reporter genes HIS3 and ADE2, since no growth was detected (Table 6). Likewise, the colorimetric reporter gene MEL1 was not activated by any of the fusion constructs, since no blue color was detected in the SD/-Trp/X-α-Gal or SD/-Leu/X-α-Gal. The Gal4-BD fusion genes and the Gal4-AD fusion gene behaved similarly to the pAS2-1 and pACT2 empty vectors, which were expressed as negative controls (Table 6).

Table 6 - Results of the baits and prey autoactivation tests.

		Growth and Blue color		
		SD/-Trp/X-α-Gal or SD/-Leu/X-α-Gal	SD/-Trp/-His/X-α-Gal or SD/-Leu/-His/X-α-Gal	SD/-Trp/-Ade/X-α-Gal or SD/-Leu/-Ade/X-α-Gal
Bait	APP	White colonies	No growth	No growth
	AICD	White colonies	No growth	No growth
	Negative control (empty pAS2-1)	White colonies	No growth	No growth
Prey	HB-EGF	White colonies	No growth	No growth
	Negative control (empty pACT2)	White colonies	No growth	No growth

5.1.2 Validation of the APP/HB-EGF interaction by yeast co-transformation

Once confirmed that APP, AICD and HB-EGF do not induce HIS3, ADE2 and MEL1 reporter genes' intrinsic activation, a yeast co-transformation assay was performed in order to confirm the interaction between APP and HB-EGF. Interaction of HB-EGF with the APP intracellular domain (AICD) was also tested, to shed light on the APP motif responsible for the interaction.

pACT2-HB-EGF (prey plasmid) and both pAS2-1-APP and pAS2-1-AICD (bait plasmids) were successfully co-transformed in yeast strain AH109 and the co-transformants were tested in SD/TDO, SD/QDO and SD/QDO/X-α-Gal medium.

The authenticity of the interaction between the HB-EGF clone and the full-length APP was confirmed by the ability to grow and turn blue on SD/QDO/X-α-Gal plates, which indicates expression of all the reporter genes HIS3, ADE2 and MEL1. In fact, the appearance was similar to the positive control that co-expressed the Gal4-BD-p53 and Gal4-AD-SV40 fusion proteins (Figure 20). The Gal4-BD and Gal4-AD empty vectors (pAS2-1 and pACT2) were co-expressed as a negative control, which, as expected showed no positive colonies (Figure 20, B). YTH tests were also carried out with yeast cells transformed with single bait or prey constructs. While all yeast constructs were able to grow on the YPD rich medium (data not shown), only co-expression of BD-bait and AD-prey fusion proteins conferred survival on SD/QDO plates. Some colonies started to appear after 2-3 days, but the plates were incubated for 8 days (TDO) or 16 days (QDO) to allow slower growing colonies to appear. According to the Clontech's MATCHMAKER YTH System User Manual, true His^+, Ade^+ colonies are robust and can grow to more than 2 mm in diameter. The small, pale colonies that may appear after 2 days but never grow more than 1 mm should not be considered as positives clones.

On the other hand, no growth of pAS2-1-AICD – pACT2-HB-EGF colonies neither in the triple DO nor in the quadruple DO was verified (Figure 20, B). This means that HIS, ADE2 and

MEL1 reporter genes were not activated and thus no interaction occurred between the Gal4-BD and Gal4-AD. Hence, we can conclude that the interaction between APP and HB-EGF is not mediated by the APP Intracellular Domain.

In conclusion, the results obtained showed that HB-EGF interacts with APP via APP domains other than the C-terminus of APP.

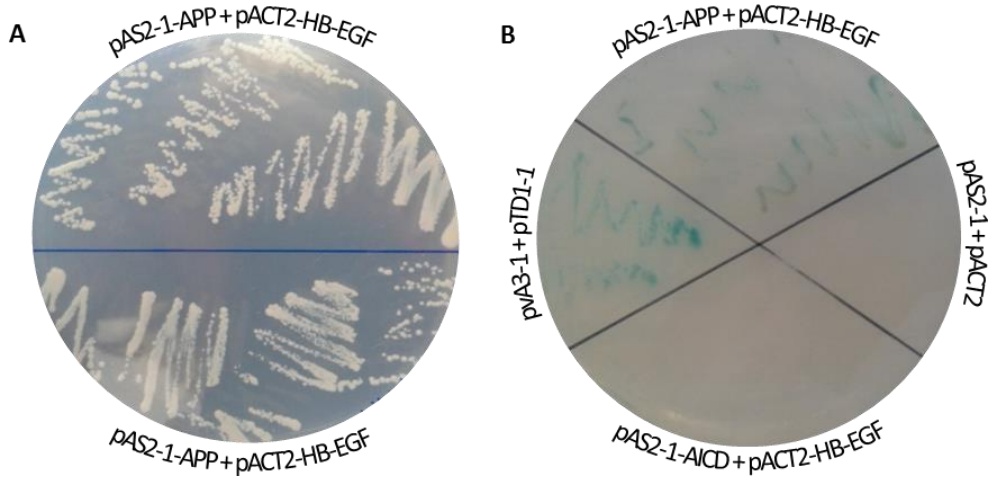

Figure 20 - Qualitative confirmation of the interaction between APP and HB-EGF by Yeast co-transformation. (A) Growth of yeast cells co-transformed with APP and HB-EGF constructs was first analyzed by streaking into quadruple dropout (QDO; -Leu, -Trp, -His, -Ade). (B) Yeast cells co-transformed with pACT2-HB-EGF+pAS2-1-APP, pACT2-HB-EGF+pAS2-1-AICD, and with the plasmid positive (pvA3-1+pTD1-1) and negative (pAS2-1+pACT2) controls were grown on QDO medium with X-α-Gal to test for α-galactosidade activity.

5.2 APP Interplay with HB-EGF

The YTH presents some intrinsic limitations that should be considered. For this reason, and although several control procedures were performed, the validation of the detected interaction by other independent methods was imperative.

5.2.1 Generation of the Myc-HB-EGF construct

In order to perform biochemical studies, mammalian expression constructs were needed. Although the APP-GFP construct was already available at the laboratory, no HB-EGF construct was available to express in mammalian cells. Therefore, subcloning procedures were performed in order to generate a ready to transfect cDNA. The pCMV-Myc plasmid was chosen for several reasons: 1) a tag fused to the HB-EGF was needed because, at the time, the anti-HB-EGF antibody was not available at the laboratory; 2) the Myc epitope has a small size, unlikely affecting the tagged protein's biochemical properties; 3) the MCS in this vector is

compatible with the MCS of Clontech's MATCHMAKER™ Two-Hybrid System Vectors, allowing direct subcloning only by using endonucleases.

5.2.2 Electrophorectic analysis of the Myc-HB-EGF cDNA construct

The Myc-HB-EGF construct was then created from pACT2-HB-EGF, using standard cloning procedures, having the insert been subcloned into the pCMV-Myc vector in frame with the Myc coding sequence. The putative Myc-HB-EGF fusion constructs were further subjected to restriction fragment analysis using *Eco*RI and *Xho*I endonucleases, to confirm the correct insertion into the mammalian expression vector. The restriction fragments were then separated by 1% agarose gel electrophoresis and the size of the observed fragments was in agreement with the expected: approximately 3.8 Kb for the pCMV-Myc vector and ~2,3 Kb for the HB-EGF insert (Figure 21).

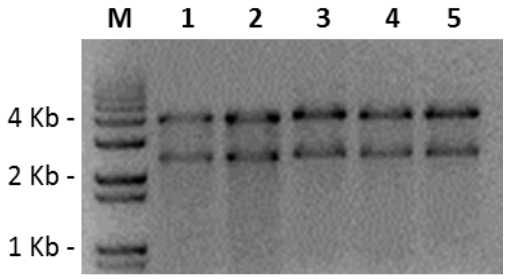

Figure 21 – Restriction fragment analysis of the pCMV-Myc-HB-EGF constructs. Lane M, 1 Kb Plus DNA Ladder. Lanes 1-5, pCMV-Myc+HB-EGF (3.8 + 2.3 Kb) fragments upon restriction with *Eco*RI and *Xho*I.

5.2.3 Optimization of Myc-HB-EGF transfection

For the functional cellular studies, we chose the immortalized HeLa cell line. This remarkably durable and prolific cell line is a widely used experimental tool for *ex vivo* assays, being of human origin and easy to transfect.

In order to optimize HeLa cells transfection with the Myc-HB-EGF construct, Myc-HB-EGF cDNA was transfected for 24h using the Turbofect™ reagent method. Different cDNA concentrations and Turbofect:DNA ratios were tested: 1 and 2 µg of Myc-HB-EGF cDNA, and 1:1 and 2:1 ratios (data not shown). The levels of HB-EGF transfection were evaluated by Western blot analysis using the anti-My-tag antibody. As we can notice by observation of Figure 22, the Turbofect™ transfection reagent rendered appreciable levels of Myc-HB-EGF transfection when using 1 µg and a 2:1 ratio. Therefore, in all subsequent experimental analysis these transfection conditions were used.

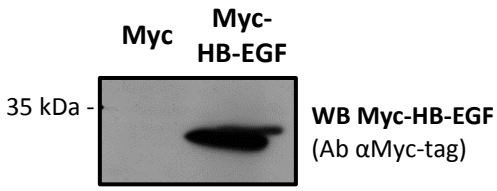

Figure 22 – Pilot experiment for detecting the expression of the transfected Myc-HB-EGF construct. The Turbofect™ transfection reagent yielded satisfactory amounts of cDNA transfection. Cells transfected with the pCMV-Myc vector were used as control.

5.2.4 Validation of the APP/HB-EGF interaction by GFP-Trap® Pull-Down assay

Several procedures may be used to validate a novel putative protein-protein interaction. Co-immunoprecipitation is a technique based on the formation of antigen-antibody complexes, most commonly used to prove that two proteins of interest are associated. However, for biochemical studies, the GFP-Trap® Pull-Down assays (Chromotek) have emerged as a fast and efficient method that enables purification of GFP-fusion proteins and their binding partners. Therefore, GFP-Trap® Pull-Down assays were performed to confirm the specific interaction between HB-EGF and APP *ex vivo* and to enable further analysis of the physiological relevance of the APP/HB-EGF interaction.

GFP-Trap® Pull-Down assays were carried out using cellular extracts obtained from HeLa cells expressing four different co-transfection conditions: 1) pEGFP-N1 and pCMV-Myc empty vectors (*EGFP:Myc*), 2) APP-GFP and the pCMV-Myc empty vector (*APP:Myc*), 3) Myc-HB-EGF and the pEGFP-N1 empty vector (*EGFP:HB-EGF*), and 4) co-transfection of both APP-GFP and Myc-HB-EGF constructs (*APP:HB-EGF*). 24 hours after transfection, cells and the respective incubation medium were harvested and subjected to GFP pull-down. Cell lysates and precipitates (*pull-down*) were resolved by 5-20% SDS-PAGE and immunoblots probed with: anti-Myc and/or anti-HB-EGF (to detect the pre-proHB-EGF Myc-HB-EGF construct and/or endogenous HB-EGF, respectively); and with anti-APP antibodies (anti N-terminus - 22C11; anti C-terminus - CT695) for endogenous APP and APP-GFP detection.

In the first experimental design, 35 mm cell culture plates were used (Figure 23). APP-GFP was detected in all APP-GFP transfected cell lysates and precipitated samples, which means that APP-GFP was successfully pulled-down, although a fainter band was observed for the APP-GFP (*APP:Myc*) pulled-down lane. Endogenous APP was only observed in the lysates and not in the pulled-down samples. Immunoblotting with anti-Myc-tag antibody detected the

Myc-HB-EGF construct in Myc-HB-EGF lysates, as expected, and in the APP:HB-EGF pulled-down sample, confirming the interaction with APP.

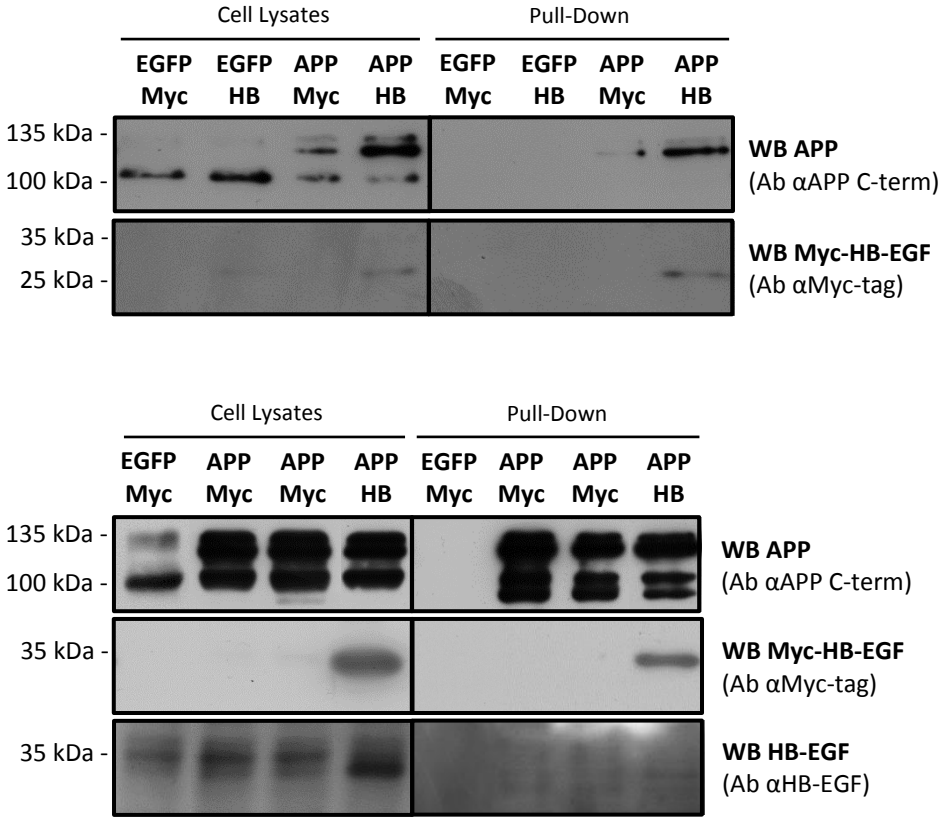

Figure 23 – Validation of APP/HB-EGF interaction by GFP-Trap pull-down assays. Immunoblot analysis of HeLa cells co-transfected with EGFP:Myc, EGFP:HB-EGF, APP:Myc and APP:HB-EGF. A – GFP-Trap pull-down of HeLa cells grown in 35 mm cell culture plates. B - GFP-Trap pull-down of HeLa cells grown in 60 mm cell culture plates. HB, HB-

In order to unravel if APP also binds to endogenous HB-EGF, the GFP-Trap® Pull-Down assay was performed in a higher amount of cellular extracts, obtained from overexpressing APP HeLa cells plated on 60 mm cell culture plates. First, the APP:Myc-HB-EGF interaction was confirmed in co-transfected pulled down samples, runned side-by-side with APP-GFP solely transfected samples. Indeed, immunoblotting with the anti-Myc-tag antibody detected the Myc-HB-EGF construct (band ~33 kDa) either in the lysate and pull-down lanes of APP-GFP and Myc-HB-EGF co-transfected samples. When membranes were probed with the anti-HB-EGF antibody, this recognized the recombinant Myc-HB-EGF as expected, but also detected various species of endogenous HB-EGF in all cell lysate lanes. Three immunoreactive proteins - of 37, 35 and 33 kDa, as deduced from co-migration with known standards - were observed in the lysates. Further, a much less abundant species of minor MW (31 kDa) was also observed. These appear to be various forms of unmodified and post-translationally modified pre-proHB-EGF. These various forms of different sizes and representing different degrees of protein

maturation were already described in cell lysates by other authors (59,61,80,81). All these bands were also detected in the APP-GFP pull-downs (and in the co-transfected lane), indicating that APP interacts with endogenous pre-proHB-EGF. Unfortunately the anti-HB-EGF antibody has a bad signal-to-noise ratio and difficult bands perception in digitalized images. Indeed, two more HB-EGF immunoreactive fainter bands appear in cell lysates (data not shown): a 25 KDa species that may represent the propeptide truncated form, proHB-EGF, being derived from the major full-length pre-proHB-EGF precursor. This species was also pulled-down by APP-GFP, being observable in APP-GFP and co-transfection pull-down lanes (data not shown). A sixth HB-EGF immunopositive faint band appeared in the expected size for soluble HB-EGF (~20kDa) in cell lysates but was barely detected in the pulled down samples and in the conditioned medium (data not shown). Of note, APP-GFP also pulled down endogenous APP (lower bands in APP-GFP pull-down lanes), what is not unexpected since APP has been reported to dimerize.

Taken together, these results indicate that APP interacts with the exogenous and endogenous pre-proHB-EGF species, and most possibly with the proHB-EGF form. Nonetheless, the bands detection was faint using the anti-HB-EGF antibody, and hence this has to be further confirmed, including if APP interacts with sHB-EGF.

5.2.5 APP/HB-EGF subcellular co-localization

The APP/HB-EGF molecular association might exert diverse effects depending on the context or subcellular compartment. In order to address the physiological relevance of the APP/HB-EGF interaction, immunocytochemistry studies were performed.

First, the subcellular distribution of the Myc-HB-EGF construct was analyzed and compared to the endogenous HB-EGF, in Myc-HB-EGF transfected cells. The anti-Myc-tag (Alexa Fluor 488; green fluorescence) and anti-HB-EGF (Texas Red, red fluorescence) antibodies were used. Fluorescence microscopy was carried out using a confocal microscope, and cells were randomly selected for analysis.

As HB-EGF shows bidirectional intracellular trafficking between the plasma membrane and ER, it was reported to localize to five different subcellular compartments: the plasma membrane, Golgi apparatus, ER, nuclear envelope, and perinuclear vesicles (56). Microphotographs revealed that Myc-HB-EGF (in green) presented a predominant subcellular distribution in the perinuclear region, in what appeared to be the ER and the Golgi apparatus, and in nearby cytoplasmic vesicles. The anti-HB-EGF labeling (in red) revealed a more diffuse distribution for the endogenous HB-EGF, being also slightly enriched at the Golgi and present in cytoplasmic vesicles distributed throughout the entire cell (Figure 24).

As expected for the N-terminally labeled full-length HB-EGF (Myc-HB-EGF), no staining could be observed neither in plasma membrane nor in the nuclear envelope. This most probably reflects the very rapid prodomain cleavage after synthesis of the precursor, or as soon as it reaches the plasma membrane (57). Likewise, very few plasma membrane staining could be observed in these cells for the endogenous HB-EGF (labeled with this antibody).

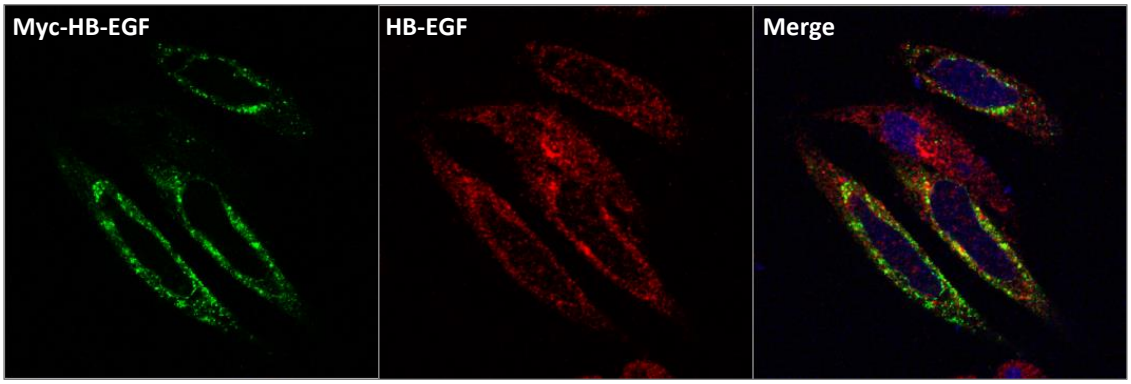

Figure 24 - Analysis of the subcellular distribution of Myc-HB-EGF (in green; anti-Myc-tag antibody) and endogenous HB-EGF (in red; anti-HB-EGF antibody). Their co-localization was also evaluated (merge).

Noticeably, low levels of co-localization between the anti-Myc-tag and anti-HB-EGF antibodies were observed, with the anti-HB-EGF antibody not recognizing efficiently the exogenous Myc-HB-EGF protein in most transfected (myc-positive) cells. This can be due to epitope masking by the myc tag in the final three dimensional conformation, a problem that did not occurred in the previous denaturing assays (GFP-Trap pull-down).

Regarding APP-GFP distribution, microphotographs of APP-GFP overexpressing cells showed the expected subcellular distribution, with APP localizing mainly in the Golgi apparatus and cytoplasmic vesicles, and with only a small fraction being present at the plasma membrane. It has been evidenced by previous work from our laboratory that fluorescently tagged APP can be observed in the endoplasmic reticulum (ER), Golgi complex, lysosomal, endocytic vesicles and plasma membrane (27,77,82). EGFP alone, by its turn, distributes diffusely through the cell cytoplasm and the nucleus, where it is found enriched.

Subsequently, the co-localization between APP and either endogenous or exogenous HB-EGF proteins was addressed in HeLa cells co-transfected with APP-GFP and Myc-HB-EGF. HB-EGF expression was detected with either the anti-Myc-tag (exogenous) or anti-HB-EGF (endogenous) antibodies (Figure 25).

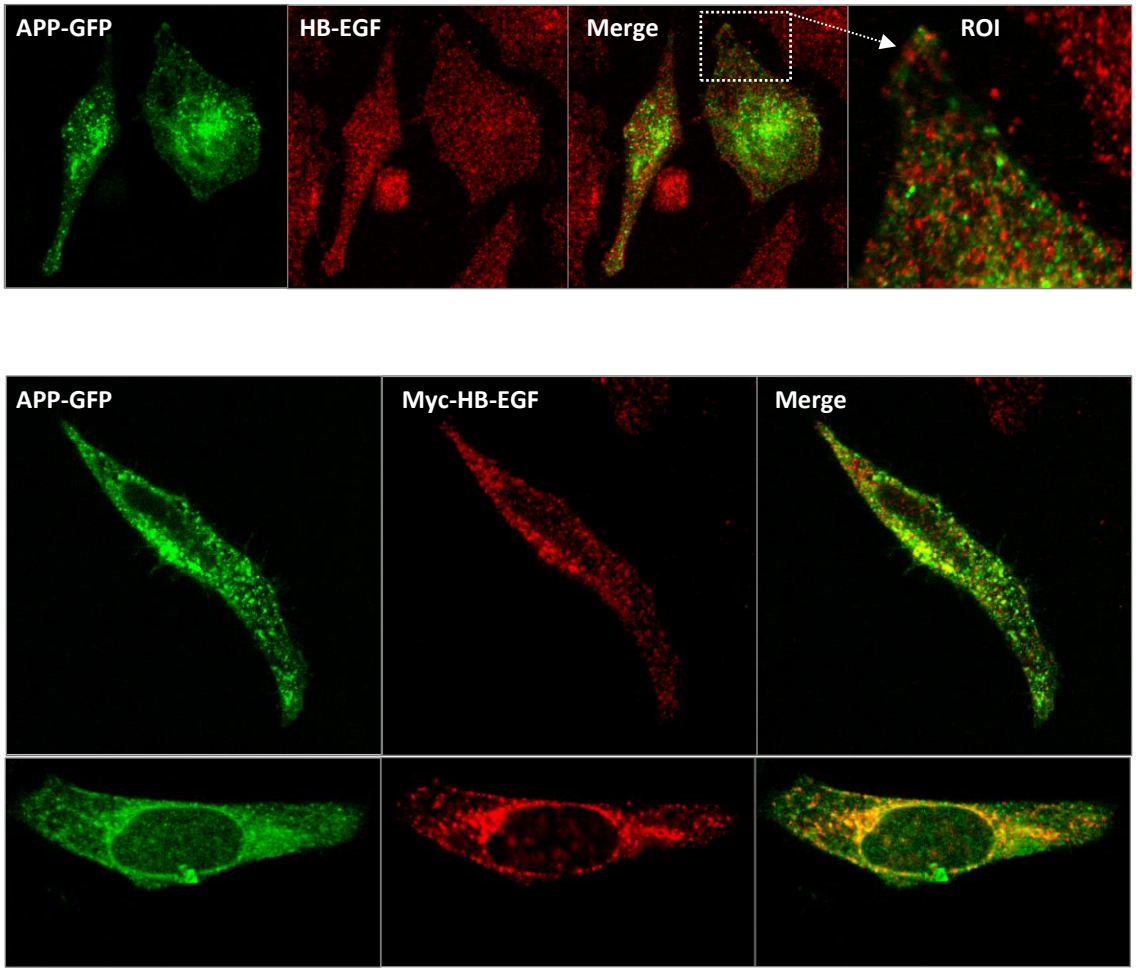

Figure 25 – Immunocytochemistry analysis of APP-GFP (green) co-localization with HB-EGF (red). Upper panel: endogenous HB-EGF (anti-HB-EGF antibody). Lower panel: transfected Myc-HB-EGF protein (anti-Myc antibody).

Confocal fluorescence microscopy showed that endogenous HB-EGF presented some degree of co-localization with APP-GFP, predominantly at small vesicles distributed throughout the cytoplasm, as showed in the magnified ROI (region of interest; Figure 25, upper panel). Recombinant HB-EGF protein seemed to co-localize with APP-GFP mainly in the Golgi apparatus and nearby vesicles (Figure 25, lower panel). Also, a higher degree of co-localization was detected when HB-EGF was overexpressed. Of note, the great majority of APP-GFP vesicles do not co-localize with HB-EGF, suggesting highly regulated interactions. The nature of the subcellular regions of co-localization, especially the cytoplasmic vesicles, will have to be further analyzed by using specific organelle markers.

5.2.6 Influence of HB-EGF overexpression in APP levels

The same four conditions used for the first pull-down assay were used to study the influence of APP and HB-EGF on each other's protein levels. To evaluate the effect of HB-EGF

overexpression in endogenous APP levels, these were quantified in HB-EGF transfected samples (*EGFP:HB-EGF*) and compared to vector samples (*EGFP:Myc*). The analysis of exogenous APP levels was performed by quantification of the APP-GFP levels in *APP:HB-EGF* and *APP:Myc* co-transfected samples (Figure 26). Of note, Ponceau S staining of total proteins bands was performed for all assays and used as loading control in the quantitative analysis.

Regarding the influence of HB-EGF overexpression in endogenous APP levels, we can observe that HB-EGF induced a 2.01±0.46 fold increase in endogenous APP. In opposition, HB-EGF induced a significant decrease in exogenous APP expression when both constructs were co-transfected (fold decrease of 0.65±0.06).

Since an increase in endogenous APP was observed, the mature and immature levels of APP were further analyzed in detail in order to understand if HB-EGF was inducing an effect specifically on one or on both forms. HB-EGF induced a fold-increase (FI) of 1.87±0.52 in the immature endogenous APP, whilst a more significant increase in mature endogenous APP expression was detected (FI of 2.82±0.61). Contrasting these results, HB-EGF induced a decrease in the amount of mature APP-GFP (0.64±0.11). So, while HB-EGF transfection seems to enhance both mature and immature endogenous APP levels, it decreases APP-GFP levels. We have further analyzed if HB-EGF overexpression affected the percentage of APP maturation and only a slight tendency for the percentage of APP maturation to increase was observed either in APP:HB-EGF co-transfected or HB-EGF transfected cells (Figure 26).

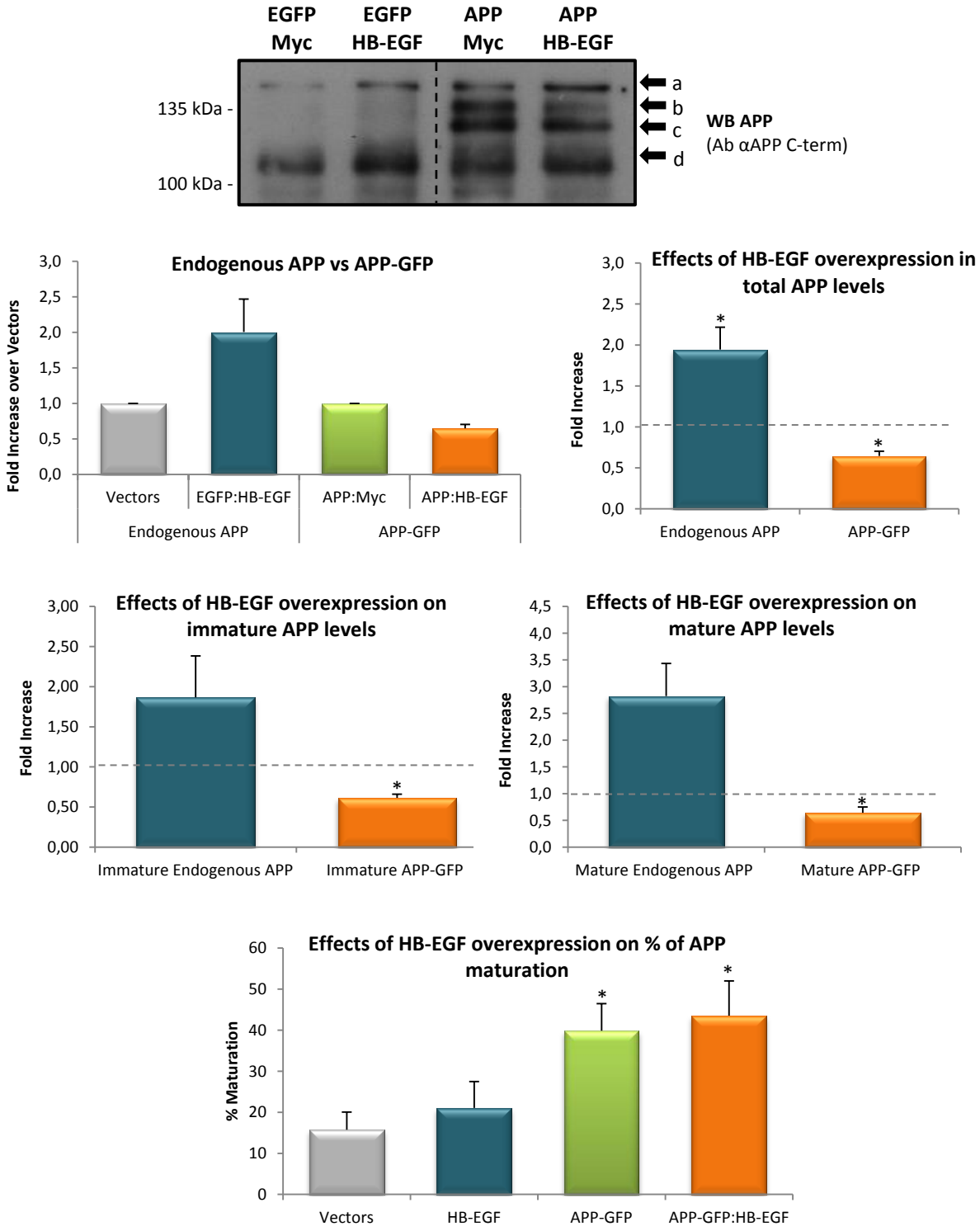

Figure 26 – Western Blot and quantitative analysis of the influence of HB-EGF overexpression in APP levels, upon 24h of HeLa cells transfection. Bands a and d, mature and immature endogenous APP. Bands b and c, mature and immature APP-GFP forms, respectively. Graphs: upper panel - endogenous APP and APP-GFP fold increase over vectors (EGFP:Myc) and APP:Myc, respectively; middle panel - mature and Immature APP fold increase over vectors (EGFP:Myc) and APP:Myc, respectively; lower panel - evaluation of % of APP maturation. Data are presented as mean ± SEM, upon correction to Ponceau. *p<0,05; **p<0,01; ***p<0,001. n=3-4.

Since the simultaneous transfection of HeLa cells with Myc-HB-EGF and APP-GFP led to a decrease in the exogenous APP levels, it was relevant to investigate if this decrease would be due to a promotion of APP processing into sAPP. Cell medium samples collected for each condition were analyzed by Western blotting with the anti-22C11 antibody (Figure 27). After soluble APP quantification, evidences showed that HB-EGF overexpression leads to a decrease both in endogenous and exogenous APP cleavage, being this decrease more accentuated for the APP:HB-EGF co-transfection condition (0.67±0.03 FD; Figure 27).

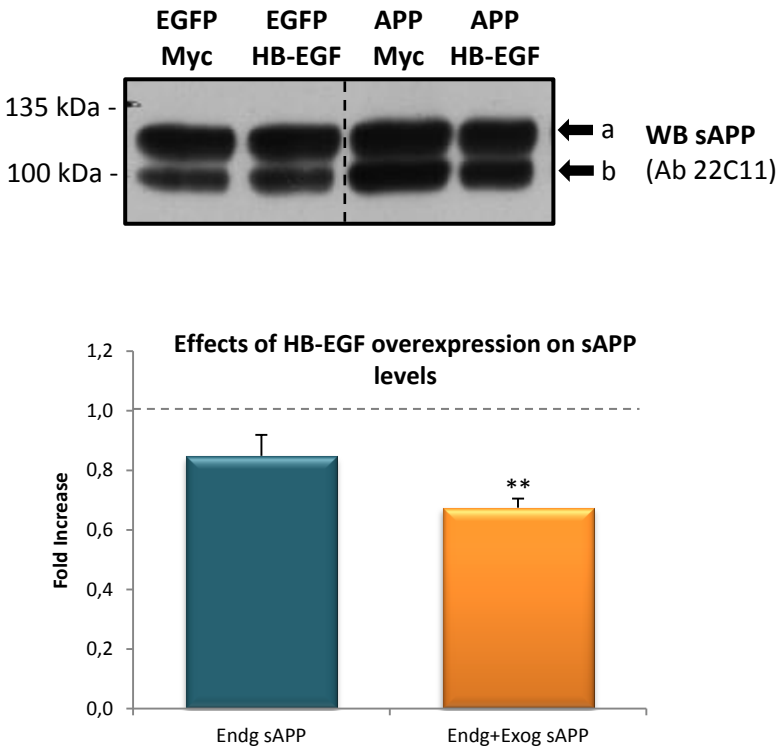

Figure 27 – Evaluation of the influence of HB-EGF overexpression on soluble APP levels in HeLa cells, upon 24h of transfection. Immunoblot: bands a and b, endogenous 751/770 sAPP isoform and exogenous sAPP, 695 isoform, respectively. Graphic: 'Endg sAPP': effect of HB-EGF transfection on endogenous sAPP levels (EGFP:Myc samples); 'Endg+Exog sAPP': effect of HB-EGF transfection (APP:HB-EGF samples) on endogenous and exogenous sAPP levels (APP:Myc samples). *p<0,05; **p<0,01; ***p<0,001. n=5.

The differential effects of HB-EGF overexpression on endogenous and exogenous APP levels led us to perform a preliminary analysis to evaluate if HB-EGF was in someway promoting APP's half-life. Hence, a cycloheximide (CHX) assay (27) was performed in pCMV-Myc vector and Myc-HB-EGF transfected cells, treated or not for 1 hr with the protein synthesis inhibitor CHX. As we can notice by observing Figure 28, cells exposed to CHX showed a significant reduction of the amount of total APP, which was consistent between HB-EGF cells and control. Thus, HB-EGF does not increase APP half-life, since this would result in none or

lower decreases in endogenous APP levels. The possibility of HB-EGF may be inducing APP gene expression will be further addressed in the future.

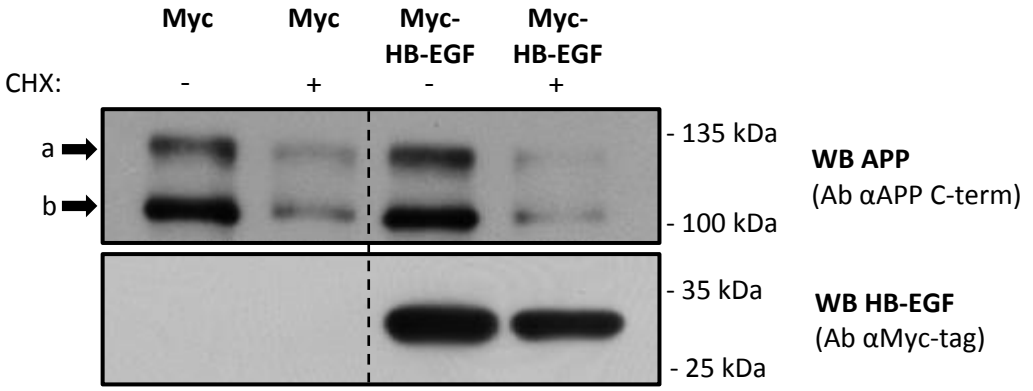

Figure 28 – Immunoblot analysis of HeLa transfected cell lysates. Cells transfected with pCMV-Myc vector or with recombinant HB-EGF were treated (+) or not (-) with cycloheximide (CHX) for 1h. Bands a and b, mature and immature endogenous APP, respectively.

5.2.7 Influence of APP overexpression in HB-EGF levels

The effects of APP overexpression on exogenous HB-EGF levels were also monitored by comparing Myc-HB-EGF levels in APP:HB-EGF versus the EGFP:HB-EGF co-transfected samples.

APP overexpression had a negative influence on the exogenous HB-EGF levels, decreasing Myc-HB-EGF levels by 0.75±0.20 when both proteins were overexpressed (representative immunoblot in Figure 33. We further intended to analyze the influence of APP-GFP transfection in endogenous HB-EGF levels, by using the anti-HB-EGF antibody, but this is not yet optimized for WB quantification; nonetheless, an increase in endogenous HB-EGF levels appears to occur when cells were transfected with APP-GFP (data not shown).

5.2.8 Influence of APP and HB-EGF overexpression in MAPK/Erk signaling

It is prior knowledge that the MAPK signaling is a main pathway activated by ligands of the EGF family. For this reason it was peremptory to investigate the influence of APP and HB-EGF/APP interaction in Erk1/2 signaling. The activation of the Erk1/2 signaling was analyzed using both anti-phosphoMAPK (Thr185/Tyr187) and anti-MAPK antibodies, in the previously analyzed samples (section 5.2.6).

Evidences showed that all the three transfection conditions promoted Erk1/2 phosphorylation, when comparing to control (vector transfected cells). Among those, EGFP:HB-EGF transfection induced the higher levels of MAP kinase phosphorylation (3.10 FI). APP:GFP followed with a FI of 1.94, and APP:HB-EGF co-expression presented a FI of 1.49 over basal levels. Hence, co-transfecting cells with APP:HB-EGF decreased MAPK phosphorylation

by ~30% (0.70 FD) relatively to APP single transfection and around 20% relatively to HB-EGF single transfection (0.80 FD) (Figure 29). Concerning MAPK levels, APP and HB-EGF co-transfection induced a FI of 1.26±0.26, with the remaining conditions not affecting MAPK levels.

When the P-MAPK/MAPK ratio, a measure of MAPK activation, was determined for each condition, the higher ratio was obtained for HB-EGF overexpressing cells (FI of 3.35), followed by APP-GFP expressing cells (2.36). APP:HB-EGF co-transfection decreased these positive effects, only activating MAPK signaling by 1.67 over basal levels (Figure 29).

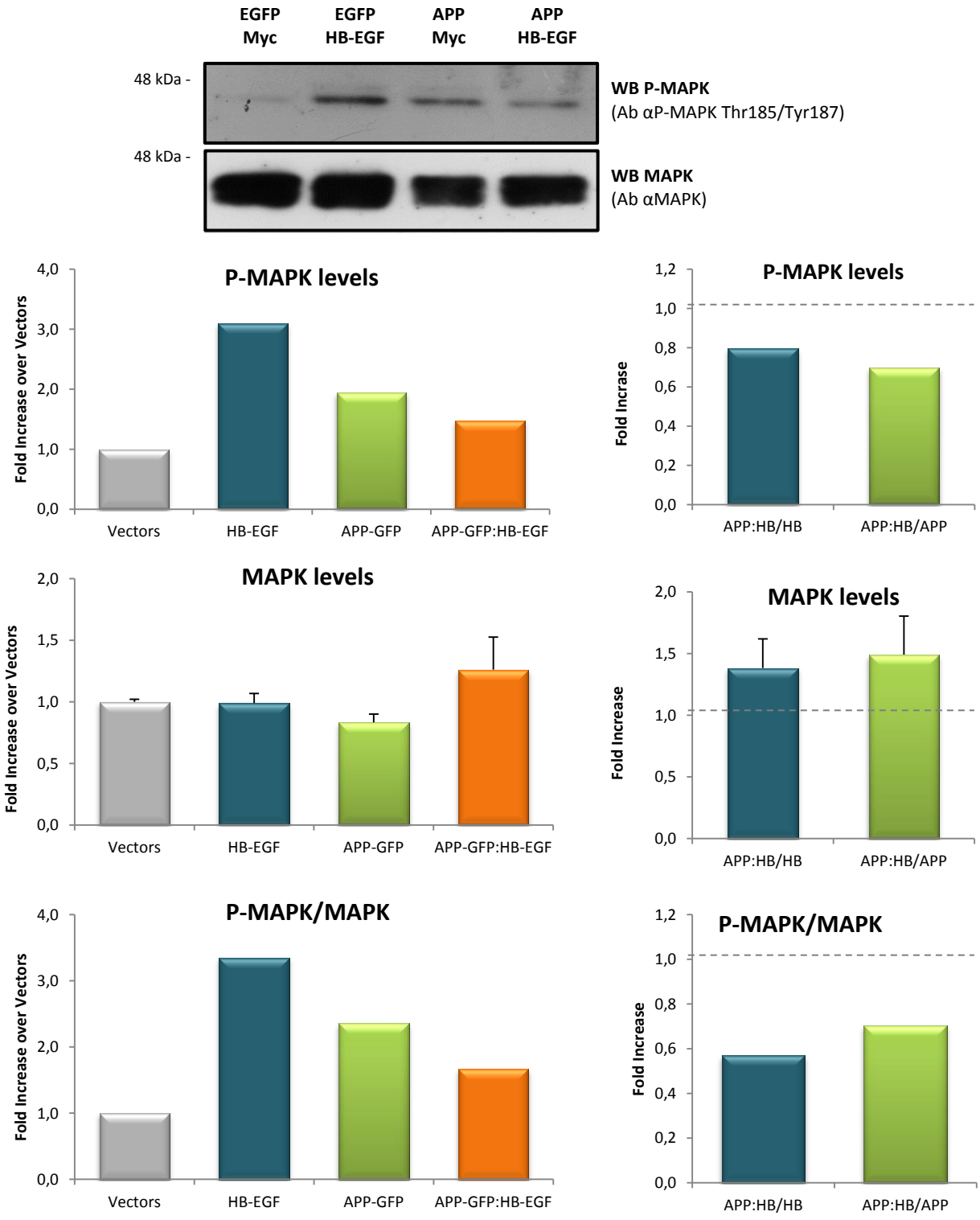

Figure 29 – Evaluation of the effect of APP and HB-EGF transfection on Erk signaling by immunoblot analysis of HeLa cells lysates. Upper and Middle: left graphs - P-MAPK and MAPK fold increases in HB-EGF, APP-GFP and APP:HB-EGF overexpressing cells, over vectors (EGFP:Myc) levels; right graphs – calculated fold increases of P-MAPK and MAPK levels by APP:HB-EGF co-transfection, over APP and HB-EGF single transfection levels. Lower panel left and right graphs: similar analyses but for the P-MAPK/MAPK ratio. Data are presented as mean ± SEM, upon correction to Ponceau. n=2 (P-MAPK levels and P-MAPK/MAPK ratio) and n=3 (MAPK levels). HB, HB-EGF.

5.2.9 Influence of APP and HB-EGF overexpression in STAT3 signaling

Another pathway already described to be activated by EGFR agonists is the STAT3 pathway. Therefore, the influence of APP and HB-EGF overexpression in STAT3 signaling was considered, being analyzed by using both anti-phosphoSTAT3 (Tyr 705) and anti-STAT3 antibodies.

Upon 24 h of transfection, no noteworthy effects on STAT3 phosphorylation (P-STAT3) were observed in either the APP-GFP, HB-EGF, or the APP:HB-EGF expressing cells. Still, APP overexpression drove the most accentuated decrease in STAT3 phosphorylation, with a fold-decrease of 0.80±0.05. STAT3 levels remained constant at the basal level (Figure 30). Protein quantification data were used to determine the P-STAT3/STAT3 ratio, a measure of STAT3 activation, for each condition. Accordant to the previous observations, the P-STAT3/STAT3 ratio presented a decrease of about 20% for the APP transfection condition (FD of 0.76±0.06), comparing to the vectors transfection. Of note, this effect has been already observed in our lab for SH-SY5Y cells (83).

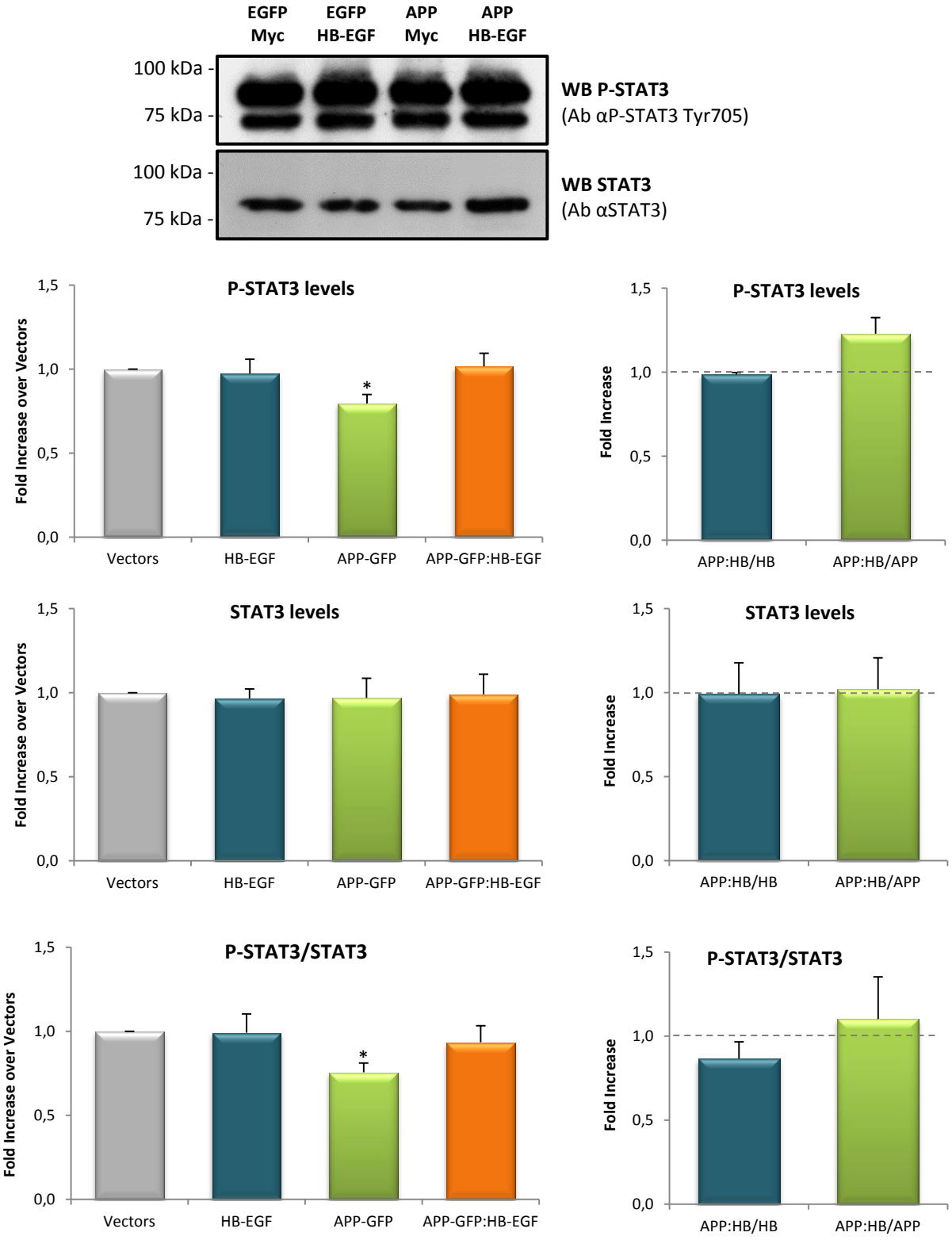

Figure 30 - Evaluation of the influence of APP and HB-EGF overexpression on STAT3 signaling by immunoblot analysis of Hela cells lysates. Upper and Middle graphs: left - P-STAT3 and STAT3 fold increase in HB-EGF, APP-GFP and APP:HB-EGF overexpressing cells, over vectors (EGFP:Myc); right: calculated fold increases on P-STAT3 and STAT3 levels in APP:HB-EGF co-transfection conditions over APP and HB-EGF single transfections. Lower graphs: similar evaluations for the P-STAT3/STAT3 ratio. Data are presented as mean ± SEM, upon correction to Ponceau. *p<0,05; **p<0,01; ***p<0,001. n=4. HB, HB-EGF.

5.3 APP Interplay with EGF

5.3.1 Influence of APP in EGF-induced signaling

Since APP was able to influence HB-EGF-induced signaling, we further evaluated if it had similar effects on EGF-induced signaling. This was conducted in pEGFP-N1 and APP-GFP transfected cells, incubated or not with 100 ng/ml of EGF for 30 min. Once again, both Erk and STAT3 signaling pathways were analyzed, and fold increases of APP over EGFP, and APP+EGF over EGFP+EGF conditions were calculated.

Again, APP declined STAT3 phosphorylation by approximately 30% in the absence of EGF (0.69±0.07 FD), and only by 12% (0,88±0.01 FD) in the presence of EGF (Figure 31). EGF itself decreased both P-STAT3 and STAT3 levels (compare EGFP+EGF vs EGFP lanes).

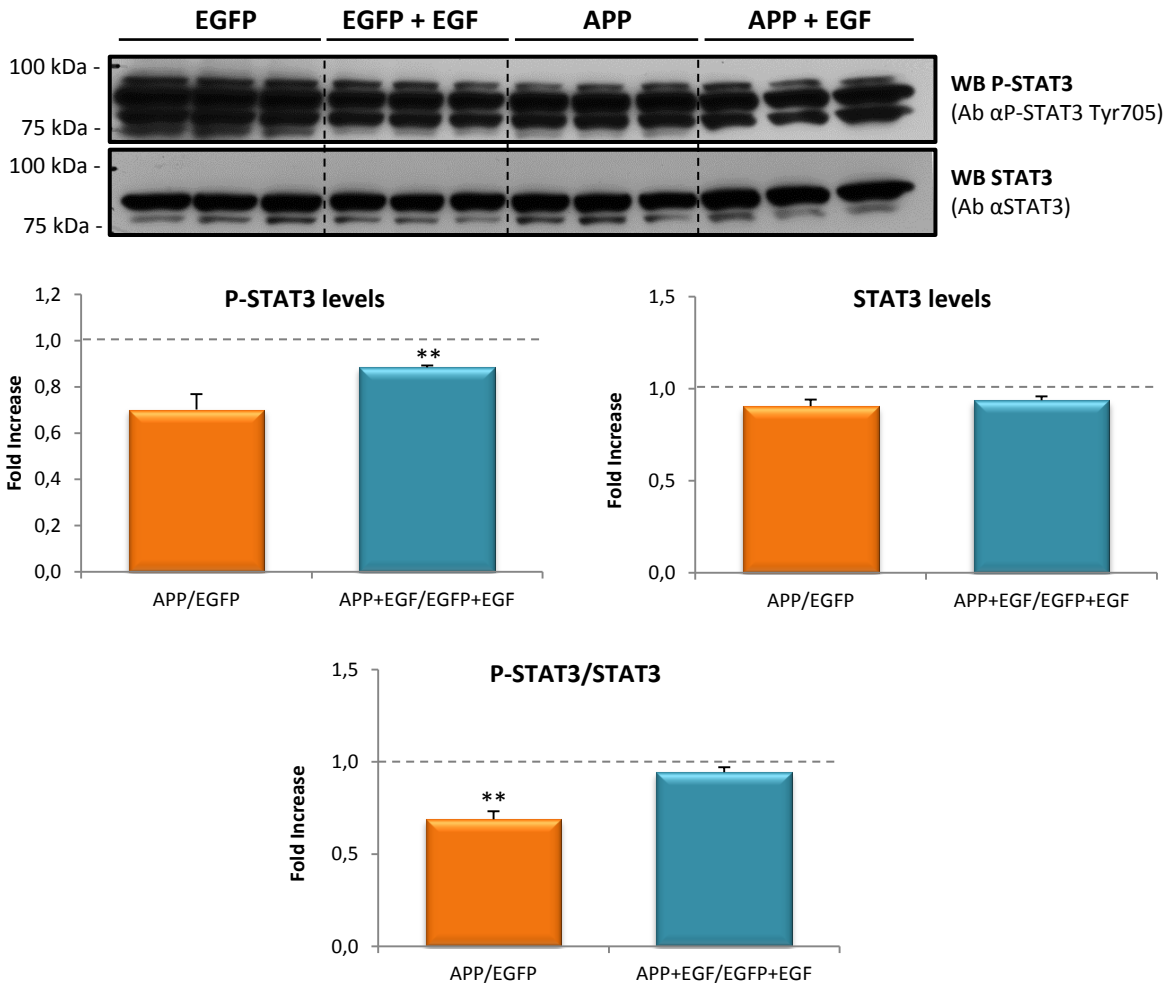

Figu**re 31** - Analysis of APP overexpression in STAT3 signaling. Upper panel – immunoblot analysis of P-STAT3 and STAT3 levels in HeLa cells transfected for 24 h with EGFP or APP-GFP, unexposed or exposed to 100 ng/ml EGF ('+EGF'). Middle and lower panel – graphic analysis of the fold increases in P-STAT3, STAT3, and P-STAT3/STAT3 ratio induced by APP-GFP transfection and EGF incubation (calculated as indicated in the x-axis). Data are presented as mean ± SEM, upon correction to Ponceau. *p<0,05; **p<0,01; ***p<0,001. n=3.

Contrasting these results, an enhancement of the Erk1/2 signaling was observed in response to EGF and to APP. EGF alone induced an enormous surge in P-MAPK levels, as expected (compare of EGFP+EGF vs EGFP lanes). For APP, in cells non treated with EGF, a fold increase of 1,94±0.24 was obtained, a double increase that is maintained in the presence of EGF (2.26±0.15). MAPK protein levels did not suffer considerable alterations. In terms of MAPK activation (P-MAPK/MAPK ratio), APP transfection induced a 2,13±0.25 FI in the absence of EGF, and a 2,21±0.16 FI in the presence of EGF (Figure 32).

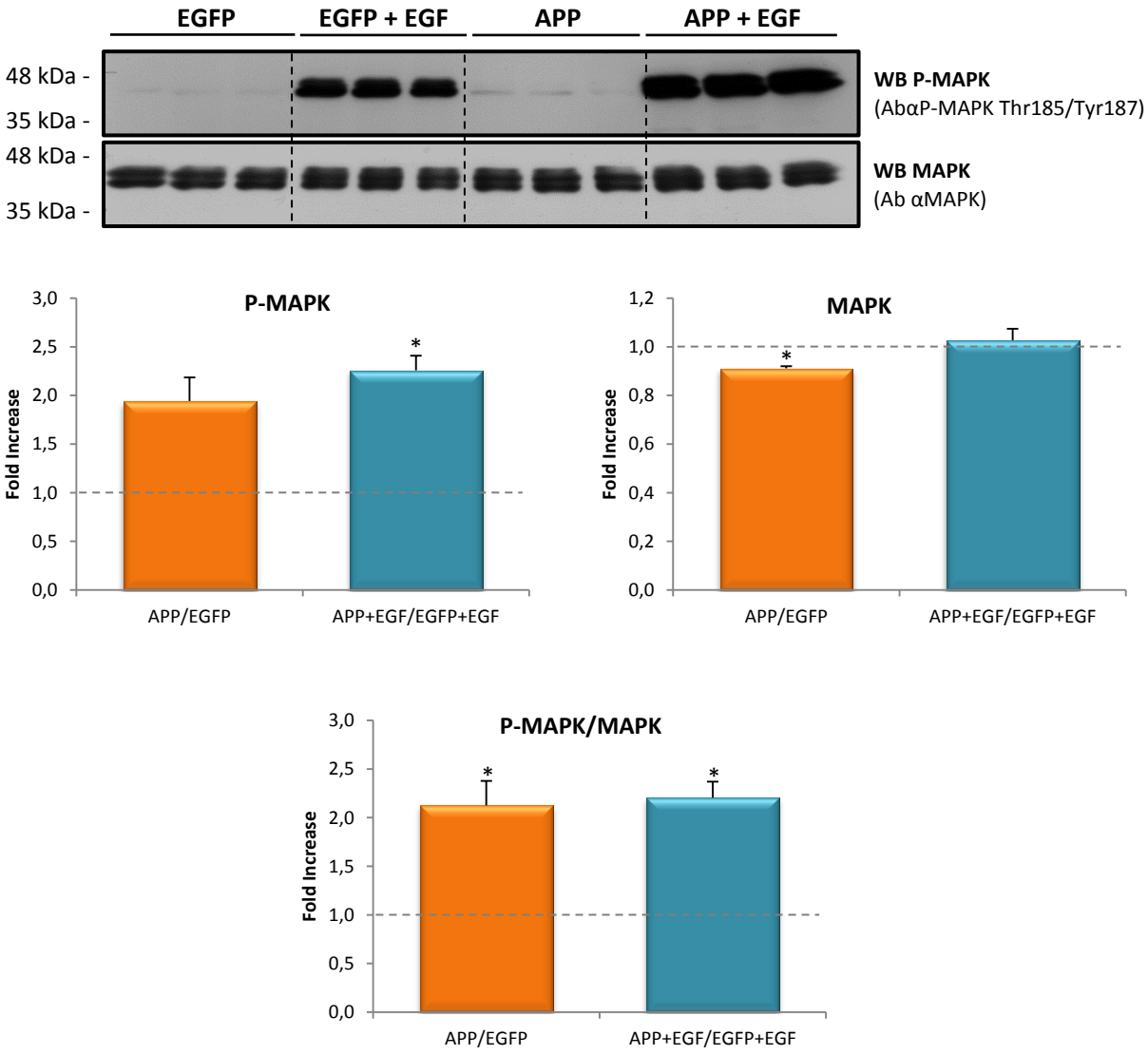

Figure 32 - Analysis of APP overexpression in MAPK signaling. Upper panel – immunoblot analysis of P-MAPK and MAPK levels in HeLa cells transfected for 24 h with EGFP or APP-GFP, unexposed or exposed to 100 ng/ml EGF ('+EGF'). Middle and lower panel – graphic analysis of the fold increases in P-MAPK, MAPK, and P-MAPK/MAPK ratio induced by APP-GFP transfection and EGF incubation (calculated as indicated in the x-axis). Data are presented as mean ± SEM, upon correction to Ponceau. *p<0,05; **p<0,01; ***p<0,001. n=3.

5.3.2 Analysis of the APP/EGF and APP/EGFR interaction by GFP-Trap® Pull-Down

Since the previously obtained results suggested a synergistic effect of APP with EGF in MAPK signaling, we further investigated the possibility of EGF and EGFR being two novel APP protein partners. With this purpose, immunoblots of the GFP pull-downs (Figure 23, 60 mm), were probed with the anti-EGF and anti-EGFR antibodies.

When blots were probed with the anti-EGF antibody, cell lysates showed three immunoreactive EGF proteins corresponding to high molecular weight species ranging 94-110 KDa. Apparent molecular masses of the different EGF species detected in the immunoblots were deduced from co-migration with known standards. Size analysis showed a major species of 110 kDa and two minor ones of 103 and 94 kDa (Figure 33). These detected species most possibly represent the precursor protein of EGF, namely prepro-EGF.

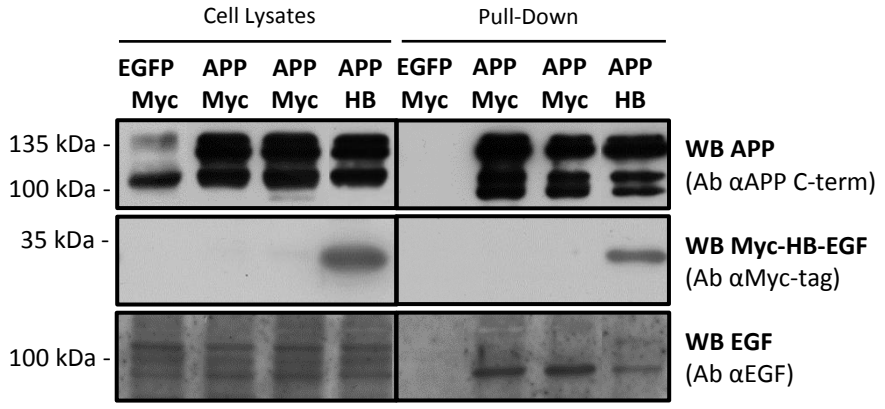

Figure 33 – Evaluation of APP binding to EGF by the GFP-Trap pull-down assay. Western Blot analysis of HeLa cells grown on 60 mm plates and co-transfected with vectors (EGFP:Myc), APP-GFP:Myc, and APP-GFP:HB-EGF. Immunodetection of APP, Myc-HB-EGF and EGF precursor in cells lysates and GFP-pull-downs was accomplished with the indicated antibodies (Ab). HB, HB-EGF.

Surprisingly, the detected lower molecular weight 94kDa species was an immunoreactive protein that was pulled-down by APP-GFP, which suggests a novel and unexpected interaction between APP and pro-EGF (Figure 33). Of note, the performed electrophoresis with 5-20% SDS-PAGE did not allow us to detect the lower molecular weight mature 6kDa EGF species, either in cell lysates or precipitated samples (data not shown).

On the other hand, our initial attempt to detect EGFR protein failed because the respective antibody was not functioning properly (data not shown).

5.3.3 APP/HB-EGF- and APP/EGF – induced alterations in cellular morphology

The effects of overexpressing APP-GFP and Myc-HB-EGF fusion proteins, solely or simultaneously, in cells morphology was also evaluated by immunocytochemistry procedures. Since appreciable effects were also observed in the biochemical analysis with EGF, the influence of EGF was also tested, having been generated two distinct sets of conditions. The first, aiming the analysis of APP-GFP and Myc-HB-EGF influence on cell morphology, consisted in four different transfection scenarios: 1) pEGFP-N1:pCMV-Myc; 2) APP-GFP:pCMV-Myc; 3) pEGFP-N1:Myc-HB-EGF, and 4) APP-GFP:Myc-HB-EGF. The second consisted in the analysis of cells exposed to EGF stimulation in three different transfection backgrounds: 1) pEGFP-N1; 2) APP-GFP and 3) APP-GFP:Myc-HB-EGF. Cells were visualized by fluorescence microscopy, and cells length was further quantified.

Vector-transfected HeLa control cells presented an average cell length of ~53µm. APP overexpression (APP:Myc) resulted in cell elongation, with an average of ~65 µm of length. Interestingly, Myc-HB-EGF transfection resulted in the most remarkable elongation, with cells presenting an average cell length of ~85 µm. On the other hand, APP-GFP and Myc-HB-EGF co-expressing cells resulted in lengths close to those of APP-GFP expressing cells.

Concerning the EGF set, a similar increase in cells length as for APP was induced by the addition of EGF to the cell medium (EGFP+EGF; ~69 µm), when comparing to vector cells (EGFP:Myc). Despite the clear increase in cell elongation induced by EGF exposure, its effect was far from the one observed for HB-EGF. Although presenting a lower cell length, HeLa cells under EGF treatment exhibited a higher degree of cell plasticity, showing several ruffles emerging from the plasma membrane. Consistent with the previous results for HB-EGF, the EGF stimulation of APP-GFP expressing cells did not prompted additional cell elongation and the cell plasticity seemed to decrease comparing to EGFP+EGF cells. When APP:HB-EGF cells were treated with EGF even lower cell lengths were observed, and this represented the closest condition to vector cells (~58 µm).

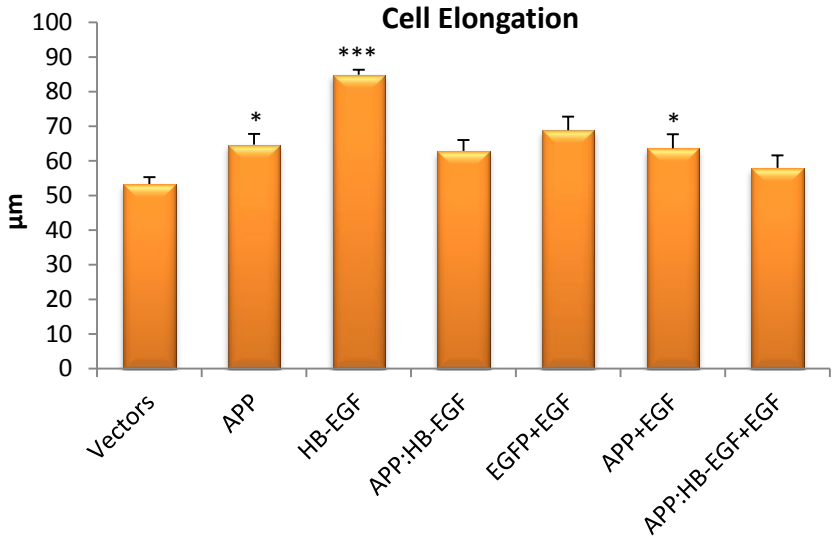

Figure 34 – Analysis of APP/HB-EGF- and APP/EGF-induced alterations in cellular morphology. Transfected HeLa cells were analyzed for cell length. *p<0,05; **p<0,01; ***p<0,001. n=3

6 Discussion

As previously mentioned, the study of PPIs is a powerful approach for inferring information about protein function. With this work we intended to study the interaction between the APP and HB-EGF proteins, and initiate the functional characterization of the complex through biochemical methods and visual analysis of subcellular distribution and co-localization.

Validation of the APP/HB-EGF interaction by yeast co-transformation. The YTH system has become one of the most popular and powerful tools to study PPIs, providing a sensitive *in vivo* assay for interaction analysis. From the YTH screen of a human brain cDNA library performed in our laboratory, HB-EGF was identified as a novel APP interactor, when using full-length APP as bait. Confirmation of the interaction in yeast was here performed by co-transformation of AH109 strain and assayed for reporter genes activation. Positive clones were obtained as accessed by their ability to grow on SD/QDO selective media and to turn blue in the presence of X-α-Gal. Hence, interaction of APP with HB-EGF was confirmed and validated by the YTH system. Additionally, HB-EGF was found not to interact with the APP intracellular domain (AICD), demonstrating that this region is not responsible for the interaction, and indicating that the interaction must occur via the APP N-terminus. Two N-terminal domains are simultaneously responsible for APP growth promoting activities, MAPK activation and heparin/HSPG binding, and may mediate APP binding to HB-EGF: the GFLD domain at E1 (10,21) and the RERMS domain at E2 (3,10,13,21). Of note, these two APP domains appear to be the relevant biological sites underlying sAPP trophic actions (6,12). Interestingly, immediately adjacent to the GFLD domain is a hydrophobic surface patch that also constitutes a putative HB-EGF binding site on APP. This has to be confirmed in further studies aiming mapping the APP domain responsible for this interaction, for example by using APP deletion mutants.

As with all detection methods, the YTH system is known to result in the detection of some false positive clones; however, the elimination of such false positives has been greatly improved by these recent YTH systems. False positive signals result from cells in which the reporter genes are active even though the bait and prey do not interact. There are several classes of false positives. For example, false positives may arise from preys that interact with DNA upstream of the reporter genes or with proteins that interact with promoter sequences. These two classes of false positives can be eliminated by the use of more than one reporter

gene under the control of different promoters, as was the case of the present work. Other false positives include interactions that occur in the YTH screen but not in a physiological context, because the partners are not co-expressed in the same cellular or subcellular environments. Hence, the new putative protein interaction found by YTH screening was further validated by other method, in order to strengthen the accuracy of PPI data and hence increase the knowledge on functional proteomics.

Validation of the APP/HB-EGF interaction by pull-down assays and subcellular co-localization. The GFP-Trap® Pull-Down is a reliable technique used to validate *ex vivo* protein interactions, and is based on the pull-down of GFP-trapped complexes. To validate the APP/HB-EGF interaction and its physiological relevance we attempted to demonstrate the complex formation between APP and Myc-HB-EGF, as well as endogenous HB-EGF, in a mammalian cell line (HeLa) transfected with APP-GFP and Myc-HB-EGF cDNAs. Immunoblot analysis using the anti-Myc-tag that recognizes the Myc-HB-EGF fusion protein, and the anti-HB-EGF antibody that recognizes the various HB-EGF species, showed that APP interacts with both the exogenous and endogenous pro-domain-containing HB-EGF forms. These results are in agreement and further extend the results obtained in the YTH, validating the APP/HB-EGF interaction.

Previous studies have shown that the HB-EGF propeptide domain is cleaved rapidly after synthesis of the precursor or readily as it reaches the cell surface, with PM-anchored HB-EGF mainly consisting of ORF_{63-208} (proHB-EGF) (37). As previously described, the HB-EGF cDNA was cloned into the pCMV-Myc vector, which contains the Myc tag in an N-terminal position relatively to the MCS. Therefore, since interaction was evidenced with the anti-Myc-tag antibody, we can point out that the APP/HB-EGF interaction is possible to occur as soon as pre-proHB-EGF is synthetized by ER-bound ribosomes and through its trafficking in the Golgi and TGN. Indeed, APP-GFP mainly co-localized with Myc-HB-EGF in the Golgi apparatus and nearby vesicles, as expected for two fusion proteins being overexpressed that follow the same secretory pathway to be membrane-targeted and medium secreted.

Facing the impossibility of detecting proHB-EGF (the form generated after prodomain cleavage) with the anti-Myc-tag antibody, the anti-HB-EGF antibody was used to evaluate whether the interaction also occurred with endogenous HB-EGF and with HB-EGF species other than pre-proHB-EGF. Of note, the immunogen used to create this antibody is a synthetic peptide derived from human HB-EGF corresponding to the 80-130 aa sequence (HB-EGF mature domain), with the antibody recognizing the pre-pro, pro, and soluble HB-EGF species. A positive interaction was detected between APP and various HB-EGF endogenous species

ranging from 31 to 37 KDa that most likely represent different degrees of post-translationally modified pre-proHB-EGF. Additionally, APP appeared to interact with a lower molecular weight form of HB-EGF (25 kDa) most possibly corresponding to proHB-EGF, although this needs further confirmation.

Further studies will also address if the mature HB-EGF domain is the region responsible for binding APP. As previously reported (57), HB-EGF can be released at a very low rate under normal culture conditions, and we have barely detected it in the conditioned medium (data not shown). Therefore, the shedding of proHB-EGF under PKC or PMA stimulation will be used to ensure the presence of sHB-EGF in detectable levels in the incubation medium. Furthermore, a construct corresponding to prodomain-truncated soluble HB-EGF was designed, and will be generated and used in subsequent studies to better characterize APP/HB-EGF binding. Cell surface protein biotinylation assays will also be pursued to specifically test for the interaction with PM-anchored proHB-EGF forms.

Very interestingly, the immunoblots probed with the CT695 antibody (recognizing the C-terminus of APP) detected not only APP-GFP but also endogenous APP in the pulled-down samples, which seems to represent APP homodimerization. Cell-bound APP was already reported to form dimers, with trans-dimerization promoting cell-cell adhesion and being mapped to the E1 and E2 APP regions (10,22). It was further shown that heparin binding to the E1 or E2 region would induce APP dimerization (13). As mentioned, heparin is also a HB-EGF interactor, and APP heparin-binding domains are involved in APP functions common to HB-EGF. Thus, the formation of a *cis* (same PM) or a trans (cell-to-cell) complex between APP, proHB-EGF and heparin and/or HPSG, with a role in cell adhesion, appears feasible and is a hypothesis that should be pursued.

The APP/HB-EGF molecular association might exert diverse effects depending on the context or subcellular compartment. Immunocytochemistry studies using the anti-Myc-tag antibody showed the expected higher localization of this pre-proHB-EGF form in the ER and Golgi (a structure extensively stained by APP-GFP) compartments, and in nearby larger vesicles possibly related to the TGN. A good degree of co-localization with APP-GFP could be observed in these regions, consistent with both proteins being processed via the secretory pathway. When using the anti-HB-EGF antibody, we could note that endogenous HB-EGF co-localizes at a much lesser extent with APP-GFP, with co-localization being occurring predominantly at small cytoplasmic vesicles distributed throughout the cell. Further experiments will be required to accomplish the identification of these cytoplasmic vesicles, namely to confirm their secretory origin. Endogenous HB-EGF also accumulates less at the ER and Golgi than Myc-HB-

EGF, which was being overexpressed, indicating that HB-EGF is normally readily packaged into secretory vesicles under normal conditions. These results suggest that endogenous HB-EGF associates with APP at/after TGN sorting and at the cell membrane. Nonetheless, endogenous HB-EGF cell surface staining was barely visible and only in a few cells, indicating that in HeLa cells, proHB-EGF (and possibly part of the sHB-EGF) must be generated intracellularly. It will be interesting to observe if the same occurs in neuronal-like cells such as the SH-SY5Y line.

Of note, an ICC procedure with both the anti-Myc-tag and anti-HB-EGF antibody performed in HB-EGF overexpressing cells, showed that the anti-HB-EGF antibody does not recognize efficiently transfected Myc-HB-EGF since very low levels of co-localization between this and the anti-myc-tag antibody occurred in Myc-HB-EGF expressing cells. It is possible that the newly synthesized Myc-HB-EGF, just before suffering any cleavage and still with the Myc tag, has the HB-EGF antibody epitope masked by the tag, impairing at some degree the antibody recognition of the recombinant Myc-HB-EGF fusion protein. This only occurred in native folding conditions such as in ICC, but not in reducing conditions such as in the WB assay.

Several growth factors and cytokines are synthesized as membrane-anchored proteins, and these are not only the precursor forms of soluble factors but also biological active molecules. Membrane-anchored forms may have different biological activity from their soluble counterparts, acting in a juxtacrine way, and their activity can be regulated by associating molecules. There are reported evidences that proHB-EGF may have opposite effects than sHB-EGF: while this always presents growth-promoting activity, proHB-EGF has the ability to suppress the growth of cancer cells through continuous and sustained EGFR phosphorylation and up-regulation (37,70). Association with APP might specifically increase some of the proHB-EGF functions, as it occurs with its association with CD9, which enhance HB-EGF binding to DT and its mitogenic activity. Together with integrin α3β1, proHB-EGF and CD9 were found to co-localize at cell–cell contact sites near adherence junctions, where EGF receptors and APP are also localized. APP may stabilize membranar proHB-EGF and deviate it for a cell adhesion and/or cell migration role, forming a complex with proHB-EGF, CD9 and integrin α3β1. Indeed, APP and integrins interact and are known to be involved in cell adhesion and migration (13,14). APP might also direct proHB-EGF for a specific receptor, either ErB1 or Erb4, with different physiological outputs (37,42,43,84).

Influence of APP and HB-EGF in each other protein levels. WB analyses showed that exogenous HB-EGF and APP-GFP levels decreased when both fusion proteins were co-transfected, when compared to their ‘solely’ transfection. The observed decay in the

exogenous APP levels propelled us to further evaluate mature and immature APP levels. The amount of mature APP-GFP was indeed suffering a considerable decline, raising some questions. First, it was considered the possibility of HB-EGF being, in someway, impairing the exogenous APP maturation process, but the percentage of mature APP-GFP against its total amounts did not decreased. Hence, Myc-HB-EGF did not hindered maturation in the secretory pathway. A second hypothesis that would suit the current results was the possibility of HB-EGF being promoting APP proteolysis to sAPP. However, HB-EGF induced a decrease in soluble APP secretion for the cell medium, for both endogenous and exogenous sAPP, allowing us to rule out this hypothesis. Further, sAPP levels in APP-GFP samples decreased to a similar extent as the full length APP-GFP levels (~65%), pointing the later as the reason for lesser sAPP. Concerning the impairment in APP-GFP levels, we can hypothesize that Myc-HB-EGF interferes with its vesicular post-TGN trafficking and/or promotes mature APP degradation via the lysosomal machinery. This hypothesis remains to be tested but an experiment to address it was already designed. Further, these results can also be co-transfection artifacts, resulting from less availability and binding to the transfection reagent in co-transfection conditions. This is feasible, since APP and HB-EGF have opposite effects on each other endogenous protein levels, as described below.

APP appears to induce a slight increase in endogenous HB-EGF, but this has to be further validated in subsequent experiments. Further, HB-EGF overexpression induced an increase in total endogenous APP, either immature or mature. The amount of the mature APP form was especially increased, confirmed by the higher percentage of APP maturation in HB-EGF overexpressing cells. In what concerns this effect, we can postulate that HB-EGF is retaining mature APP in secretory vesicles and/or at the plasma membrane, so that they can act synergistically in cell surface adhesion and interacting with proteins of the extracellular matrix, since both appear to be involved in membrane-matrix stabilization.

Concerning the raise in the endogenous APP levels, two feasible explanations were purposed: HB-EGF can be somehow promoting APP's half-life or, in a neurotrophin-like scenario (85,86), promoting APP gene transcription. Through the use of radioactivity-based techniques, the half-life of total cellular APP was estimated to be of approximately 1 h (29). After exposing cells for 1h to cycloheximide (an inhibitor of protein synthesis), we observed that the amounts of endogenous APP suffered a significant and similar decline in both control and Myc-HB-EGF expressing cells. This suggests that the increase of endogenous APP is not due to an increase in APP's half-life because, if this was the case, the decrease in APP protein levels would not be as accentuated as in control condition (87). Thus, the remarkable upregulation in endogenous APP levels is likely due to a positive regulation of APP gene

transactivation, potentially through the nuclear translocated HB-EGF C-terminus. As already observed for neurotrophins such as NGF and BDNF, APP may sustain long-term signaling for HB-EGF. Neurotrophins also lead to increased APP levels (by gene transactivation) and, later on, to its cleavage to sAPP and AICD. These topics here addressed will need further investigation through mRNA studies and the use of HB-EGF deletion constructs.

Influence of APP and HB-EGF overexpression in Erk and STAT3 signaling. Concerning the influence of HB-EGF and APP overexpression in Erk signaling, we could observe that HB-EGF overexpression led to a 3,10 FI in MAPK activation, which corroborates several previous studies reporting that HB-EGF signals preferentially through the MAPK signaling pathway. Very interestingly, APP overexpression alone drove the second highest effects on the rate of MAPK activation (FI of ~2). While APP:HB-EGF co-transfection still induced an increase in MAPK activation over control condition, it decreased the rate of MAPK activation relatively to HB-EGF, suggesting that APP/HB-EGF interaction does not necessarily leads to MAPK activation. Concerning the effects in STAT3 signaling, HB-EGF, either alone or co-expressed with APP-GFP, did not affect this pathway. Further, it was realized that APP-GFP overexpression *per se* slightly decreased the rate of STAT3 phosphorylation.

When APP is associated with pre-pro and proHB-EGF in HeLa cells the Erk signaling is not preferentially activated, which may, in part, be due to the induced decrease of soluble APP secretion. Indeed, it is previous knowledge that sAPP promotes the Erk signaling activation (88,89). Similarly, impairment in soluble HB-EGF secretion may be occurring, which would contribute to this scenario, and this will be further pursued.

APP effects on EGF-induced signaling. As expected for EGF itself, it prompted a 170±20 FI in MAPK phosphorylation, comparing to the basal condition. Consistent with the previous obtained results for the influence of APP overexpression in MAPK signaling, also in these experiments APP alone was able to again drive a 2-fold increase in MAPK phosphorylation. Very interestingly, a remarkable result was obtained when APP overexpressing cells were exposed to EGF treatment. APP overexpression led to a ~2,3 FI increase in P-MAPK levels, comparing to cells transfected with the EGFP vector and treated with EGF. This means that APP acts synergistically with EGF to significantly enhance MAPK activation, and hence promoting sEGF-induced Erk signaling.

The influence of APP in the STAT3 signaling was confirmed by this set of studies, resulting in a decrease on STAT3 phosphorylation of approximately 30%; nonetheless, this decrease was abolished under EGF stimulation. Therefore, unlike for Erk signaling, APP is not

prone to signal through the STAT3 cascade but may not totally impair it when it is activated by other signals.

Analysis of the APP/EGF and APP/EGFR interaction by GFP-Trap Pull-Down. Towards analyzing the possibility of APP to interact with two more proteins involved in the EGFR signaling pathway, namely EGF itself and EGFR, the immunoblots of the APP:HB-EGF pull-down experiments (60 mm) were probed for these two proteins.

First, the anti-EGF antibody was used and the presence of three immunoreactive proteins, ranging from 94-110 kDa, was demonstrated in HeLa cell lysates, which most likely represent pre-proEGF and proEGF species with different glycosylation degrees. Similar maturation of the membrane-associated proEGF was previously reported in rat kidney (57). Further, these authors have described that HeLa cells transiently transfected with pre-proEGF cDNA first produce the EGF high molecular weight precursor, proEGF, and that this precursor is membrane anchored, being expressed at the cell surface as shown by biotinylation experiments (57). Similarly to human HB-EGF, the EGF species detected in HeLa cell lysates are most possibly pre-pro and proEGF, found intracellularly and at the cell surface. Of note, data reported on mouse EGF are similar to those obtained for mouse HB-EGF and suggests that the proEGF is the form that is preferentially found at the cell surface.

Surprisingly, the 94 kDa immunoreactive species was also clearly detected in APP pull-down precipitates, evidencing a novel interaction between APP and a proEGF species. Further experimental studies will be needed in order to understand what species these bands may represent, to confirm this novel interaction, and to study whether the same result is obtained for the 6 kDa soluble EGF form. Indeed, this result raises the question if the EGF domain is the main region promoting binding to APP, and this has to be further tested. Of note, the HB-EGF heparin-binding domain lies mostly N-terminal to the EGF-like domain but partially overlaps with this. In addition, it would also be interesting to evaluate if proHB-EGF competes with pro-EGF for APP.

Due to the remarkable results obtained with the EGF studies and since HeLa cells express endogenous EGFR at physiological levels at the cell surface, this receptor was also tested for binding to APP. Unfortunately, our initial attempt to detect EGFR protein failed since the antibody was not working properly and failed to recognize the endogenous EGFR protein in all tested cell lysates.

We may hypothesize that while EGFR is a high affinity cell surface receptor for proEGF and proHB-EGF, APP functions as a lower affinity receptor for these (and other precursors of growth factors and cytokines), regulating their autocrine and juxtacrine roles. Indeed, APP-GFP

overexpression was observed to induce a sustained but low response in the MAPK activation (2.0 FI), while EGFR activation via sEGF resulted in a fast and robust MAPK activation (increased by ~170 times in 30 min). Further, these pathways may compete, since AICD leads to a long-term decrease in EGFR levels, and/or APP may signal through EGFR, what needs to be further addressed.

APP/HB-EGF- and APP/EGF – induced alterations in cellular morphology. Very interestingly, HB-EGF overexpression rendered a significant promotion of cell elongation, with cells presenting an average cell length of ~85 µm, comparing to the ~53 µm measured in vector transfected cells (Figure 34). While cells treatment with EGF also resulted in cell elongation, it was considerably inferior to the one induced by HB-EGF, with EGF main effect being to induce cell plasticity. A parallel can be drawn with the effects reported for HB-EGF in neurite outgrowth, via activation of the ERK signaling pathway, an effect never been reported for EGF (84).

When APP was co-transfected with HB-EGF, it appears that the cell elongation prompted by HB-EGF was inhibited to APP values, similarly to what occurred in Erk activation assays. This points out that, besides apparently not signaling through Erk (or STAT3), the physiological function of the APP/HB-EGF interaction is probably not to mediate cell differentiation. When APP-GFP cells were stimulated with EGF, no significant alteration on cell elongation could be observed (Figure 34).

7 Conclusions

We have here first described the interaction between APP and cellular HB-EGF. Taken together, results indicate that the HB-EGF binding domain in the APP protein is most likely located at the APP N-terminus, most probably at one of the APP heparin-binding motifs responsible for APP trophic role. This hypothesis needs further confirmation, together with the hypothesis that the prodomain and/or the mature domain on HB-EGF are responsible for APP binding. Outstandingly, we also first describe the physical interaction between APP and cellular EGF, a widely known mitogenic and trophic factor, strengthening the hypothesis that the EGF domain is the region that binds to APP.

In a first set of experiments, we have observed that while APP and EGF seem to have a synergistic effect in promoting EGF-induced Erk signaling, the same does not occur for APP and HB-EGF, that appear to have opposite effects in this respect. Nonetheless, the experimental conditions tested were different, and this signaling interference has still to be evaluated in APP overexpressing cells exposed to soluble HB-EGF. It will be also important to tests whether the APP 'basal' effect in MAPK phosphorylation is mediated by its binding to proEGF and/or proHB-EGF, by e.g. siRNA interfering assays.

The relevance of these interactions will certainly be further addressed by us. Due to their tissue distribution, APP and EGF interaction should be of major importance regulating non-brain tissues, while APP and HB-EGF interaction may be of higher functional relevance in neuronal tissues, where it is known to be expressed at much higher levels than EGF (44,50). APP and HB-EGF role in brain show quite an overlap. In fact, HB-EGF and APP/sAPP have been implicated in neuronal survival, glial/stem cell proliferation and differentiation, contributing to adult neurogenesis in the dentate gyrus of the hippocampus (49). Importantly, evidences suggest that HB-EGF may be one of the important contributors to synaptic plasticity and memory formation in the hippocampus, determinant functions also reported for APP, and found impaired in AD.

In summary, our recent findings place HB-EGF and EGF as important players in multiple steps of APP signaling, and vice-versa. The identification of novel putative APP interactors such as these will always represent a hallmark in molecular biology studies, since they can potentially help to understand the biology of APP, and, ultimately, better characterize APP-related AD pathogenesis.

8 References

1. Zhang H, Ma Q, Zhang Y, Xu H. Proteolytic processing of Alzheimer's β-amyloid precursor protein. Journal of neurochemistry. 2012 Jan;120 Suppl:9–21.

2. Ling Y, Morgan K, Kalsheker N. Amyloid precursor protein (APP) and the biology of proteolytic processing: relevance to Alzheimer's disease. The International Journal of Biochemistry & Cell Biology. 2003 Nov;35(11):1505–35.

3. Strooper B De, Annaert W. Proteolytic processing and cell biological functions of the amyloid precursor. Journal of cell science. 2000;113:1857–70.

4. Selkoe D. The cell biology of β-amyloid precursor protein and presenilin in Alzheimer's disease. Trends in Cell Biology. 1998 Nov 1;8(11):447–53.

5. Selkoe D. Alzheimer ' s Disease : Genes , Proteins , and Therapy. Physiological Reviews. 2001;81(2):741–66.

6. Chow VW, Mattson MP, Wong PC, Gleichmann M. An Overview of APP Processing Enzymes and Products. Neuromolecular Medicine. 2010;12(1):1–12.

7. Thinakaran G, Koo EH. Amyloid Precursor Protein Trafficking , Processing , and Function. Journal of Biological Chemistry. 2009;283(44):29615–9.

8. Henriques AG, Vieira SI, Da Cruz e Silva EF, Da Cruz e Silva OAB. A-beta promotes Alzheimer's disease-like cytoskeleton abnormalities with consequences to APP processing in neurons. Journal of neurochemistry. 2010;113:761–71.

9. Cummings JL. Alzheimer's Disease. New England Journal of Medicine. 351:56–67.

10. Reinhard C, Hébert SS, De Strooper B. The amyloid-beta precursor protein: integrating structure with biological function. The EMBO journal. 2005 Dec 7;24(23):3996–4006.

11. King GD, Turner RS. Adaptor protein interactions : modulators of amyloid precursor protein metabolism and Alzheimer ' s disease risk ? Experimental Neurology. 2004;185:208–19.

12. O'Brien RJ, Wong PC. Amyloid Precursor Protein Processing and Alzheimer's Disease. Annual Reviews of Neuroscience. 2011;1987:185–204.

13. Zheng H, Koo EH. Biology and pathophysiology of the amyloid precursor protein. Molecular Neurodegeneration. BioMed Central Ltd; 2011;6(1):27.

14. Zhang Y, Thompson R, Zhang H, Xu H. APP processing in Alzheimer's disease. Molecular brain. BioMed Central Ltd; 2011 Jan;4(1):3.

15. Da Cruz e Silva EF, Da Cruz e Silva OA. Protein phosphorylation and APP metabolism. Neurochemical Research. 2003;28(10):1553–61.

16. Kang J, Lemaire HG, Unterbeck A, Salbaum JM, Masters CL, Grzeschik KH, et al. The precursor of Alzheimer's disease amyloid A4 protein resembles a cell-surface receptor. Nature. 1987;6106:733–6.

17. Schmechel D, Goldgaber D, Burkhart D, Gilbert J, Gajdusek D RA. Cellular localization of messenger RNA encoding amyloid-beta-protein in normal tissue and in Alzheimer disease. Alzheimer Dis Assoc Disord. 1988;2:96–111.

18. Tanzi RE, Gusella JF, Watkins PC, Bruns GA, St George- Hyslop P, Van Keuren, M.L., Patterson D, et al. Amyloid beta protein gene: cDNA, mRNA distribution, and genetic linkage near the Alzheimer locus. Science. 1987;235:880–4.

19. Suzuki T, Nakaya T. Regulation of Amyloid β-Protein Precursor by Phosphorylation and Protein Interactions. The Journal of Biological Chemistry. 2008;283(44):29633–7.

20. Suzuki T, Oishi M, Marshak DR, Czernik AJ, Nairn AC, Greengard P. Cell cycle,dependent regulation of the phosphorylation and metabolism of the Alzheimer amyloid precursor protein. The EMBO journal. 1994;13(5):1114–22.

21. Kong GK, Miles LA, Crespi GAN, Morton CJ, Ling H, Kevin N, et al. Copper binding to the Alzheimer ' s disease amyloid precursor protein. Eur Biophys J. 2008;37:269–79.

22. Soba P, Eggert S, Wagner K, Zentgraf H, Siehl K, Kreger S, et al. Homo- and heterodimerization of APP family members promotes intercellular adhesion. The EMBO journal. 2005 Oct 19;24(20):3624–34.

23. Small SA, Gandy S. Sorting through the Cell Biology of Alzheimer ' s Disease : Intracellular Pathways to Pathogenesis. Neuron. 2006;52:15–31.

24. Evin G, Weidemann A. Biogenesis and metabolism of Alzheimer's disease Abeta amyloid peptides. Peptides. 2002;23(7):1285–97.

25. Schettini G, Govoni S, Racchi M RG. Phosphorylation of APP-CTF-AICD domains and interaction with adaptor proteins: signal transduction and/or transcriptional role – relevance for Alzheimer pathology. Journal of Neurochemistry. 2010;115:1299–308.

26. Müller UC, Zheng H. Physiological functions of APP family proteins. Cold Spring Harbor perspectives in medicine. 2012 Feb;4:a006288.

27. Vieira SI, Rebelo S, Esselmann H, Wiltfang J, Lah J, Lane R, et al. Retrieval of the Alzheimer's amyloid precursor protein from the endosome to the TGN is S655 phosphorylation state-dependent and retromer-mediated. Molecular Neurodegeneratio. BioMed Central Ltd; 2010 Jan;5:40.

28. Bayer TA, Wirths O, Majtényi K, Hartmann T, Multhaup G, Beyreuther K CC. Key Factors in Alzheimer's Disease: β-amyloid Precursos Protein Processing, Metabolism and Intraneuronal Transport. Brain Pathology. 2001;11:1–11.

29. Haass C, Kaether C, Thinakaran G, Sisodia S. Trafficking and proteolytic processing of APP. Cold Spring Harbor perspectives in medicine. 2012 May;2(5):a006270.

30. Saito Y, Sano Y, Vassar R, Gandy S, Nakaya T, Yamamoto T, et al. X11 proteins regulate the translocation of amyloid beta-protein precursor (APP) into detergent-resistant membrane and suppress the amyloidogenic cleavage of APP by beta-site-cleaving enzyme in brain. The Journal of biological chemistry. 2008 Dec 19;283(51):35763–71.

31. Wang Z. Presynaptic and postsynaptic interaction of the amyloid precursor protein promotes peripheral and central synaptogenesis. Journal of Neuroscience. 2009;29(35):10788–801.

32. Lu D.C., Rabizadeh S., Chandra E., Shayya R., Ellerby L.M., Ye X., Salvesen G.S., Koo E.H. BDE. A second cytotoxic proteolytic peptide derived from amyloid beta-protein precursor. Nature Medicine. 2000;6:397–404.

33. Cohen S, Carpenter G. Epidermal Growth Factor. Journal of Biological Chemistry. 1990;265(14):7709–12.

34. Beerli RR, Hynes NE. Epidermal growth factor-related peptides activate distinct subsets of ErbB receptors and differ in their biological activities. The Journal of biological chemistry. 1996 Mar 15;271(11):6071–6.

35. Adam RM. Role of HB-EGF in cancer [Internet]. 2010 [cited 2013 Feb 2]. Available from: http://atlasgeneticsoncology.org/Deep/HB-EGFinCancerID20090.html

36. Iwamoto R, Mekada E. Heparin-binding EGF-like growth factor: a juxtacrine growth factor. Cytokine & growth factor reviews. 2000 Dec;11(4):335–44.

37. Raab G, Klagsbrun M. Heparin-binding EGF-like growth factor. Biochimica et biophysica acta. 1997 Dec 9;1333(3):F179–99.

38. Iwamoto R, Yamazaki S, Asakura M, Takashima S, Hasuwa H, Miyado K, et al. Heparin-binding EGF-like growth factor and ErbB signaling is essential for heart function. Proceedings of the National Academy of Sciences of the United States of America. 2003 Mar 18;100(6):3221–6.

39. Pathway Central: EGF Pathway [Internet]. [cited 2013 Feb 2]. Available from: http://www.sabiosciences.com/pathway.php?sn=EGF_Pathway

40. Sun D, Bullock MR, Altememi N, Zhou Z, Hagood S, Rolfe A, et al. The effect of epidermal growth factor in the injured brain after trauma in rats. Journal of neurotrauma. 2010 May;27(5):923–38.

41. Mekada E, Iwamoto R. HB-EGF : Basis Sequence - Mouse, UCSD-Nature Molecule Pages [Internet]. [cited 2013 Feb 2]. Available from: http://www.signaling-gateway.org/molecule/query?afcsid=A002932&type=abstract

42. Nishi E, Prat A, Hospital V, Elenius K, Klagsbrun M. N-arginine dibasic convertase is a specific receptor for heparin-binding EGF-like growth factor that mediates cell migration. The EMBO journal. 2001 Jul 2;20(13):3342–50.

43. Elenius K, Paul S, Allison G, Sun J, Klagsbrun M. Activation of HER4 by heparin-binding EGF-like growth factor stimulates chemotaxis but not proliferation. The EMBO journal. 1997 Mar 17;16(6):1268–78.

44. Oyagi A, Hara H. Essential roles of heparin-binding epidermal growth factor-like growth factor in the brain. CNS neuroscience & therapeutics. 2012 Oct;18(10):803–10.

45. Mishima K, Higashiyama S, Nagashima Y et al. Regional distribution of heparin-binding epidermal growth factor-like growth factor mRNA and protein in adult rat forebrain. Neurosci Lett. 1996;213:153–6.

46. Hayase Y, Higashiyama S, Sasahara M, Amano S, Nakagawa T, Taniguchi N HF. Expression of heparin-binding epidermal growth factor-like growth factor in rat brain. Brain Res. 1998;784:163–78.

47. Nakagawa T, Sasahara M, Hayase Y et al. Neuronal and glial expression of heparin-binding EGF-like growth factor in central nervous system of prenatal and early-postnatal rat. Devolpmental Brain Research. 1998;108:263–72.

48. Imudia AN, Kilburn BA, Petkova A, Edwin SS, Romero R, Armant DR. Expression of heparin-binding EGF-like growth factor in term chorionic villous explants and its role in trophoblast survival. Placenta. 2009;29(9):784–9.

49. Kunlin Jin, Xiao Ou Mao, Yunjuan Sun, Lin Xie, Lan Jin, Eiichiro Nishi, Michael Klagsbrun DG. Heparin-binding epidermal growth factor-like growth factor: hypoxia-inducible expression in vitro and stimulation of neurogenesis in vitro and in vivo. The Journal of neuroscience. 2002 Jul 1;22(13):5365–73.

50. Zhou Y, Besner GE. Heparin-binding epidermal growth factor-like growth factor is a potent neurotrophic factor for PC12 cells. Neuro-Signals. 2010 Jan;18(3):141–51.

51. Oyagi A, Moriguchi S, Nitta A et al. Heparin-binding EGF-like growth factor is required for synaptic plasticity and memory formation. Brain Research. 2011;1419:97–104.

52. Peng H, Wen TC, Tanaka J et al. Epidermal growth factor protects neuronal cells in vivo and in vitro against transient forebrain ischemia- and free radical-induced injuries. Journal of Cerebral Blood Flow & Metabolism. 1998;18:349–60.

53. Farkas L, Krieglstein K. Heparin-binding epidermal growth factor-like growth factor (HB-EGF) regulates survival of midbrain dopaminergic neurons. Journal of Neural Transmission. 2002;109:267–77.

54. Edwards JP, Zhang X, Mosser DM. The Expression of Heparin-Binding Epidermal Growth Factor-Like Growth Factor by Regulatory Macrophages. Journal of Immunology. 2010;182(4):1929–39.

55. Hieda M, Isokane M, Koizumi M, Higashi C, Tachibana T, Shudou M, et al. Membrane-anchored growth factor, HB-EGF, on the cell surface targeted to the inner nuclear membrane. The Journal of cell biology. 2008 Feb 25;180(4):763–9.

56. Hieda M, Koizumi M, Higashi C, Tachibana T, Taguchi T, Higashiyama S. The cytoplasmic tail of heparin-binding EGF-like growth factor regulates bidirectional intracellular trafficking between the plasma membrane and ER. FEBS Open Bio. Federation of European Biochemical Societies; 2012 Jan;2:339–44.

57. Le Gall SM, Auger R, Dreux C, Mauduit P. Regulated cell surface pro-EGF ectodomain shedding is a zinc metalloprotease-dependent process. The Journal of biological chemistry. 2003 Nov 14;278(46):45255–68.

58. Suzuki M, Raab G, Moses M a, Fernandez C a, Klagsbrun M. Matrix metalloproteinase-3 releases active heparin-binding EGF-like growth factor by cleavage at a specific juxtamembrane site. The Journal of biological chemistry. 1997 Dec 12;272(50):31730–7.

59. Goishi K, Higashiyama S, Klagsbrun M, Nakano N, Umata T, Ishikawa M, et al. Phorbol ester induces the rapid processing of cell surface heparin-binding EGF-like growth factor: conversion from juxtacrine to paracrine growth factor activity. Molecular biology of the cell. 1995 Aug;6(8):967–80.

60. Nanba D, Higashiyama S. Dual intracellular signaling by proteolytic cleavage of membrane-anchored heparin-binding EGF-like growth factor. Cytokine & Growth Factor Reviews. 2004 Feb;15(1):13–9.

61. Gechtman Z, Alonso JL, Raab G, Ingber DE, Klagsbrun M. The shedding of membrane-anchored heparin-binding epidermal-like growth factor is regulated by the Raf/mitogen-activated protein kinase cascade and by cell adhesion and spreading. The Journal of biological chemistry. 1999 Oct 1;274(40):28828–35.

62. Blobel CP, Carpenter G, Freeman M. The Role od Protease Activity in ErbB Biology. Experimental Cell Research. 2010;315(4):671–82.

63. Izumi Y, Hirata M, Hasuwa H, Iwamoto R, Umata T, Miyado K, et al. A metalloprotease-disintegrin, MDC9/meltrin-gamma/ADAM9 and PKCdelta are involved in TPA-induced ectodomain shedding of membrane-anchored heparin-binding EGF-like growth factor. The EMBO journal. 1998 Dec 15;17(24):7260–72.

64. Herrlich A, Klinman E, Fu J, Sadegh C, Lodish H. Ectodomain cleavage of the EGF ligands HB-EGF, neuregulin1-beta, and TGF-alpha is specifically triggered by different stimuli and involves different PKC isoenzymes. FASEB journal : official publication of the Federation of American Societies for Experimental Biology. 2008 Dec;22(12):4281–95.

65. Toki F, Nanba D, Matsuura N, Higashiyama S. Ectodomain shedding of membrane-anchored heparin-binding EGF like growth factor and subcellular localization of the C-terminal fragment in the cell cycle. Journal of cellular physiology. 2005 Mar;202(3):839–48.

66. Naglich JG, Metherall JE, Russel DW, Eidels L. Expression cloning of a difteria toxin receptor: identity with a heparin-binding EGF-like growth factor precursor. Cell. 1992;(69):1051–61.

67. Nakamura K, Mitamura T, Takahashi T, Kobayashi T, Mekada E. Importance of the major extracellular domain of CD9 and the epidermal growth factor (EGF)-like domain of

heparin-binding EGF-like growth factor for up-regulation of binding and activity. The Journal of biological chemistry. 2000 Jun 16;275(24):18284–90.

68. Higashiyama S, Iwamoto R, Goishi K, Raab G, Taniguchi N, Klagsbrun M, et al. The membrane protein CD9/DRAP 27 potentiates the juxtacrine growth factor activity of the membrane-anchored heparin-binding EGF-like growth factor. The Journal of cell biology. 1995 Mar;128(5):929–38.

69. Raab G, Kover K, Paria BC, Dey SK, Ezzell RM, Klagsbrun M. Mouse preimplantation blastocysts adhere to cells expressing the transmembrane form of heparin-binding EGF-like growth factor. Development. 1996;(122):637–45.

70. Miyoshi E, Higashiyama S, Nakagawa T, Hayashi N, Taniguchi N. Membrane-anchored heparin-binding epidermal growth factor-like growth factor acts as a tumor survival factor in a hepatoma cell line. The Journal of biological chemistry. 1997 May 30;272(22):14349–55.

71. Prenzel N, Zwick E, Daub H, Leserer M, Abraham R, Wallasch C UA. EGF receptor transactivation by G-protein-coupled receptors requires metalloproteinase cleavage of proHB-EGF. Nature. 1999;402:884–8.

72. Nanba D, Mammoto A, Hashimoto K, Higashiyama S. Proteolytic release of the carboxy-terminal fragment of proHB-EGF causes nuclear export of PLZF. The Journal of cell biology. 2003 Nov 10;163(3):489–502.

73. Jessmon P, Kilburn B a, Romero R, Leach RE, Armant DR. Function-specific intracellular signaling pathways downstream of heparin-binding EGF-like growth factor utilized by human trophoblasts. Biology of reproduction. 2010 May;82(5):921–9.

74. Fields S, Song O. A novel genetic system to detect protein-protein interactions. Nature. 1989;340:245–6.

75. Causier B, Davies B. Analysing protein-protein interactions with the yeast two-hybrid system. Plant Mol Biol. 2002;50:855–70.

76. Timóteo SC. Identification of Protein Complexes in Alzheimer's Disease. 2012;

77. Vieira SI, Rebelo S, Domingues SC, Da Cruz e Silva EF, O.A. da C e S. S655 phosphorylation enhances APP secretory traffic. Molecular and Cell ular Biochemistry. 2009;328(1-2):145–54.

78. Da Cruz e Silva OA, Fardilha M, Henriques AG, Rebelo S, Vieira S, Da Cruz Silva EF. Signal transduction therapeutics: relevance for Alzheimer's disease. Journal of Molecular Neuroscience. 2004;23(1-2):123–42.

79. Romero-Calvo I, Ocón B, Martínez-Moya P, Suárez MD, Zarzuelo A, Martínez-Augustin O, et al. Reversible Ponceau staining as a loading control alternative to actin in Western blots. Analytical biochemistry. 2010 Jun 15;401(2):318–20.

80. Minoru Ono, Gerhard Raab, Keneth Lau, Judith A. Abraham MK. Purification and Characterization of Transmembrane Forms of Heparin-binding EGF-like Growth Factor. The Journal of biological chemistry. 1994 Dec 9;269(49):31315–21.

81. Higashiyamas S, Lauq K, Besners GE, Abraham A. Structure of Heparin-binding EGF-like Growth Factor. Journal of Biological Chemistry. 1992;267(9):6205–12.

82. Da Cruz e Silva OA, Vieira SI, Rebelo S, Da Cruz e Silva EF. A model system to study intracellular trafficking and processing of the Alzheimer's amyloid precursor protein. Neurodegenerative Disease. 2004;196–204.

83. Cerqueira R. APP and APP phosphorylation in Gα o -induced STAT3 signaling. 2012;

84. Zhou Y, Besner GE. Heparin-binding epidermal growth factor-like growth factor is a potent neurotrophic factor for PC12 cells. Neuro-Signals. 2010 Jan;18(3):141–51.

85. Ruiz-León Y PA. Induction of tyrosine kinase receptor b by retinoic acid allows brain-derived neurotrophic factor-induced amyloid precursor protein gene expression in human sh-sy5y neuroblastoma cells. Neuroscience. 2003;120:1019–26.

86. Holback S, Adlerz L IK. Increased processing of APLP2 and APP with concomitant formation of APP intracellular domains in BDNF and retinoic acid-differentiated human neuroblastoma cells. Journal of Neurochemistry. 2005;95:1059–68.

87. Liu M, Dhanwada KR, Birt DF, Hecht S, Pelling JC. Increase in p53 protein half-life in mouse keratinocytes following UV-B irradiation. Carcinogenesis. 1994 Jun;15(6):1089–92.

88. Turner P.R., O'Connor K., Tate W.P. AWC. Roles of amyloid precursor protein and its fragments in regulating neural activity, plasticity and memory. Progress in Neurobiology. 2003;70:1–32.

89. Gakhar-Koppole N., Hundeshagen P., Mandl C., Weyer S.W., Allinquant B., Muller U. and CF. Activity requires soluble amyloid precursor protein alpha to promote neurite outgrowth in neural stem cell-derived neurons via activation of the MAPK pathway. European Journal of Neurosciences. 2008;28:871–82.

9 Appendix

Culture media and solutions

I. Bacterial media

- **LB (Luria-Bertani) Medium**

To 950 mL of deionised H_2O add:

LB	25 g
Agar	15 g (for plates only)

Shake until the solutes have dissolved. Adjust the volume of the solution to 1 L with deionised H_2O. Sterilize by autoclaving.

- **SOB Medium**

To 950 mL of deionised H2O add:

SOB Broth	25.5 g

Shake until the solutes have dissolved. Add 10 mL of a 250mM KCl (prepared by dissolving 1.86g of KCl in 100 mL of deionised H_2O). Adjust the pH to 7.0 with 5N NaOH. Just prior to use add 5 mL of a sterile solution of 2M $MgCl_2$ (prepared by dissolving 19 g of $MgCl_2$ in 90 mL of deionised H2O). Adjust the volume of the solution to 1 L with deionised H_2O and sterilize by autoclaving).

- **SOC Medium**

SOC is identical to SOB except that it contains 20 mM glucose. After the SOB medium has been autoclaved, allow it to cool to 60°C and add 20 mL of a sterile 1M glucose (this solution is made by dissolving 18 g of glucose in 90 mL of deionised H_2O; after the sugar has dissolved, adjust the volume of the solution to 1 L with deionised H_2O and sterilize by filtration through a 0.22-micron filter.

II. Yeast Media

- **SD synthetic medium**

To 800 mL of deionised H2O add:

Yeast nitrogen base without amino acids (DIFCO)	6.7 g
Agar (for plates only)	15 g

Shake until the solutes have dissolved. Adjust the volume to 850mL with deionized H_2O and sterilize by autoclaving. Allow medium to cool to 60°C and add glucose to 2% (50 mL of a sterile 40% stock solution) and 100 mL of the appropriate 10x dropout solution.

- **10x Dropout solution (10x DO)**

This solution contains all but one or more of the following components:

	10x concentration (mg/L)	SIGMA #
L-Isoleucine	300	I-7383
L-Valine	1500	V-0500
L-Adenine hemisulfate salt	200	A-9126
L-Arginine HCl	200	A-5131
L-Histidine HCl monohydrate	200	H-9511
L-Leucine	1000	L-1512
L-Lysine HCl	300	L-1262
L-Methionine	200	M-9625
L-Phenylalanine	500	P-5030
L-Threonine	2000	T-8625
L-Tryptophan	200	T-0254
L-Tyrosine	300	T-3754
L-Uracil	200	U-0750

10x dropout supplements may be autoclaved and stored for up to 1 year.

- **YPD medium**

To 950 mL of deionised H_2O add:

YPD	50 g
Agar	15 g (for plates only)

Shake until the solutes have dissolved. Adjust the volume to 1 L with deionized H_2O and sterilize by autoclaving. Allow medium to cool to 60°C and add glucose to 2% (50 mL of a sterile 40% stock solution).

- **TE Buffer (pH 7.5)**

10 mM Tris-HCl (pH 7.5)

1 mM EDTA (pH 8.0)

III. Cell culture Solutions and Immunocytochemistry

- **DMEM Medium**

For a final volume of 1 L, dissolve one pack of DMEM powder (with L-glutamine and 4500 mg glucose/L; Sigma Aldrich) in deionized H_2O and add 3.7 g $NaHCO_3$ (Sigma Aldrich). Adjust to pH 7.4. Sterilize by filtering through a 0,2 μm filter and store at 4°C.

- **Complete DMEM (HeLa cells)**

For a final volume of 1 L, when preparing DMEM medium adjust to pH 7.4 and before sterilizing add: 100 mL (10% v/v) Fetal bovine Serum (FBS; Gibco BRL, Invitrogen). Notes: FBS is heat-inactivated for 30 min at 56°C. For cell maintenance, prior to pH adjustment add 100 U/mL penicillin and 100 mg/mL streptomycin (100 mL Streptomycin/Penicilin/Amphotericin solution (Gibco BRL, Invitrogen)).

- **PBS (1x)**

For a final volume of 500 ml, dissolve one pack of BupH Modified Dulbecco's Phosphate Buffered Saline Pack (Pierce) in deionised H_2O. Final composition:

8 mM Sodium Phosphate

2 mM Potassium Phosphate

140 mM Sodium Chloride

10 mM Potassim Chloride

Sterilize by filtering through a 0.2 μm filter and store at 4°C.

- **4% Paraformaldehyde Fixative solution**

For a final volume of 100 mL, add 4g of paraformaldehyde to 25 mL deionised H_2O. Dissolve by heating the mixture at 58°C while stirring. Add 1-2 drops of 1 M NaOH to clarify the solution and filter (0.2 μm filter). Add 50 mL of 2X PBS and ajust the volume to 100 mL with deionised H_2O.

IV. Solutions for proteins manipulation

SDS-PAGE and Immunoblotting Solutions

- **(4x) LGB (Lower gel buffer)**

To 900 ml of deionised H_2O add:

Tris	181.65 g
SDS	4 g

Mix until the solutes have dissolved. Adjust the pH to 8.9 and adjust the volume to 1L with deionised H2O.

- **(5x) UGB (Upper gel buffer)**

To 900 ml of deionised H_2O add:

Tris	75.69 g

Mix until the solute has dissolved. Adjust the pH to 6.8 and adjust the volume to 1 L with deionised H_2O.

- **30% Acrylamide/0.8% Bisacrylamide**

To 70 ml of deionised H_2O add:

Acrylamide	29.2 g
Bisacrylamide	0.8 g

Mix until the solute has dissolved. Adjust the volume to 100 ml with deionised water. Filter through a 0.2 µm filter and store at 4°C.

- **10% APS (ammonium persulfate)**

In 10 ml of deionised H_2O dissolve 1 g of APS. Note: prepare fresh before use.

- **10% SDS (sodium dodecilsulfate)**

In 10 ml of deionised H_2O dissolve 1 g of SDS.

- **Resolving (lower) gel solution for gradient gels (60 ml)**

	5%	**20%**
H_2O	17,4 ml	2,2 ml
30% Acryl/0.8% Bisacryl solution	5 ml	20 ml
LGB (4x)	7,5 ml	7,5 ml
10% APS	150 µL	150 µL
TEMED	15 µL	15 µL

- **Stacking (upper) gel solution (20 ml)**

	3,5%
H_2O	13,2 ml
30% Acryl/0.8% Bisacryl solution	2,4 ml
UGB (5x)	4,0 ml
10% APS	200 µL
10% SDS	200 µL
TEMED	20 µL

- **(4x) Loading Gel Buffer**

1 M Tris solution (pH 6.8)	2.5 mL (250 mM)
SDS	0.8 g (8%)
Glicerol	4 ml (40%)
β-Mercaptoetanol	2 ml (2%)
Bromophenol blue	1 mg (0.01%)

Adjust the volume to 10 ml with deionised H_2O. Store in darkness at room temperature.

- **1 M Tris (pH 6.8) solution**

To 150 ml of deionised H_2O add:

Tris base	30.3 g

Adjust the pH to 6.8 and adjust the final volume to 250 ml.

- **10x Running Buffer**

Tris	30.3 g (250 mM)
Glycine	144.2 g (2.5 M)
SDS	10 g (1%)

Dissolve in deionised H2O, adjust the pH to 8.3 and adjust the volume to 1 L.

- **1x Transfer Buffer**

Tris	30.3 g (250 mM)
Glycine	144.2 g (192 mM)

Mix until solutes dissolution. Adjust the pH to 8.3 with HCl and adjust the volume to 800 ml with deionised H_2O. Just prior to use add 200 ml of methanol (20%).

- **10x TBS (Tris buffered saline)**

Tris	12.11 g (10 mM)
NaCl	87.66 g (150 mM)

Adjust the pH to 8.0 with HCl and adjust the volume to 1L with deionised H_2O.

- **10x TBST (TBS+Tween)**

Tris	12.11 g (10 mM)
NaCl	87.66 g (150 mM)
Tween 20	5 ml (0.05%)

Adjust the pH to 8.0 with HCl and adjust the volume to 1L with deionised H2O.

- **Membranes Stripping Solution (500 ml)**

Tris-HCl (pH 6.7)	3.76 g (62.5 mM)
SDS	10g (2%)
β-mercaptoethanol	3.5 ml (100 mM)

Dissolve Tris and SDS in deionised H_2O and adjust with HCl to pH 6.7. Add the β-mercaptoethanol and adjust volume to 500 ml.

- **ECL home-made (250 ml)**

Solution A - ECL luminol solution (Stock solution):

20 mM luminol (in DMSO) *	1.25 ml (100µM)
100 mM 4-iodophenol (in DMSO) *	5 ml (2mM)
0.1 M Tris (pH 9.35)	125 ml (50 mM)

Adjust volume to 250 ml with deionised H_2O. * Protect from the light; conserve at -20°C

Solution B – Hydrogen peroxide

Pull-down solutions

- **Lysis buffer (5 ml)**

50 mM Tris (pH 8)	250 µl of 1M Tris (pH 8)
25% glycerol	1250 µl 100% glycerol
0.5% Gepac-ca-630 (NP40)	250 µl 10% NP40
200 mM NaCl	200 µl 5M NaCl
β-mercaptoethanol	0,35 µl β-mercaptoethanol

1 mM PMSF	50 µl 100 mM PMSF
Protease inhibitor cocktail	5 µl of protease inhibitor cocktail

Keep all on ice.

- **Wash buffer (20 ml)**

10 mM Tris (pH 8)	200 µl of 1M Tris (pH 8)
0.1% Gepac-ca-630 (NP40)	200 µl 10% NP40
150 mM NaCl	600 µl 5M NaCl
0.25 mM EDTA	40 µl 0.25M EDTA
1 mM PMSF	200 µl 100 mM PMSF
Protease inhibitor cocktail	20 µl of protease inhibitor cocktail

Keep all on ice.

V. Solutions for DNA manipulation

- **50x TAE Buffer Tris base**

Tris base	242 g
Glacial acetic acid	57.1 mL
0.5M EDTA (pH 8.0)	100 mL

- **TE Buffer (pH 7,5)**

10 mM Tris-HCL pH 7,5
1 mM EDTA pH 8,0

- **6x Loading Buffer (LB)**

Bromophenol blue	0.25%
Glycerol	30%

- **Competent Cell Solutions**

Solution I (1L):

$MnCl_2.4H_2O$	9.9 g
$CaCl_2.2H_2O$	1.5 g

Glycerol	150 g
KHAc 1M	30 mL

Adjust the volume of the solution to 1 L with deionised H_2O. Adjust pH to 5.8, filter through a 0.2 µm filter and store at 4°C.

Solution II (1L):

0.5M MOPS (pH 6.8)	20 mL
RbCl	1.2 g
$CaCl_2.2H_2O$	11g
Glycerol	150 g

Adjust the volume of the solution to 1 L with deionised H_2O. Filter through a 0.2 µm filter and store at 4°C.

- **Miniprep Solutions**

Solution I:

50 mM glucose

25 mM Tris.HCl pH 8.0

10 mM EDTA

Solution II:

0.2 N NaOH

1% SDS

Solution III:

3 M potassium acetate

2 M glacial acetic acid

- **Midiprep Solutions**

Cell Resuspension Solution:

50 mM Tris-HCl (pH 7.5)

10 mM EDTA

100 µg/mL RNAase A

Cell Lysis Solution:

0.2 M NaOH

1% SDS

Neutralization Solution:

4.09 M Guanidine hydrochloride (pH 4.8)

759 mM potassium acetate

2.12 M Glacial acetic acid

Column Wash Solution:

60 mM potassium acetate

8.3 mM Tris-HCl (pH 7.5)

0.04 mM EDTA

60 % ethanol

Plasmids

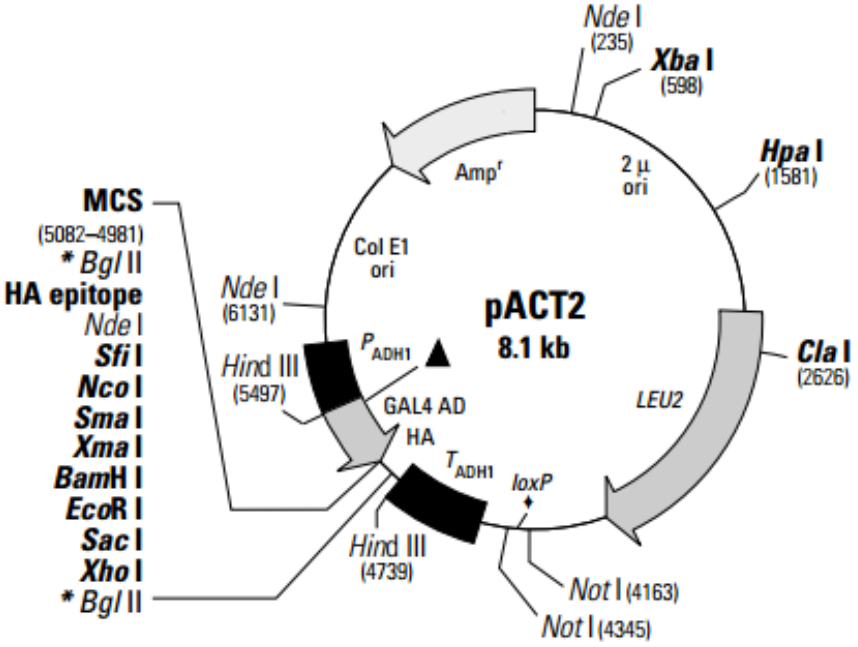

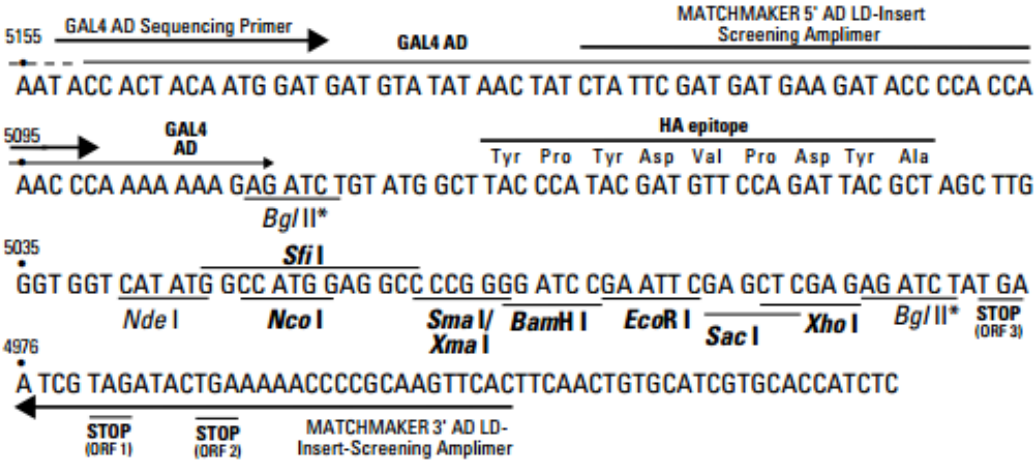

pACT2 (Clontech) map and multiple cloning sites. Unique sites are in bold. pACT2 is used to generate a hybrid containing the GAL4 AD, an epitope tag and a protein encoded by a cDNA in a fusion library. The hybrid protein is expressed at medium levels in yeast host cells from an enhanced, truncated ADH1 promoter and is targeted to the nucleus by the SV40 T-antigen nuclear localization sequence. pACT2 contains the LEU2 gene for selection in Leu$^-$ auxotrophic yeast strains.

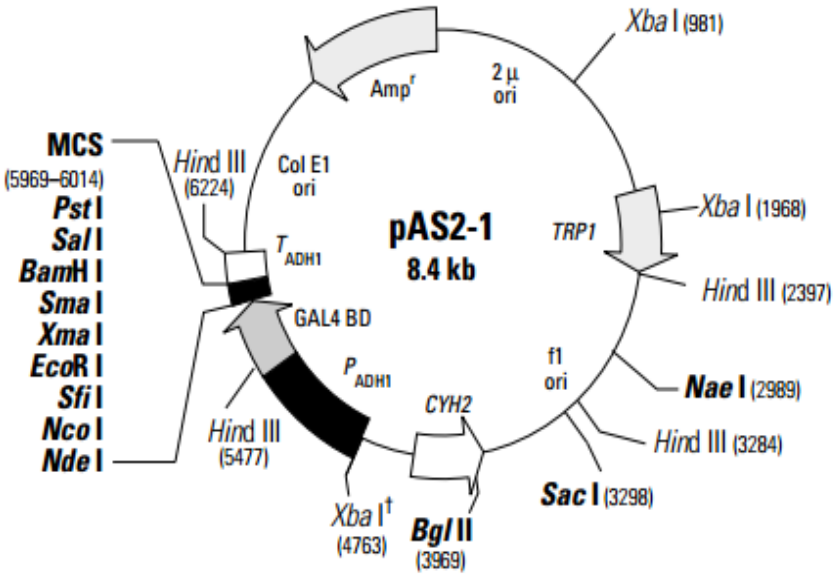

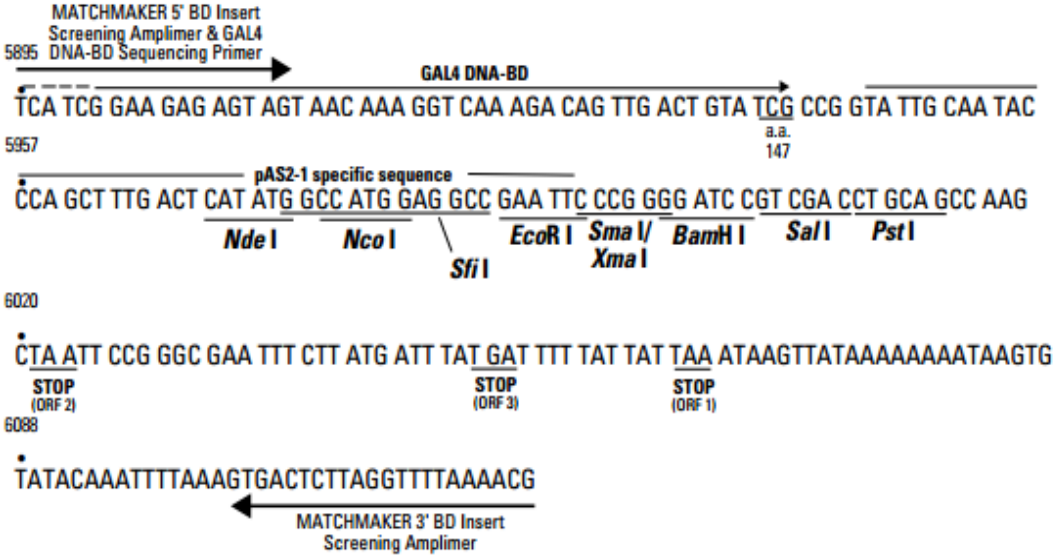

pAS2-1 (Clontech) map and multiple cloning sites. Unique restriction sites are coloured blue. pAS2-1 is a cloning vector used to generate fusions of a bait protein with the GAL4 DNA-BD. The hybrid protein is expressed at high levels in yeast host cells from the full-length ADH1 promoter. The hybrid protein is targeted to the yeast nucleus by nuclear localization sequences. pAS2-1 contains the TRP1 gene for selection in Trp^- auxotrophic yeast strains.

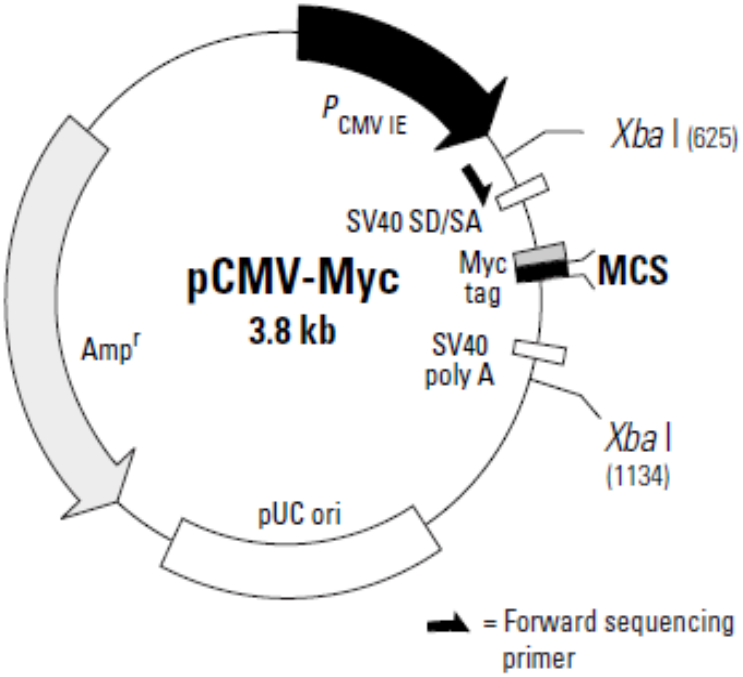

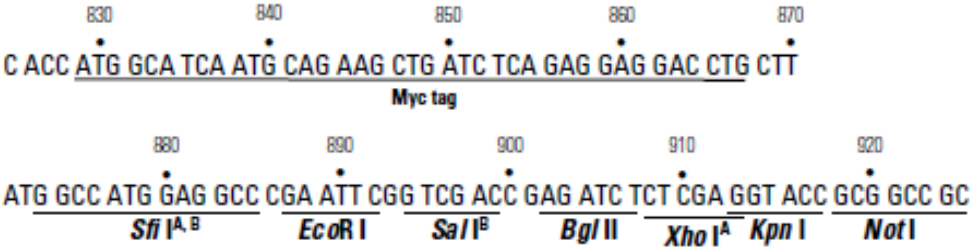

pCMV-Myc (Clontech) restriction map and multiple cloning sites. Unique restriction sites are in bold. pCMV-Myc is a mammalian expression vector with an N-terminal c-Myc epitope tag. This vector possesses the ampicillin resistance gene for selection in E. coli.

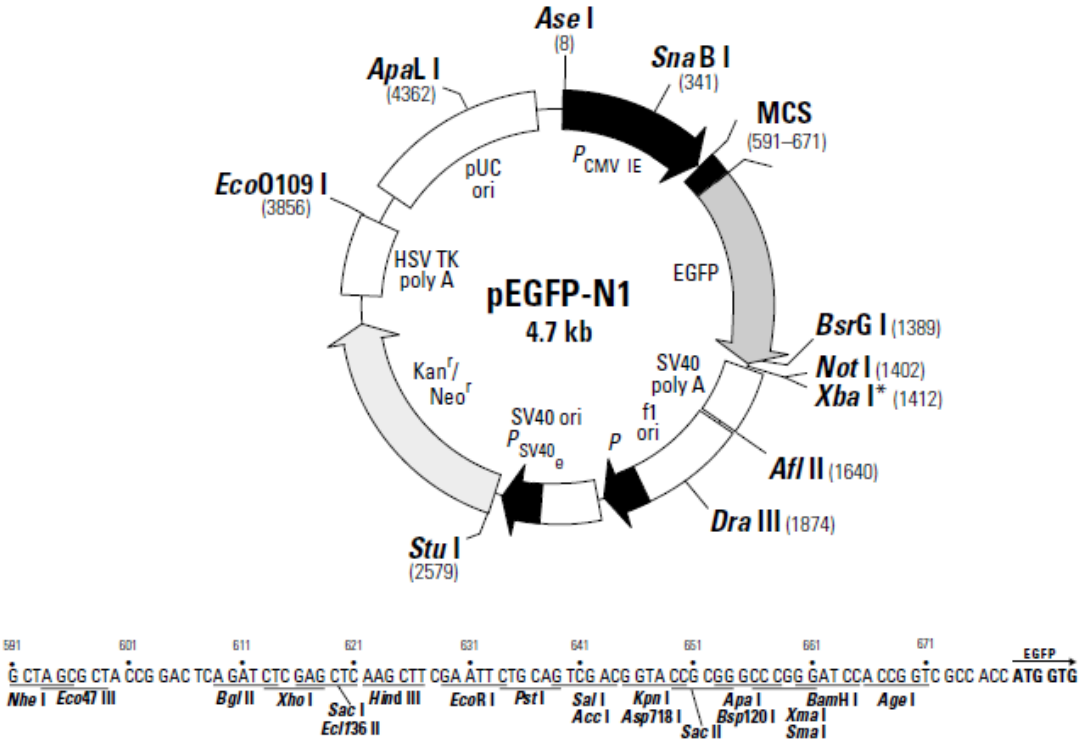

pEGFP-N1 (Clontech) restriction map and multiple cloning sites. Unique restriction sites are in bold. pEGFP-N1 is a mammalian expression vector with the EGFP coding sequence located in a C-terminal position to the MCS. This vector possesses the kanamicin resistance gene for selection in E. coli.